International Journal of Distributed Sensor Networks

Advances in Cognitive Radio Sensor Networks

Guest Editors: Hyung Seok Kim, Waleed Ejaz, Khalid Al-Begain, Al-Sakib Khan Pathan, and Najam ul Hasan

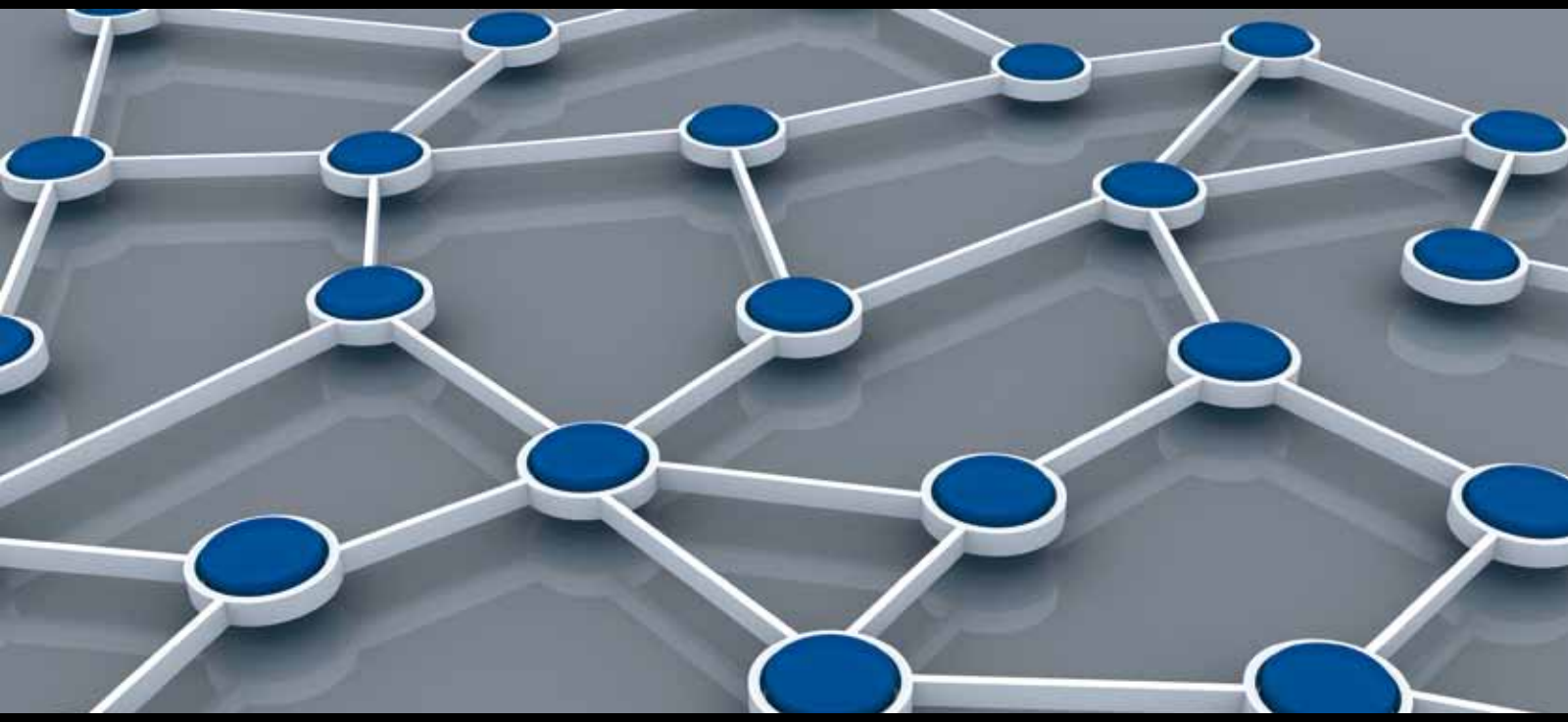

Advances in Cognitive Radio Sensor Networks

International Journal of Distributed Sensor Networks

Advances in Cognitive Radio Sensor Networks

Guest Editors: Hyung Seok Kim, Waleed Ejaz,
Khalid Al-Begain, Al-Sakib Khan Pathan, and Najam ul Hasan

Editorial Board

Contents

Hindawi Publishing Corporation
International Journal of Distributed Sensor Networks
Volume 2014, Article ID 631624, 3 pages
http://dx.doi.org/10.1155/2014/631624

Editorial

Advances in Cognitive Radio Sensor Networks

Hyung Seok Kim,[1] Waleed Ejaz,[1] Khalid Al-Begain,[2] Al-Sakib Khan Pathan,[3] and Najam ul Hasan[4]

[1] *Sejong University, Seoul 143 747, Republic of Korea*
[2] *University of South Wales, Pontypridd CF37 1DL, UK*
[3] *International Islamic University Malaysia (IIUM), 53100 Kuala Lumpur, Malaysia*
[4] *National University of Computer and Emerging Sciences, Islamabad 44000, Pakistan*

Correspondence should be addressed to Hyung Seok Kim; hyungkim@sejong.ac.kr

Received 22 January 2014; Accepted 22 January 2014; Published 9 March 2014

Advances in wireless communication have changed the customs and the living style of people today, and the demand for wireless communication with high speeds and ubiquitous connectivity continues to increase. Currently a number of different wireless networks, for example, cellular networks and wireless local area networks, are in place to support mobile services but still new emerging applications require more support to meet communication requirements. Cognitive radio (CR) networks have emerged in response to the demand of these emerging applications as one form of several new wireless networks. A variety of new challenges and issues have also arisen with these new networking technologies, which have created many new research opportunities. While designing these emerging networks, it is not only important to realize innovative applications, but also crucial to investigate how to achieve the optimum bandwidth and energy efficiency, due to the scarcity of the network resources (bandwidth, channel, energy, storage, and so on). Such investigation requires a multidisciplinary effort that encompasses areas of signal processing, communication, control, and information theory. The major focus of this special issue is investigating how to achieve efficient use of spectral resources with low power consumption in the cognitive radio networks.

Increasing demand for spectral resources has introduced the issue of efficient spectrum utilization. CR technology indeed allows opportunistic access to the spectrum. CR employs the concept of dynamic spectrum access (DSA) to improve spectrum utilization efficiency and communication quality. In addition to many other wireless systems taking advantage of DSA, several challenges and requirements of a wireless sensor network (WSN) can be met by using CR; therefore, some proposals suggested embedding CR within such networks. That gives rise to a new term, known as cognitive radio sensor network (CRSN).

Despite the advantages offered by CRSN, embedding CR in sensors has also introduced several challenges. In addition to the challenges inherited from WSN, there are some unique challenges related to CRSN including definitions of channel, channel availability, channel heterogeneity channel quality, control channel assignment, and transmission channel assignment. This motivates the design of a new medium access mechanism for CRSN that can cope with all these challenges. Currently, WSNs have been used in a number of different applications ranging from surveillance and remote monitoring to healthcare; thereby, while designing protocol suite for CRSN, the underlying application also needs to be taken into consideration.

CRSN mainly is composed of two parts: sensing and access policy. Briefly, sensing policy determines the set of channels to be sensed, the order in which the channels should be sensed, and duration of each sensing. After identifying the spectrum holes, access policy determines access related issues as to whether to access the band or not.

Sensing Policy. Spectrum sensing is the prerequisite of DSA. In DSA, the sensors opportunistically access the spectrum; hence, they need to gather the spectrum usage information via a spectrum sensing process prior to transmission. For spectrum sensing in CRSN, a sensing policy needs to be defined that answers the following questions.

(i) Which set of channels is the most suitable to be sensed?

(ii) What should the schedule be for sensing the channels?

(iii) Which technique will be the most suitable for sensing?

(iv) What should be the duration of sensing?

(v) Should the sensor sense collaboratively or not?

(vi) How should the sensor collaborate?

(vii) In collaborative sensing, how many sensors should sense a channel?

Access Policy. In CRSN, when a node senses an event signal, it communicates its reading using DSA over an available spectrum band (determined based on sensing policy) to satisfy the application specific requirement. As multiple CRSNs are sharing the available spectrum without harming the licensed user communication, an access policy needs to be defined. In CRSN, the access policy needs to answer the following questions.

(i) Which channel (control channel) should be used for the exchange of control messages?

(ii) Which channels should be used for data?

(iii) How should data channels be assigned to users?

(iv) How should channel switching be ensured in case of licensed user appearance?

(v) What should the maximum transmission frame length be?

(vi) What should the transmission parameter be, such as power, modulation, and error coding mechanisms?

(vii) How can the Quality of Service (QoS) of the different applications be ensured?

In a nutshell, there is indeed some critical benefits of cognitive radio based wireless sensor networks like opportunistic channel usage for bursty traffic, dynamic spectrum access, deployment of multiple sensor networks without hampering each other's operation on the same area, adaptive reduction of power consumption, conformity to different spectrum regulations in different locations, and so on. That is why this research field has attracted many researchers in the recent times. The challenges, however, are many, some of which are explored and analyzed in the accepted articles in this special issue, with some interesting solutions and proposals.

Contributions of Accepted Papers. A. Raza et al. in their paper entitled "*Consensus-based distributive cooperative spectrum sensing for mobile ad hoc cognitive radio networks*" proposed a consensus-based distributed cooperative spectrum sensing scheme (CDCSS) in CR mobile ad hoc networks which is inspired by novel biological mechanisms. CDCSS works on mobile nodes in distributive network without using a centralized entity to improve the sensing performance in cognitive radio mobile ad hoc networks.

F. Ye et al. in their paper entitled "*The user requirement based competitive price model for spectrum sharing in cognitive radio networks*" analyzed the competitive price game model for spectrum sharing in CR networks with multiple primary users and secondary users and proposed a user requirement based competitive price game model for the calculation of the shared spectrum size of cognitive user in Bertrand game.

W. B. Tessema et al. in their paper entitled "*Channel hopping sequences for rendezvous establishment in cognitive radio sensor networks*" proposed two channel hopping sequences to establish a link in CRSNs with and without the assumption of global clock synchronization. Under the assumption of global clock synchronization, authors first propose synchronous channel hopping sequence in which the sequences can overlap with each other in all available channels at different time slots and the rendezvous spread out over. Next, under the assumption that CR users are not synchronized with each other, authors proposed asynchronous channel hopping sequence in which CR users can get a rendezvous channel within a bounded time, although they start hopping at any time slot.

J. Kim et al. in their paper entitled *"A rendezvous scheme for self-organizing cognitive radio sensor networks"* proposed a hopping sequence algorithm to achieve a successful rendezvous within a single period in a CR network. With the proposed algorithm, called hopping sequence guaranteeing rendezvous within a single period, CR nodes can rendezvous in a single period and reliably exchange control message with each other.

M. O. Mughal et al. in their paper entitled "*Energy detection in multihop cooperative diversity networks: an analytical study*" presented a study of detection performance of energy detector in relay based multihop cooperative diversity networks operating over independent Rayleigh fading channels. In particular, upper bound average detection probability expressions are obtained for three scenarios: (i) multihop cooperative relay communication; (ii) multihop cooperative relay communication with direct link and maximum ratio combiner at destination; and (iii) multihop cooperative relay communication with direct link and selection combiner at destination.

E. Romero et al. in their paper entitled "*A game theory based strategy for reducing energy consumption in cognitive WSN*" presented a new game theory based strategy to optimize energy consumption in WSNs. This strategy takes advantage of a new opportunity offered by cognitive wireless sensor networks: the ability to change the transmission and reception channel.

S. M. Kamruzzaman et al. in their paper entitled "*Channel-slot aggregation diversity based slot reservation scheme for cognitive radio ad hoc networks*" proposed a channel-slot aggregation diversity based slot reservation scheme, called

channel-slot aggregation diversity based slot reservation, for CR ad hoc networks. Power control mechanism along with doze mode operation is adopted to improve the spectrum and energy efficiencies. Furthermore, the proposed method efficiently utilizes the channel bandwidth by assigning unused slots to new CR users and enlarging the frame length when the number of slots within the frame is insufficient to support the demand of neighboring CR users. An effective frame recovery method is also presented that shrinks the frame length in an efficient way.

We hope that the papers in this special issue would be beneficial for the research community to get some ideas to find future research topics related to this area.

Hyung Seok Kim
Waleed Ejaz
Khalid Al-Begain
Al-Sakib Khan Pathan
Najam ul Hasan

Hindawi Publishing Corporation
International Journal of Distributed Sensor Networks
Volume 2014, Article ID 872780, 12 pages
http://dx.doi.org/10.1155/2014/872780

Research Article

Channel Hopping Sequences for Rendezvous Establishment in Cognitive Radio Sensor Networks

Widist Bekulu Tessema, Byeongung Kim, Junhyung Kim, Wooseong Cho, and Kijun Han

School of Computer Science and Engineering, Kyungpook National University, Daegu 702-701, Republic of Korea

Correspondence should be addressed to Kijun Han; kjhan@knu.ac.kr

Received 23 August 2013; Revised 9 December 2013; Accepted 23 December 2013; Published 24 February 2014

Academic Editor: Najam ul Hasan

In Cognitive Radio sensor networks, a pair of Cognitive Radio (CR) users wishing to communicate should first agree on a specific channel called control channel. Communication rendezvous is used to establish a control channel between CR users. Channel Hopping (CH) protocol is a sequence-based approach that provides an effective method for implementing rendezvous without relying on a Common Control Channel (CCC). In this approach, all CR users hop to the same rendezvous channel and hence this channel will serve as a control channel between them. In this paper, we propose two Channel Hopping Sequences (CHS) to establish a link in CR sensor networks with and without the assumption of global clock synchronization. Our schemes provide successful communication rendezvous within a bounded time interval. Theoretical analysis and simulation results showed that both schemes outperform the existing schemes used for similar purpose in terms of many performance criteria.

1. Introduction

Wireless sensor networks (WSN) are being used in many industrial and application areas, including industrial process monitoring, healthcare applications, home automation, and traffic control [1]. In last decade, various communication systems use industrial, scientific, and medical (ISM) band for exchanging information due to its licence-free nature [1, 2]. As a result, the ISM band becomes more congested. The concept of Cognitive Radio (CR) has recently initiated great interest to get full potential of the radio spectrum [3]. If a Primary User (PU) is currently not using the band, the secondary user changes its transmission parameters to take advantage of the band. After detecting the vacant frequency bands, a CR user selects the best available spectrum hole for opportunistic communications and it vacates the channel when the PUs returns. It also applies the same phenomenon to a control channel. Hence, a particular channel cannot be fixed as a control channel forever and the control channel can vary from time to time. CR networks involve extensive exchange of control messages to coordinate critical network functions, which are broadcasted on a preassigned Common Control Channel [4]. However, not only is a static control channel allocation contrary to the opportunistic access paradigm, but also the implementation of a CCC for all the CR users is a challenging task [4]. Furthermore, the sudden appearance of a PU may lead to loss of connectivity among SUs [4, 5].

Communication rendezvous enables CR users to communicate with each other. A pair of CR users wishing to communicate should first agree on a specific channel called control channel. Communication rendezvous are used to establish a control channel between CR users. Most of the existing MAC protocols for CR networks relay on a dedicated global or local control channel [7–10]. However, those approaches suffer from the problem of control packet overhead, and the dynamic nature of spectrum availability makes it difficult to rely on a CCC. In contrast, Channel Hopping (CH) protocol is a sequence-based control channel design that provides an effective method for implementing rendezvous without relying on a CCC [7]. One of the rendezvous channels are assigned to be a control channel. The CH sequence determines the order with which the CR users visit all of the available rendezvous channels. The main aim of this design is to diversify the control channel allocation over spectrum and time spaces in order to minimize the impact

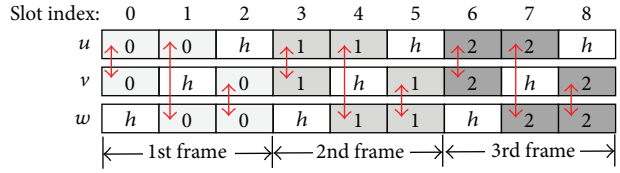

Figure 1: Quorum-based CH system [6].

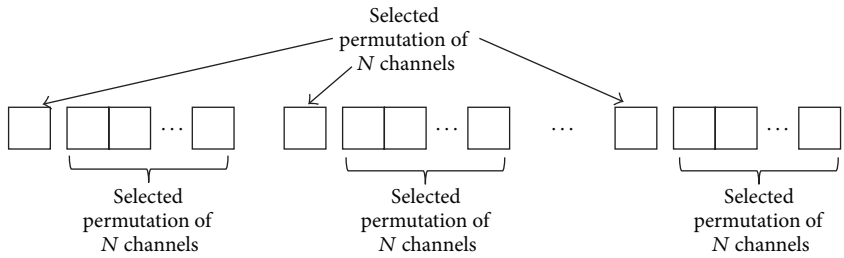

Figure 2: Building a sequence for SeqR [7].

of PU activity. In this approach, all CR users hop on a set of sequences of rendezvous channels. When two CR users want to communicate with each other, they hop to the same rendezvous channel and hence this channel will serve as a control channel between them.

In this paper, we propose two Channel Hopping Sequences to establish a link in CR sensor networks with and without the assumption of global clock synchronization. Under the assumption of global clock synchronization, we first propose Synchronous Channel Hopping Sequence (S-CHS) in which the sequences can overlap with each other in all available channels at different time slots and the rendezvous spread out over. Next, under the assumption that CR users are not synchronized with each other, we propose Asynchronous Channel Hopping Sequence (A-CHS) in which CR users can get a rendezvous channel within a bounded time although they start hopping at any time slot.

The rest of this paper is organized as follows. We describe related works in Section 2. The S-CHS and the A-CHS protocols are explained in Section 3. Performance evaluation of the proposed schemes is given in Section 4. Finally, we conclude the paper in Section 5.

2. Related Works

2.1. Quorum-Based Channel Hopping (QCH). The quorum-based mechanism [6] achieves CCC establishment through CHS satisfying the property of intersection (Figure 1). Based on this property, four CH systems are constructed. The first system (M-QCH) minimizes the upper-bound of the Time to Rendezvous (TTR) value by using the majority and minimal cyclic quorum systems. The second system (L-QCH) evenly distributes the rendezvous points over different time slots during a CH period. The third system (A-QCH) guarantees rendezvous only on two distinct channels between any two CHS's without requirement for global clock synchronization. The fourth system, A-MOCH mechanism, presumes that the rotation closure property of quorum-based system must be satisfied by one commonly available channel. The advantage of such assumption can enable one rendezvous in N^2 time slots where N refers to the total number of channels.

2.2. Sequence-Based Rendezvous (SeqR). The SeqR mechanism [11] constructs nonorthogonal CHS using permutation of the channels as presented in Figure 2. The selected permutation appears $N + 1$ times in the sequence: the permutation appears N times contiguously once the permutation appears interspersed with the other N permutations. For example, if $N = 5$, a permutation (3, 2, 5, 1, 4) is selected at random, and the following sequence is produced;

$$\mathbf{3}, 3, 2, 5, 1, 4, \mathbf{2}, 3, 2, 5, 1, 4, \mathbf{5}, 3, 2, 5, 1, 4, \mathbf{1}, 3, 2, 5, 1, 4, \mathbf{4}, 3, 2, 5, 1, 4. \quad (1)$$

Note that the original permutation appears 6 times in the sequence, including once mixed with the other 5 appearances of the permutation. This sequence is then repeated infinitely. The expected TTR is bounded by $N^2 + N$. Consequently, it may take a long time to find a neighbouring node on a channel for the exchange of control information, especially when the number of available channels is large.

2.3. Efficient Channel Hopping (ETCH). ETCH (SYNC-ETCH) and Asynchronous ETCH (ASYNC-ETCH) mechanisms are presented in [12]. The SYNC-ETCH consists of three parts: rendezvous scheduling, rendezvous channel assignment, and CHS execution. A newly joining node executes SYNC-ETCH to establish a control channel with another node as follows. First, the node constructs a set of CHS guaranteeing the satisfaction of the overlap requirement. After completing the CHS construction, the node synchronizes to the existing nodes and starts the CH process according to the CHS execution scheme of SYNC-ETCH. Particularly, PU activities are high on SYNC-ETCH because

0	1	2
1	2	0
2	0	1

Figure 3: Cayley table for a set $S = \{0, 1, 2\}$.

C_{00}	C_{01}	$\cdots$	$C_{0\,N-2}$	$C_{0\,N-1}$	$C_{0\,N-2}$	$C_{0\,N-3}$	$\cdots$	C_{00}
$\cdots$	$\cdots$	$\cdots$	$\cdots$	$\cdots$	$\cdots$	$\cdots$	$\cdots$	$\cdots$
C_{i0}	C_{i1}	$\cdots$	$C_{i\,N-2}$	$C_{i\,N-1}$	$C_{i\,N-2}$	$C_{i\,N-3}$	$\cdots$	C_{i0}
$\cdots$	$\cdots$	$\cdots$	$\cdots$	$\cdots$	$\cdots$	$\cdots$	$\cdots$	$\cdots$
$C_{N-1\,0}$	$C_{N-1\,1}$	$\cdots$	$C_{N-1\,N-2}$	$C_{N-1\,N-1}$	$C_{N-1\,N-2}$	$C_{N-1\,N-3}$	$\cdots$	$C_{N-1\,0}$

Figure 4: Illustration of reflected Cayley table.

each node randomly selects a sequence after completing a pre-started sequence (the sequence to be selected might be suffering from PU appearance). Similar to SYNC-ETCH, ASYNC-ETCH also first constructs a set of CHS when a CR node joins the network. The difference is that the node does not need to synchronize to the existing nodes unlike ASYNC-ETCH.

3. Proposed Schemes

In this section, we propose two Channel Hopping Algorithms that generate CHS to establish a link in CR sensor network with and without the assumption of global clock synchronization: Synchronous Channel Hopping Sequence (S-CHS) and Asynchronous Channel Hopping Sequence (A-CHS). In both algorithms, it is assumed that CR users have N available channels, and they are capable of sensing PUs signal. The PUs can establish connection on $N - 1$ channels. We also assume that each CR users has a single half-duplex radio.

3.1. S-CHS. S-CHS is based on the assumption of global clock synchronization. The algorithm to generate S-CHS is divided into three parts: construction of Cayley table, reflection, and cyclic shift and catenation.

3.1.1. Construction of Cayley Table to Get All Possible Permutations. We use Cayley table [13] for designing the hopping sequences because it simplifies the permutation operation on a given set. The Cayley table produces all possible permutations of a set. The permutation of a set can be obtained by integer addition modulo operation which is a mathematical tool that helps in getting numbers which are less than the pivoting number (the divisor). The Cayley table, denoted by C, over the set $S = \{0, 1, \ldots, N - 1\}$ is made through integer addition modulo operation as follows:

$$C = \left\{c_{ij}\right\}, \quad c_{ij} = \frac{(i + j)}{Z(N)}, \quad \forall (i, j) \in \{0, 1, \ldots, N - 1\}, \quad (2)$$

where $Z(N)$ denotes modulo operation with a positive integer N.

An example for a set $S = \{0, 1, 2\}$ is shown in Figure 3. Let us take modulo operation on the first row of the Cayley table: $(0 + 0)\%\ (3) = 0$, $(0 + 1)\%\ (3) = 1$, $(0 + 2)\%\ (3) = 2$. All results 0, 1, and 2 are less than 3 (divisor) which is the number of available rendezvous channels.

3.1.2. Reflection of Cayley Table. We construct the reflected Cayley table by appending all elements except the last element to the end of each row of a given Cayley table in the reverse order. For the ith row of the Cayley table $\{c_{i0}, c_{i1}, \ldots, c_{iN-1}\}$, its reflected row will be $\{c_{i0}, c_{i1}, \ldots, c_{iN-2}, c_{iN-1}, c_{iN-2}, c_{iN-3}, \ldots, c_{i1}, c_{i0}\}$. Repeating the same operation on all rows, we get the reflected Cayley table as illustrated in Figure 4. As shown in this figure, each row of the reflected Cayley table has $(2N - 1)$ elements.

3.1.3. Construction of S-CHS by Cyclic Shifting and Catenation. We define the k-order cyclic shift (or rotation) operation by shifting a vector to the right direction by k positions in a cyclic manner. If we perform one-order cyclic shifting on an N-code array $A^0 = \{a_0, a_1, \ldots, a_{N-1}\}$, we get $A^1 = \{a_{N-1}, a_0, a_1, \ldots, a_{N-2}\}$. Similarly, the 2-order shifted vector will be $A^2 = \{a_{N-2}, a_{N-1}, a_0, a_1, \ldots, a_{N-3}\}$. In general, we have the k-order shifted vector $A^k = \{a_{N-k}, a_{N-k+1}, \ldots, a_0, \ldots, a_{N-k-1}\}$. Now, we perform cyclic shifting on each row of the reflected Cayley table. For example, if we perform cyclic shifting operation on the reflected Cayley table for the set $S = \{0, 1, 2\}$, we get 5 different tables by 0-order to 5-order cyclic shifting as shown in Figure 5. Note that each row of the reflected Cayley table has 5 elements.

Finally, we make hopping sequences by catenating all elements from the first to the last row of the reflected Cayley table. For example, for a set $\{0, 1, 2\}$, we get a hopping sequence $\{0, 1, 2, 1, 0, 1, 2, 0, 2, 1, 2, 0, 1, 0, 2\}$ by catenating all elements of the first reflected Cayley table illustrated in

0	1	2	1	0
1	2	0	2	1
2	0	1	0	2

(a) C^0 (reflected Cayley table)

0	0	1	2	1
1	1	2	0	2
2	2	0	1	0

(b) C^1 (1-order cyclic shift)

1	0	0	1	2
2	1	1	2	0
0	2	2	0	1

(c) C^2 (2-order cyclic shift)

2	1	0	0	1
0	2	1	1	2
1	0	2	2	0

(d) C^3 (3-order cyclic shift)

1	2	1	0	0
2	0	2	1	1
0	1	0	2	2

(e) C^4 (4-order cyclic shift)

Figure 5: Cyclic shifting of reflected Cayley table for a set $\{0, 1, 2\}$.

	T_0	T_1	T_2	T_3	T_4	T_5	T_6	T_7	T_8	T_9	T_{10}	T_{11}	T_{12}	T_{13}	T_{14}
H_0	0	1	2	1	0	1	2	0	2	1	2	0	1	0	2
H_1	0	0	1	2	1	1	1	2	0	2	2	2	0	1	0
H_2	1	0	0	1	2	2	1	1	2	0	0	2	2	0	1
H_3	2	1	0	0	1	0	2	1	1	2	1	0	2	2	0
H_4	1	2	1	0	0	2	0	2	1	1	0	1	0	2	2

Figure 6: Illustration of S-CHS for CR sensor network with 3 channels.

Figure 5(a). Similarly, we can construct 4 other hopping sequences from the reflected Cayley tables illustrated in Figures 5(b)–5(e). Figure 6 shows these five hopping sequences constructed from the reflected Cayley tables shown in Figure 5. From this figure, we can observe that any two of five hopping sequences are overlapped at some time slot. If we denote these hopping sequences by H_i ($i = 0, 1, 2, 3, 4$), then the first hopping sequence (H_0) has the same element "0" with H_1 at the time slot T_0. In other words, H_0 coincides with H_1 at the time slot T_0. Similarly, H_0 coincides with H_2 at the time slot T_3, and it also coincides with H_3 and H_4 at the time slot T_1 and T_4, respectively. We express the coincidences between any two sequences as follows:

$$\begin{aligned} &H_0 \cap H_1 = \{0\} \text{ at } T_0, \qquad H_0 \cap H_2 = \{1\} \text{ at } T_3, \\ &H_0 \cap H_3 = \{1\} \text{ at } T_1, \qquad H_0 \cap H_4 = \{0\} \text{ at } T_4, \\ &H_1 \cap H_2 = \{0\} \text{ at } T_1, \qquad H_1 \cap H_3 = \{1\} \text{ at } T_4, \\ &H_1 \cap H_2 = \{0\} \text{ at } T_1, \qquad H_1 \cap H_3 = \{1\} \text{ at } T_4, \\ &H_2 \cap H_4 = \{1\} \text{ at } T_0, \qquad H_3 \cap H_4 = \{0\} \text{ at } T_3. \end{aligned} \tag{3}$$

It is interesting that the coincidence happens in a cyclic manner. This is because cyclic shifting operation is performed on the reflected Cayley table to make hopping sequences. The length of S-CHS is $N(2N-1)$ since the reflected Cayley table has N rows, each of which has $(2N-1)$ elements.

With S-CHS, any given two hopping sequences can coincide periodically. Figure 7 shows periodical rendezvous points and the mean TTR when two sequences H_1 and H_2 are used for hopping sequences in CR sensor network with 3 channels. We can see that they periodically coincide with a period of 5 time slots.

3.2. A-CHS. When CR users are not synchronized with each other, the assumption for S-CHS is no longer valid. Although CR users start hopping at any time slot, they should get a rendezvous channel within a bounded TTR. In the preceding section, we used reflection properties together with Cayley table and cyclic rotations in order to establish a set of hopping sequences. In S-CHS, reflection operation is performed about the last element. Instead, in A-CHS, reflection is performed about certain imaginary point (channel) which is not member of currently available channels. The easiest way for generating such a point is to have duration (time slot) during which no channel access or no frequency hopping is present. Let us denote such silent duration by B (meaning "blank"). To generate A-CHS, this silent channel is appended at the end of the channel members for reflection. Then, A-CHS is constructed by reflecting all channel members about the silent duration (denoted by H_0) as depicted in Figure 8. So, the hopping sequence for A-CHS will be $H_0 = \{0, 1, 2, \ldots, N-1, B, N-1, N-2, \ldots, 2, 1, 0\}$. If we denote shifted (or delayed) versions of H_0 by H_d (d means delay), then the hopping sequence H_0 must satisfy such a condition that $H \cap H_d \neq$ empty for any possible values of d. In a CR sensor network with N channels, the possible delays are $0, 1, 2, \ldots$ or $2N$ because the sequence H_0 has $(2N+1)$ members.

For instance, in a CR sensor network with three channels, we get a hopping sequence $H_0 = \{0, 1, 2, B, 2, 1, 0\}$. In this example, the CR user has clock drift ($d = 0, 1, \ldots,$ or 7) as shown in Figure 9. The sequence H_0 is taken as reference.

Figure 10 demonstrates when and where two CR users rendezvous with A-CHS in 3-channel CR sensor network. In this figure, two values in each entry mean rendezvous channel and rendezvous time, respectively. For example, two sequences H_0 and H_1 coincide on channel 0 at time slot T_7. So, in this case, the TTR becomes 8 by counting the elapsed time slots. Averaging TTR over all possible delays ($d = 1, 2 \ldots, 6$), the average TTR will be 7.5 time slots. And the maximum TTR (denoted by MTTR) will be 10 time slots when $d = 5$.

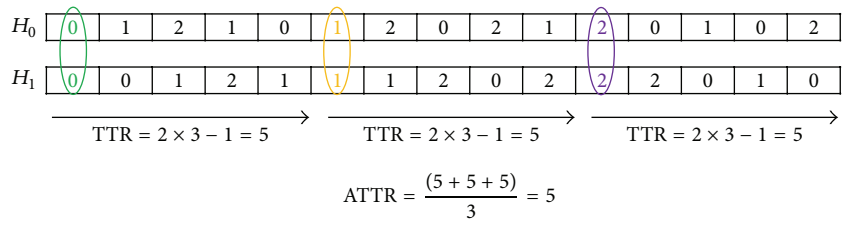

Figure 7: Average TTR using S-CHS for CR sensor network with 3 channels.

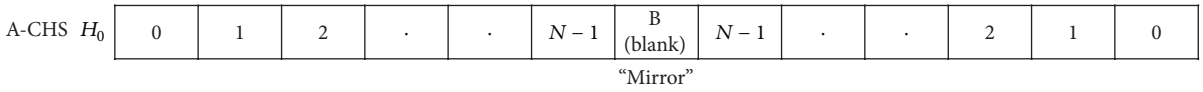

Figure 8: Construction of A-CHS by addition of silent duration and reflection about silent duration.

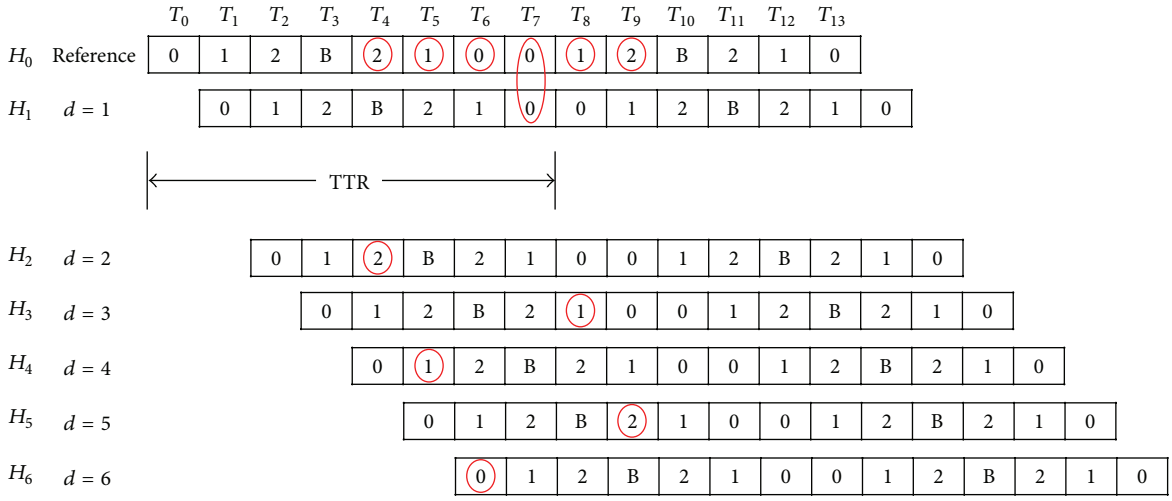

Figure 9: Rendezvous demonstration with A-CHS.

H_1	Ch 0 T_7					
H_2	Ch 2 T_4	Ch 0 T_8				
H_3	Ch 1 T_8	Ch 2 T_5	Ch 0 T_9			
H_4	Ch 1 T_5	Ch 1 T_5	Ch 2 T_6	Ch 0 T_{10}		
H_5	Ch 2 T_9	Ch 1 T_6	Ch 1 T_{10}	Ch 2 T_7	Ch 0 T_{11}	
H_6	Ch 0 T_6	Ch 2 T_{10}	Ch 1 T_5	Ch 1 T_{11}	Ch 2 T_8	Ch 0 T_{12}
	H_0	H_1	H_2	H_3	H_4	H_5

Figure 10: Demonstration of rendezvous with A-CHS in 3-channel CR sensor network. (Two values in each entry mean rendezvous channel and rendezvous time, resp.).

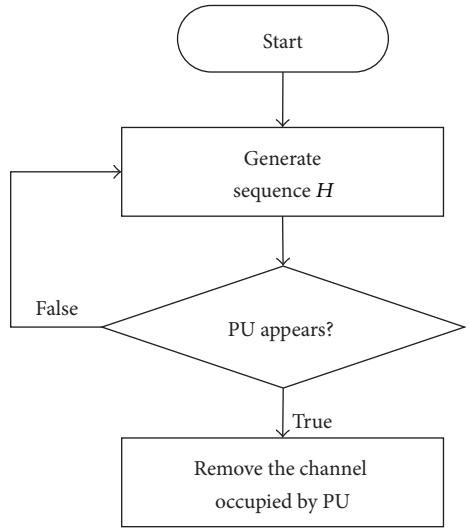

Figure 11: Rendezvous mechanism for PU appearance.

3.3. Mechanism for PU Appearance. The presence of PU disturbs or completely jams secondary user's activity. The appearance of PU may lead to link breakage. So, SUs need to have mechanism through which they will sense PU presence. The channel at which the PU stays must not be used by the SU until the PU ceases out of the channel. Hence CR users must be provided with a procedure through which they deal with the arising of the PU on a channel. The simplest way is that a CR user must be forbid from hopping those channels which is using by a PU [14]. The mechanism of this type of rendezvous for PU appearance is depicted in Figure 11.

4. Performance Evaluation

We evaluate our scheme in terms of five performance criterion, including TTR (ATTR and MTTR), effect by PU appearance, average channel load, channel utilization ratio, and degree of overlap. Comparison targets are two synchronous CH protocols such as M-QCH, SYNC-ETCH, and three asynchronous CH protocols such as SeqR, ASYNC-ETCH, and A-MOCH.

The performance evaluation is carried out by both theoretical and simulation study. The layout of the CR sensor networks is considered to have 2 to 10 rendezvous channels (Table 1). The SUs are considered to be inside the coverage area of the PU. During the simulation, we randomly check the availability of the PU using Poisson distribution. The rendezvous channels are disabled for a random time period upon the appearance of the PU. The senders always obey the receiver sequence and this process is repeated until the simulation ends.

4.1. TTR Performance. We first studied the performance of S-CHS and A-CHS in terms of TTR. TTR refers to the time needed by any two CR devices for rendezvous using hopping sequences, and it is computed by the number of time slots elapsed from the reference time to the rendezvous time.

Table 1: Parameters used for simulation.

Parameters	Values
Number of channels	2~10
PU appearance pattern	Poisson distribution
Duration of PU activity	Exponential distribution
Transmission range	250 m

Bounded and short TTR helps in minimizing the channel access delay. As seen in the preceding section, with S-CHS, two CR nodes periodically rendezvous every $(2N - 1)$ time slots (including the time slot it is currently hopping at) in a CR sensor network with N channels. The rendezvous channels are evenly distributed over all channels. In other words, rendezvous happens on all channels with the same probability. The Average TTR (ATTR) with S-CHS becomes $2N - 1$. And the Maximum TTR (MTTR) with S-CHS also becomes $2N - 1$:

$$\text{ATTR} = 2N - 1, \tag{4}$$

$$\text{MTTR} = 2N - 1. \tag{5}$$

In A-CHS, we can easily get TTR for N-channel CR sensor network by generalizing the example in Figure 3. Considering all possible clock drifts (delays), we have

$$\text{TTR} = \begin{cases} N + 1 + \dfrac{d}{2} & \text{for } d = 0, 2, 4, \ldots, 2N \\ 2N + 1 + \dfrac{(d+1)}{2} & \text{for } d = 1, 3, 5, \ldots, 2N - 1. \end{cases} \tag{6}$$

Averaging TTR for all possible values of d, we get ATTR by

$$\text{ATTR} = E[\text{TTR}] = 2N + 1.5. \tag{7}$$

Also, we have MTTR by

$$\text{MTTR} = 3N + 1. \tag{8}$$

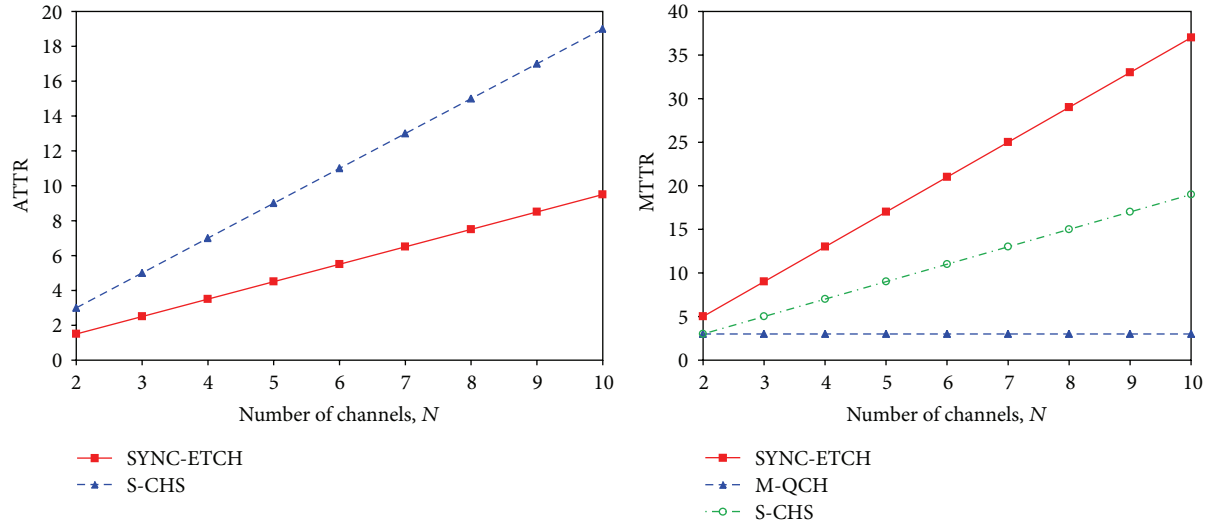

(a) ATTR and MTTR with synchronous protocols

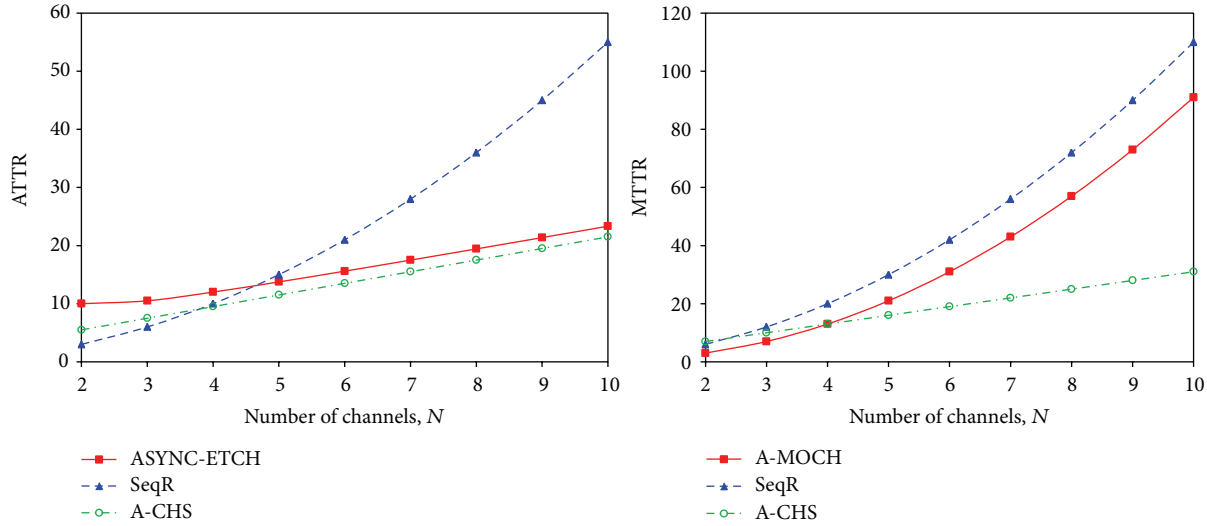

(b) ATTR and MTTR with asynchronous protocols

Figure 12: TTR performance of Channel Hopping Protocols.

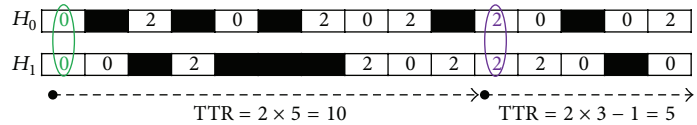

$$\text{ATTR} = \frac{(10 + 5)}{2} = 7.5$$

Figure 13: Effect of a PU on S-CHS.

Figure 12 shows ATTR and MTTR with Channel Hopping Protocols. As seen from this figure, A-CHS provides a better performance than other asynchronous CH protocols in terms of TTR (both ATTR and MTTR) for almost all values of N. So, A-CHS can be used to reduce the delay of MAC protocols for CR sensor network. S-CHS and M-QCH achieve shorter MTTR than SYNC-ETCH since S-CHS utilizes all available channels for rendezvous between two sequences, whereas SYNC-ETCH only utilizes a single point for rendezvous.

4.2. TTR Dependency on PU Arising [14]. The following example illustrates an assumption that SUs sense appearance of PU at channel 1 and then prohibit themselves from hopping

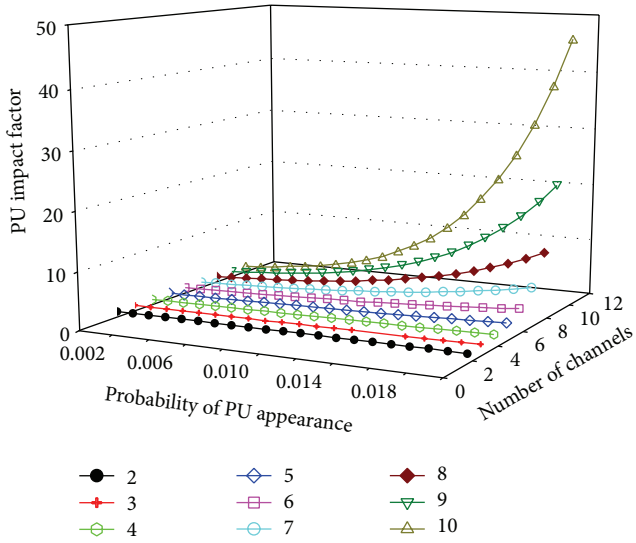

(a) PU impact factor with S-CHS (when N and p are varied)

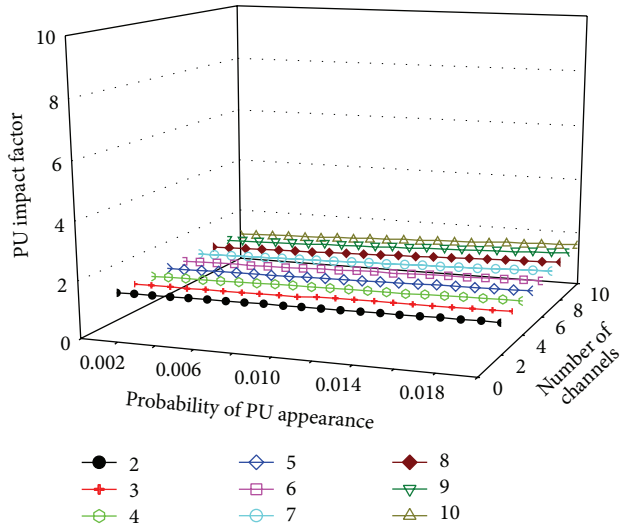

(b) PU impact factor with A-CHS (when N and p are varied)

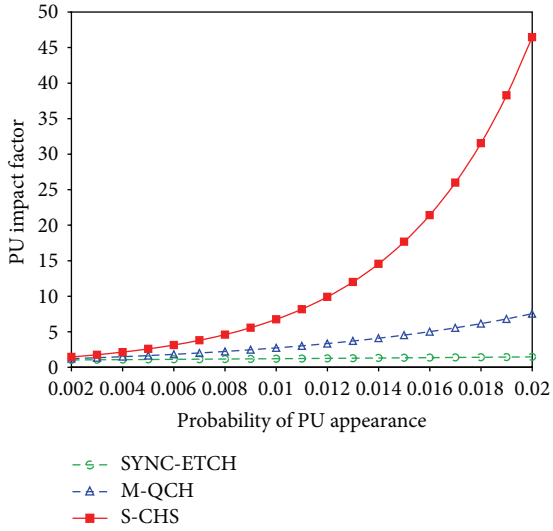

(c) PU impact factor with synchronous protocols (when $N = 10$)

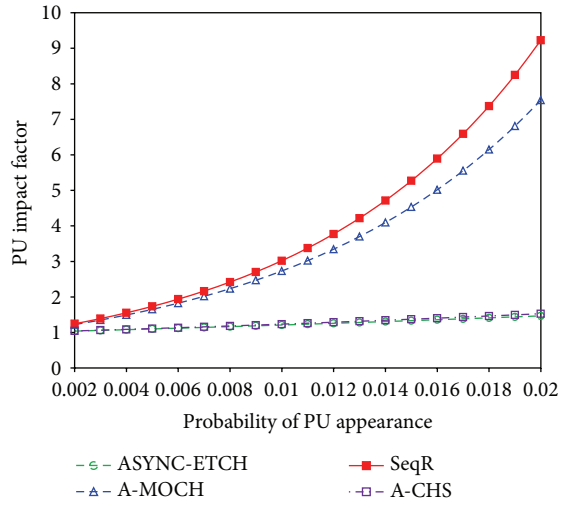

(d) PU impact factor with asynchronous protocols (when $N = 10$)

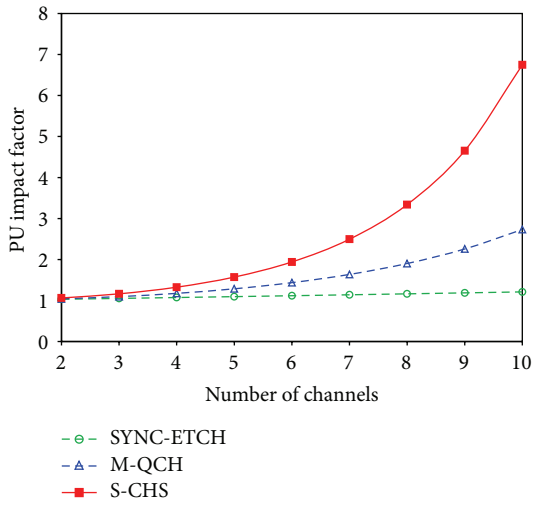

(e) PU impact factor with synchronous protocols (when $p = 0.01$)

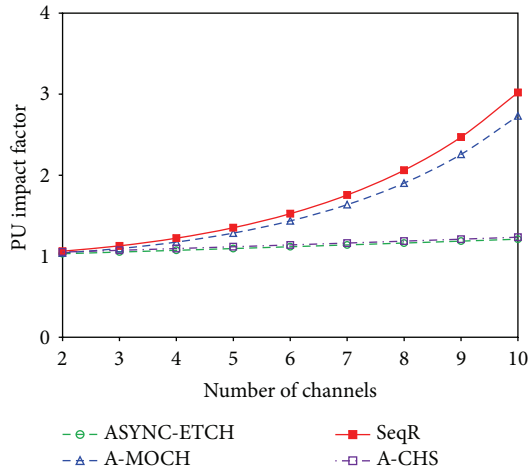

(f) PU impact factor with asynchronous protocols (when $p = 0.01$)

Figure 14: PU impact factor.

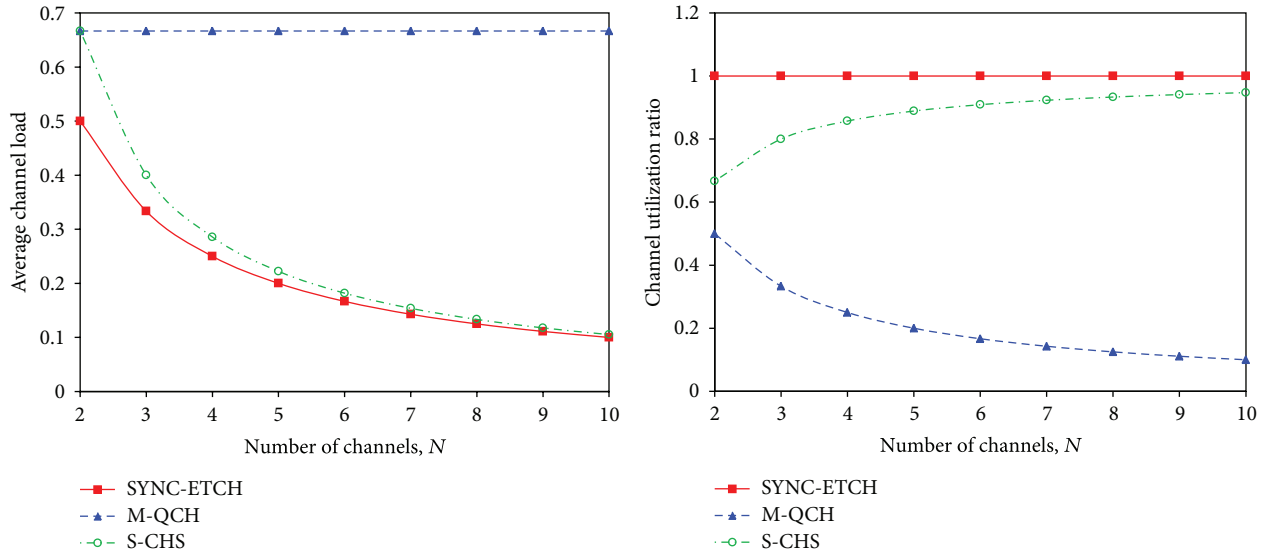

(a) Average channel load and utilization ratio with synchronous protocols

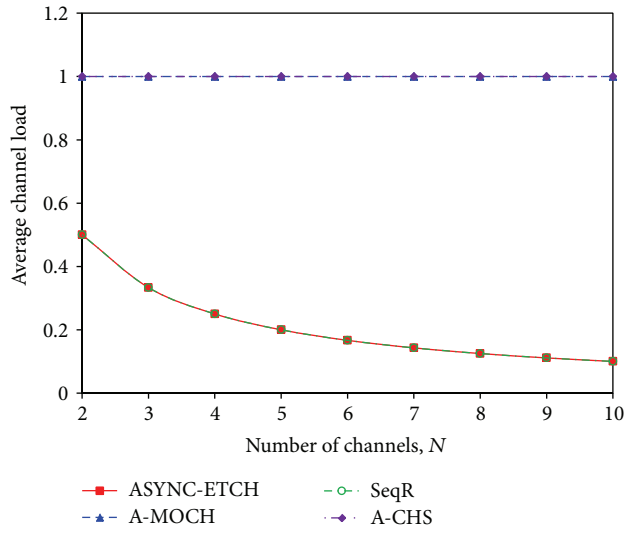

(b) Average channel load with asynchronous protocols

FIGURE 15: Average channel load and utilization ratio with the Channel Hopping Protocols.

at that channel until the PU leaves the channel. In Figure 13, the shadow part designates the interval when channel 1 is occupied by PU.

The occupation of a channel by PU highly affects the TTR of S-CHS and A-CHS since the channel is no more available for the rendezvous until the PU leaves the channel. For example, in Figure 13, the time to the next rendezvous will be doubled due to the occupancy of channel 1 by PU. In this case, ATTR is given by $(10 + 5)/2 = 7.5$.

More generally, assuming that p is the probability of a PU appears on a channel for a time slot T, then the probability that the PU will occupy this particular channel during the period is given by

$$P_{\mathrm{PU}} = 1 - (1 - p)^{T}, \tag{9}$$

where T refers to the time required for hopping a sequence [14].

As described earlier, the period of hopping sequence with S-CHS is $N(2N - 1)$. The average number of channels occupied by PU during a period of hopping sequence (denoted by M) will be

$$M = N \cdot P_{\mathrm{PU}} = N\left(1 - (1 - p)^{N(2N-1)}\right). \tag{10}$$

So, we get ATTR under impact of PU appearance by

$$\mathrm{ATTR}' = \frac{N}{N - M}\mathrm{ATTR}. \tag{11}$$

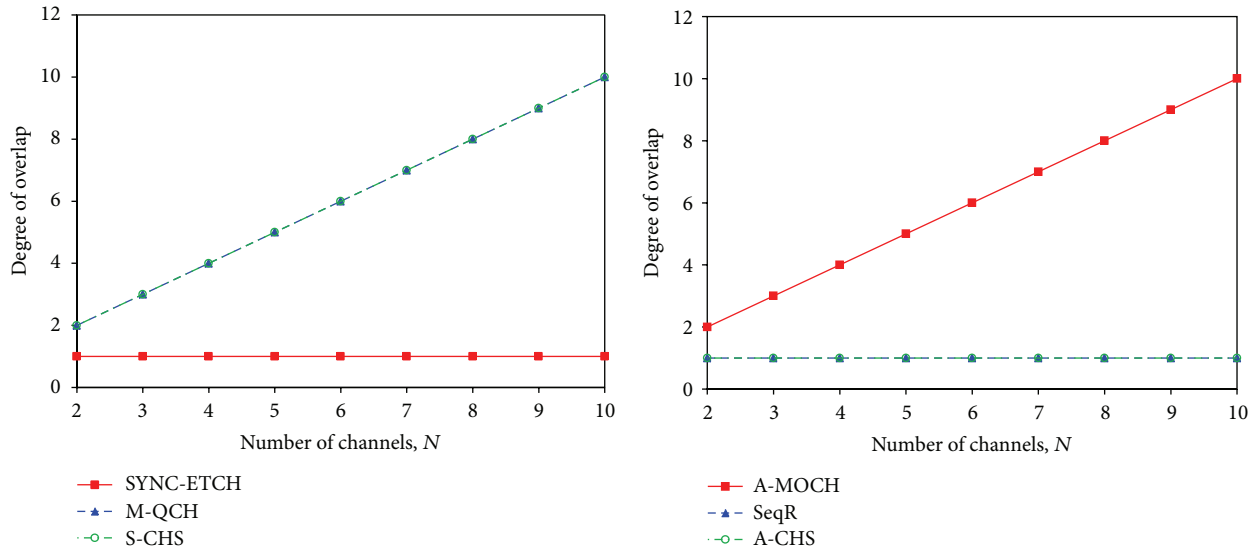

(a) Synchronous protocols (b) Asynchronous protocols

Figure 16: Degree of overlap with Channel Hopping Protocols.

Using (4) and (11), we can express the effect of PU appearance on ATTR performance by the following impact factor:

$$f = \frac{\text{ATTR}'}{\text{ATTR}} = \frac{N}{N-M} = \frac{1}{(1-p)^{N(2N-1)}}. \quad (12)$$

Similarly, considering that the length of hopping sequence in A-CHS is $2N + 1$, the impact factor in A-CHS is given by

$$f = \frac{\text{ATTR}'}{\text{ATTR}} = \frac{1}{(1-p)^{2N+1}}. \quad (13)$$

As seen in Figure 14, when the number of channels is small, the PU appearance does not cause a significant change in ATTR with S-CHS. But, for large N (more specifically $N > 7$), the PU appearance exponentially increases ATTR in S-CHS. In contrast, the A-CHS is not significantly affected by the appearance of PU regardless of the number of available channels. We can see that ATTR with A-CHS does not rise meaningfully for all values of N although the probability of PU appearance increases, and thus A-CHS shows a very stable performance in ATTR under the impact of PU appearance.

4.3. Channel Load and Utilization Performance. Channel load is defined as the average fraction of nodes that any two CR nodes rendezvous on the same channel. Channel utilization ratio means the ratio of the number of utilized rendezvous channels to the total number of available channels. A large value of channel utilization ratio indicates that more channels are used for rendezvous. Figure 15 supports this fact. We can that S-CHS outperforms M-QCH in terms of average channel load and the channel utilization as we expected in the theoretical analysis. We can see that channel utilization ratio is inversely proportional to the number of channels in SYNC-ETCH, ASYNC-TECH, and SeqR. This figure also indicates that S-CHS provides similar performance in terms of the channel load and channel utilization ratio. As previously described, rendezvous channels are evenly distributed over all channels in both S-CHS and M-QCH. As a result, S-CHS and M-QCH will be more susceptible for channel congestion problem. Different pairs of sender and receiver normally construct default as well as different alternative hopping sequences. Therefore, the rendezvous points of these hopping sequences are different and their convergence is very low in case of A-MOCH mechanism. In addition, in a given period, the rendezvous channels are not found with equal probabilities. Such unfair distributions may result in traffic load to a certain channels over the others.

4.4. Degree of Overlapping Performance. The overlapping or the intersection of two sequences in a hopping sequence period (counted by the number of time slots) is called degree of overlapping. Figure 16 shows that A-CHS, SYNC-ETCH, and SeqR are only overlapped at a single rendezvous point between any two given sequences. But, the degree of overlapping linearly increases as the number of available channels is increased in S-CHS, M-QCH, and A-MOCH.

4.5. Summary. The comparison in terms of five different metrics, that is, ATTR, degree of overlapping, average channel load, MTTR, and channel utilization, is shown in Table 2. N and p denote the number of available channels and the probability of PU's appearance on a channel in a time slot, respectively.

5. Conclusion

In this paper, we proposed two Channel Hopping Mechanisms to establish a control channel in CR sensor networks:

Table 2: Comparison of Channel Hopping Schemes.

CH protocols	ATTR	MTTR	PU impact factor	Average channel load	Channel utilization ratio	Degree of overlap
Synchronous CH						
SYNC-ETCH	$\frac{2N-1}{2}$	$4N-3$	$\frac{1}{(1-p)^{2N-1}}$	$\frac{1}{N}$	1	1
M-QCH	N/A	3	$\frac{1}{(1-p)^{N^2}}$	$\frac{2}{3}$	$\frac{1}{N}$	N
S-CHS	$2N-1$	$2N-1$	$\frac{1}{(1-p)^{N(2N-1)}}$	$\frac{1}{N-0.5}$	$\frac{N-1}{N-0.5}$	N
Asynchronous CH						
ASYNC-ETCH	$\frac{2N^2+N}{N-1}$	—	$\frac{1}{(1-p)^{2N-1}}$	$\frac{1}{N}$	N/A	At least 1
A-MOCH	N/A	N^2-N+1	$\frac{1}{(1-p)^{N^2}}$	1	N/A	N
SeqR	$\frac{N^2+N}{2}$	N^2+N	$\frac{1}{(1-p)^{N(N+1)}}$	$\frac{1}{N}$	N/A	1
A-CHS	$2N+1.5$	$3N+1$	$\frac{1}{(1-p)^{2N+1}}$	1	N/A	1

S-CHS and A-CHS. S-CHS performs connection establishment assuming global clock synchronization while A-CHS is based on the assumption that CR users start hopping at any time. Theoretical and simulation results showed that our schemes provide successful communication rendezvous within a bounded time interval. Moreover, A-CHS provides the best performance in terms of TTR, ant thus it can be used to reduce delay of MAC protocols. TTR performance with S-CHS is significantly affected by the appearance of PU as the number of available channels is increased whereas A-CHS shows a very stable performance in the ATTR under the effect of PU appearance although the number of channels is increased. S-CHS shows a very good performance in terms of average channel load and the channel utilization. The degree of overlapping linearly increases as the number of available channels is increased in S-CHS, whereas A-CHS is only overlapped at a single rendezvous point between any two given sequences.

Conflict of Interests

The authors declare that there is no conflict of interests regarding the publication of this paper.

Acknowledgments

This work was supported by the IT R&D Program of MSIP/KEIT (10041145, Self-Organized Software platform (SoSp) for Welfare Devices). This work was supported by the National Research Foundation of Korea (NRF) Grant funded by the Korean government (MSIP) (2011-0029034). This work was supported by the Brain Korea 21 Plus Program.

References

[1] D. Puccinelli and M. Haenggi, "Wireless sensor networks: applications and challenges of ubiquitous sensing," *IEEE Circuits and Systems Magazine*, vol. 5, no. 3, pp. 19–29, 2005.

[2] G. Zhou, J. A. Stankovic, and S. H. Son, "Crowded spectrum in wireless sensor networks," in *Proceedings of the EmNets*, Cambridge, Mass, USA, May 2006.

[3] O. B. Akan, O. B. Karli, and O. Ergul, "Cognitive radio sensor networks," *IEEE Network*, vol. 23, no. 4, pp. 34–40, 2009.

[4] N. ul Hasan, W. Ejaz, K. Manzoor, and H. S. Kim, "GSM: gateway selection mechanism for strengthening inter-cluster coordination in cognitive radio ad hoc networks," *EURASIP Journal on Wireless Communications and Networking*, vol. 2013, p. 171, 2013.

[5] S. Liu, L. Lazos, and M. Krunz, "Cluster-based control channel allocation in opportunistic cognitive radios networks," *IEEE Transaction on Mobile Computing*, vol. 11, no. 10, pp. 1436–1449, 2012.

[6] K. Bian, J.-M. Park, and R. Chen, "A quorum-based framework for establishing control channels in dynamic spectrum access networks," in *Proceedings of the 15th Annual ACM International Conference on Mobile Computing and Networking (MobiCom '09)*, pp. 25–36, New York, NY, USA, September 2009.

[7] T. Chen, H. Zhang, G. M. Maggio, and I. Chlamtac, "CogMesh: a cluster-based cognitive radio network," in *Proceedings of the 2nd IEEE International Symposium on New Frontiers in Dynamic Spectrum Access Networks*, pp. 168–178, Dublin, Ireland, April 2007.

[8] B. Hamdaoui and K. G. Shin, "OS-MAC: an efficient MAC protocol for spectrum-agile wireless networks," *IEEE Transactions on Mobile Computing*, vol. 7, no. 8, pp. 915–930, 2008.

[9] K. R. Chowdhury and I. F. Akyldiz, "OFDM-based common control channel design for cognitive radio Ad Hoc networks," *IEEE Transactions on Mobile Computing*, vol. 10, no. 2, pp. 228–238, 2011.

[10] K. Bian, J.-M. Park, and R. Chen, "Control channel establishment in cognitive radio networks using channel hopping," *IEEE Journal on Selected Areas in Communications*, vol. 29, no. 4, pp. 689–703, 2011.

[11] L. A. DaSilva and I. Guerreiro, "Sequence-based rendezvous for dynamic spectrum access," in *Proceedings of the 3rd IEEE Symposium on New Frontiers in Dynamic Spectrum Access Networks (DySPAN '08)*, pp. 440–446, Chicago, Ill, USA, October 2008.

[12] Y. Zhang, Q. Li, G. Yu, and B. Wang, "ETCH: efficient channel hopping for communication rendezvous in dynamic spectrum access networks," in *Proceedings of the IEEE INFOCOM*, pp. 2471–2479, Shanghai, China, April 2011.

[13] http://en.wikipedia.org/wiki/Cayley_table.

[14] J. H. Kim, G. S. Park, and K. J. Han, "A rendezvous scheme for self-organizing cognitive radio sensor networks," *International Journal of Distributed Sensor Networks*, vol. 2014, Article ID 315874, 10 pages, 2014.

Hindawi Publishing Corporation
International Journal of Distributed Sensor Networks
Volume 2014, Article ID 382414, 13 pages
http://dx.doi.org/10.1155/2014/382414

Research Article

Channel-Slot Aggregation Diversity Based Slot Reservation Scheme for Cognitive Radio Ad Hoc Networks

S. M. Kamruzzaman, Abdullah Alghamdi, Abdulhameed Alelaiwi, and Mohammad Mehedi Hassan

College of Computer and Information Sciences, King Saud University, P.O. Box 51178, Riyadh 11543, Saudi Arabia

Correspondence should be addressed to S. M. Kamruzzaman; smzaman@ksu.edu.sa

Received 7 September 2013; Revised 10 December 2013; Accepted 23 December 2013; Published 17 February 2014

Academic Editor: Najam ul Hasan

In cognitive radio (CR) ad hoc networks, spectrum efficiency and energy efficiency are vitally important because spectrum availability is opportunistic in nature and mobile CR nodes usually have limited energy. Aiming to improve network throughput along with improving spectrum and energy efficiencies, this paper proposes a channel-slot aggregation diversity based slot reservation (CADSR) scheme by which each CR node can utilize multiple slots in different channels simultaneously and efficiently utilize the power control mechanism with only a single CR transceiver. The proposed scheme dynamically assigns channel-slots to CR nodes using the diversity technique according to the topology density of the network and the bandwidth requirement, allowing CR nodes to join and leave the network at any time in a distributed way. A dynamic frame length expansion and shrinking scheme has also been introduced that improves the slot utilization. Extensive simulation results show that the proposed mechanism achieves significant performance improvement in network throughput, energy efficiency, and end-to-end delay.

1. Introduction

Cognitive radio (CR) technology has been proposed for improving the spectrum efficiency by allowing unlicensed users, referred to as CR users, to utilize dynamically the temporarily vacant spectrum of the licensed band assigned to primary users (PUs) without harmful interference or collisions to them [1]. In cognitive radio ad hoc networks (CRANs) there is no central controlling unit, while all the CR users are independent to join and leave the network at any time and, hence, a good coordination mechanism is required to allocate resources for smooth operation.

The uncertain availability of the radio spectrum imposes exceptional challenges in CRANs. The distributed multihop architecture, the dynamic network topology, and the spectrum availability varying in time and space domain are some of the critical factors [1, 2]. Due to these, CR users experienced the performance degradation by the activity of PUs. Since PU activity varies both in frequency and time domain, incorporating diversity technique in developing coordinating mechanism for CRANs can provide an effective solution in order to address this challenge.

In CRANs with multiple channels, channel aggregation (CA) has been proposed as an effective approach to improve the spectrum utilization. In CA, CR users are capable of aggregating multiple contiguous or noncontiguous channels that are unused by PUs to support high data rate services [3, 4]. IEEE 802.22 wireless regional area network (WRAN) standard supports CA technique to aggregate up to 3 contiguous TV channels to meet the high data rate requirements [5, 6].

In mobile ad hoc networks, energy conservation is of prime importance where nodes are battery powered with limited energy. A key challenge in such networks is how to prolong the lifetime of the networks. In order to lengthen the network lifetime and to improve the energy efficiency, energy-efficient scheme, which consumes less energy, is essential [7].

In CRANs, network throughput, spectrum efficiency, and energy efficiency are vital important performance measures. Naturally, the network throughput of wireless networks can

be improved by increasing the transmit power. However, in CRANs, it is not true and will degrade the spectrum and energy efficiencies. The mutual interference and packet collisions are unavoidable in CRANs due to distributed nature. In this network, if one node increases the transmit power, its neighbor nodes will suffer more serious interference and hence neighbor nodes can only transmit with lower rates, which will degrade the network throughput. Moreover, high transmit power will cause more packet collisions, which is harmful to the network throughput. In addition, when the throughput gain cannot match the power consumption, increasing transmit power will also cause the degradation of spectrum and energy efficiencies [8]. On the other hand, with low transmit power communication may fail due to short coverage range and spectrum resources will be underutilized. Thus, power control mechanism, which allows wireless nodes, to vary transmit power level to transmit packets, play important roles to improve the network performances in terms of network throughput, spectrum efficiency and energy efficiency.

Time division multiple access (TDMA) is a conventional wireless communication technique that has the ability to provide the collision-free packet transmission regardless of the traffic load. Each frequency band is divided into several timeslots. A set of such periodically repeating timeslots is known as the frame. Each node is assigned one or more timeslots in each frame, and the node transmits only in those slots. The TDMA approaches usually use the fixed number of timeslots in a frame. This works well for static networks. The primary drawback of such reservation-based TDMA schemes is that they waste the timeslots reserved for those nodes that have no packets to transmit [9]. However, in CRANs, some CR nodes may not have always messages to transmit. In such cases, the timeslots dedicated to them remain unused, which degrades the network performance. Moreover, since CR nodes are mobile, if a CR node moves out of its coverage range, its assigned slots will remain unused. Again, it should be allocated slot(s) in the frame being used in the new area where it moves. However, use of a fixed number of timeslots in a frame may not handle such situations effectively as there may be the shortage of timeslots.

For addressing all these issues and to achieve the aforementioned goals, in this paper, we propose a channel-slot aggregation diversity based slot reservation scheme, called CADSR, for cognitive radio ad hoc networks. The proposed diversity technique is based on the well-known software-defined radio that allows each node to simultaneously utilize a group of channel-slots with only one CR transceiver. Power control mechanism along with doze mode operation is adopted to improve the spectrum and energy efficiencies. Furthermore, the proposed method efficiently utilizes the channel bandwidth by assigning unused slots to new CR users and enlarging the frame length when the number of slots within the frame is insufficient to support the demand of neighboring CR users. An effective frame recovery method is also presented that shrinks the frame length in an efficient way.

The rest of the paper is organized as follows. Section 2 describes the related work. The system model is presented in Section 3. The proposed diversity based scheme is described in Section 4. We present the performance evaluation using computer simulation in Section 5, and finally in Section 6 we conclude the paper.

2. Related Work

In CRANs, medium access control (MAC) protocols are responsible for dynamically accessing the opportunistic channel for packet transmission. Designing an efficient MAC protocol for CR networks is a challenging issue. One of the most important targets in cognitive MAC protocol design is how to efficiently use available channels and limited power budget to increase the network throughput [2, 10, 11]. Many researchers suggested several ways of improving the spectral efficiency in CR networks to mitigate the spectrum scarcity crisis by balancing the underutilized license bands and overutilized unlicensed bands [12–14].

In CR networks, channel aggregation techniques have been proposed in many MAC protocols. A number of research works proposed recently on CA to improve spectrum utilization in CRNs can be found in [4, 15, 16]. Several CA strategies were proposed and analyzed in the literature, where CR users aggregate a constant or variable number of channels. In order to efficiently utilize available channel resources, which vary dynamically with time and locations, under limited power resources, we propose, in this paper, a diversity technology called channel-slot aggregation diversity.

There have been many studies for applying TDMA to ad hoc networks. However, most of them do not take into account the autonomous behaviors of the mobile nodes, and thus they cannot assign slots for new incoming nodes. Dynamic TDMA resource allocation concept emerged to overcome this drawback. Dynamic TDMA improves slot utilization of the scheme by dynamically deallocating unused slots and allocating new slots when necessary. Many TDMA based dynamic slot assignment schemes have been proposed for ad hoc networks [17–24].

The unifying slot assignment protocol (USAP) proposed in [17] considers the autonomous behaviors of new users and assigns a frame to each user. Each frame has a fixed number of slots. It reserves the first slot of each frame for signaling. It allows nodes to assign a slot dynamically using the reserved slot, but slot utilization is very low due to its fixed frame length. Moreover, when the network expands, the channel utilization becomes low due to a large number of unassigned slots. USAP multiple access (USAP-MA) proposed in [18] improves USAP by reducing the number of unassigned slots taking into account the number of users in the network topology. It utilizes an adaptive broadcast cycle to change the frame length and frame cycle dynamically. However, this method does not indicate when to change the frame length or how to select a slot to be assigned to a new user. Furthermore, the use of this method also wastes an excessive number of slots and results in lower channel utilization.

A dynamic TDMA slot assignment (DTSA) approach based on USAP has been proposed in [19]. This method

takes into account more autonomous behaviors of users in a multi-hop ad hoc network. However, the channel assignment method is still preplanned, where a slot is preassigned to each user. The preassigned slot is not released even when the user has no data to transmit. Therefore, it results in lower channel utilization. Furthermore, this approach cannot provide more slots when a user requires them to deal with burst traffic.

An evolutionary-dynamic TDMA slot assignment protocol (E-DTSAP) for ad hoc networks has been proposed in [20]. According to the topology density of the network and the bandwidth requirement, the E-DTSAP protocol changes the frame length and the transmission schedule dynamically. Moreover, it allows the transmitter to reserve one or more unscheduled slots from the set of unassigned slots in its neighborhood by coordinating the announcement and confirmation with the neighboring users up to two hops away. However, this protocol is for single channel and mobility of nodes is not considered in this proposal. Moreover, a dynamic frame length expansion and recovery method, called dynamic frame length channel assignment (DFLCA), has been proposed in [21]. This strategy is designed to make better use of the available channels by taking advantage of the spatial reuse concept. However, this scheme is also designed for single channel network.

A self-stabilizing TDMA (STDMA) scheme was proposed in [22], where the slots are divided in a hierarchical manner. First, blocks of timeslots in a frame are divided among the cluster heads of the clusters. Cluster heads then assign their allocated timeslots among the member nodes. Doing so, this approach prevents the possible interferences among the transmissions of nodes in different clusters. However, the STDMA approach uses a fixed number of timeslots and hence may fall in shortage of slots when the number of member nodes increases. It may not make efficient use of unused slots too, causing unwanted delay in the network.

A fast dynamic slot assignment scheme, called F-DSA, is proposed in [23] to reduce timeslot access delay for a newly arrived node in ad hoc networks. F-DSA simplifies the slot assignment process by using minislots to share control packet for short periods. However, overhead in this scheme is high. An adaptive TDMA slot assignment protocol (ATSA) is proposed in [24] for vehicular ad hoc networks. ATSA divides different sets of timeslots according to vehicles moving in opposite directions. When a node accesses the networks, it chooses a frame length and competes with a slot based on its direction and location to communication with the other nodes.

We have proposed a dynamic slot reservation scheme based on channel-slot aggregation diversity technique for cognitive radio mobile ad hoc networks. Proposed CADSR scheme successfully overcomes the shortcomings of the other existing mechanisms (a preliminary version of this scheme can be found in [25]), where each node is allowed to simultaneously utilize a group of channel-slots with only one CR transceiver. In this scheme power control mechanism along with doze mode operation is adopted to further improve the spectrum and energy efficiencies. Furthermore, the frame length is dynamically enlarging and shortening based on the number of nodes and the traffic demand. The proposed method works in such a way that it minimizes the contentions, the number of packet losses, and the queuing delay, which ensures very good network performance.

3. System Model

We consider an energy-constrained CR ad hoc network comprised of N CR nodes (users). Suppose that CRAN contains one common control channel (CCC) and L orthogonal frequency data channels (indexed by $1, 2, \ldots, L$). The CCC with central frequency f_0 belongs to the CR service provider [26, 27], which is basically used to exchange control packets. The data channels with central frequencies $\{f_1, \ldots, f_L\}$ are licensed to PUs and exploited opportunistically by CR users. A summary of various symbols and variables used in this paper is shown as follows.

Summary of various symbols and variables:

A_e^t, A_e^r: the efficient areas of the transmitter and receiver antennas

c: the speed of light

a_l: average activity factor of each channel

f: channel frequency

d: distance between the transmitter and the receiver

g_{UV}^0: the control channel power gain of the node pairs U, V

$G_t(f), G_r(f)$: The gains of the transmitter and receiver antennas

h_t, h_r: heights of the transmitter and receiver antennas

j: common available channel

K: system loss factor

L: number of channels

(l, t): communication segment with l channel and t timeslot

$\mathrm{LUS}_{l,t}$: segment state for the segment with l channel and t timeslot

M: number of primary users (PUs)

N: number of CR users

$P_{\mathrm{inf}}(l)$: received interference

$P_{\mathrm{min}}^{\mathrm{inf}}$: the maximum tolerable interference power

$P_{\mathrm{max}-u}(l)$: maximal allowed transmit power

P_{max}: maximum transmit power

P_r^{ATIM}: the received power of the ATIM packet

$P_r^U(V)$: the received power at node V from node U

P_t^U: the transmission power of node U

Q: number of packets

R: transmission rate

$\mathrm{SINR}_{\mathrm{th}}$: threshold for signal to interference plus noise ratio

T: number of timeslots

α: the path loss coefficient

$Z_l(t)$: the activity states of l channels at time t.

We assume that PUs randomly choose channels from the channel pool for their data transmissions and usage of each channel is modeled as an independent and identically distributed renewal process with ON (or active) and OFF (or idle) states. In ON state, PU is active (present) and the channel cannot be used by CR users. On the other hand, in OFF state, PU is inactive (absent) and CR users can utilize the channels without causing any harmful interference to PUs. The activity sates of l channels at time t in any location within the area are given as

$$Z_l(t) = \begin{cases} 1, & \text{if channel } l \text{ is ON at } t,\ l \in L, \\ 0, & \text{otherwise.} \end{cases} \quad (1)$$

Let the duration of ON and OFF states for l channels be exponentially distributed with the mean $1/\lambda_l$ and $1/\mu_l$. Thus, we can characterize the average activity factor of each channel as

$$a_l = \frac{\mu_l}{\lambda_l + \mu_l}. \quad (2)$$

The probability that the lth channel is not being used by PU is $1 - a_l$.

The number and the locations of the PUs are considered unknown to the CR users. A link can be made between two CR users, if there exists one or more common channel available to both users. We assume that all CR users are equipped with a single half-duplex CR transceiver, which consists of a reconfigurable transceiver and a scanner. The CR transceiver is based on the software-defined radio so that it can realize channel-slot aggregation, which allows the CR users to use multiple channels with different transmit power simultaneously.

For accessing a channel, a CR user must sense channels first and can access the channels only if any of these L channels is not being used by PUs. Any efficient spectrum sensing scheme proposed in the literature can be used to detect the locally available channels. As we mainly focus on designing how CR users efficiently access and utilize limited spectrum resources to improve the performance of CRANs, such as throughput, spectrum efficiency, and energy efficiency, we assume that CR users can obtain reliable sensing results at the end of the sensing period.

In the CR network, a total number of L channels are shared by PUs and CR users. Every PU occupies only one channel while a CR user may aggregate multiple channels by channel-slot aggregation technique. We assume that the arrivals of PUs and CR users are subject to independent Poisson distributions with arrival rates λ_p and λ_c, respectively.

We consider that CR node exchanges control packets with maximum power $P_{\max}$ and transmit data as well as acknowledgement (ACK) packet on controlled power. A radio signal can be correctly decoded by the intended receiver only if the signal to interference plus noise ratio (SINR) is above a certain hardware-dependent threshold, SINR_{th}. The higher value of SINR ensures that more packets can be transmitted reliably. Depending on the modulation scheme, different threshold values of SINR_{th} are valid. The radio propagation model between two nodes follows the two-ray ground reflection model [2, 28]. If we consider that nodes U and V indicate the sender and receiver, respectively, then the received power at node V from node U is given by

$$P_r^U(V) = P_t^U G_t(f) G_r(f) \frac{h_t^2 h_r^2}{d^\alpha K}, \quad (3)$$

where P_t^U is the transmission power of node U, $G_t(f)$ and $G_r(f)$ denote the gains of the transmitter and receiver antennas, respectively, d is the distance between the transmitter and receiver, K is the system loss factor, h_t and h_r are the heights of the transmitter and receiver antennas, respectively, and α is the path loss coefficient with range of 2–4. According to [28], the gains of the transmitter and receiver antennas can be written as

$$G_t(f) = \frac{4\pi A_e^t f^2}{c^2}, \qquad G_r(f) = \frac{4\pi A_e^r f^2}{c^2}, \quad (4)$$

where A_e^t and A_e^r represent the efficient areas of the transmitter and receiver antennas, c is the speed of light, and f is the carrier center frequency.

4. Proposed CADSR Scheme

The channel access mechanism of the proposed channel-slot aggregation diversity based slot reservation (CADSR) scheme is shown in Figure 1. The system time is divided into frames. A frame consists of a sensing window, an ad hoc traffic indication messages (ATIM) window, and a communication widow. The synchronization of the CR users is done with the help of periodic beaconing. In sensing window (sensing phase), every CR user carries out channel sensing to get the spectrum opportunity. In ATIM window (reservation phase), all CR users tune their radio interfaces to the control channel (CH_0) and transmit/receive control packets for resource reservation. It is noted that during ATIM window only the control channel is used. Control packets exchanging is based on a kind of CSMA/CA protocol. In communication window (data transmission phase), CR users transmit/receive their traffic by using all $L + 1$ channels (CH_0–CH_L). The communication window is time slotted. A timeslot consists of the data (packet) transmission time, the corresponding ACK transmission time, and the guard times. The guard time includes the propagation delay and the transition time from transmitting mode to receiving mode.

We assume that CR users are synchronized by a periodic beacon signal, so that all nodes begin their beacon interval at the same time. Whenever a CR user wants to join in a network, it first listens to beacon signal for at least one frame interval on the control channel to synchronize itself with that network. If it does not hear any beacon signal in that period, it starts sending periodic beacon signal assuming itself to be

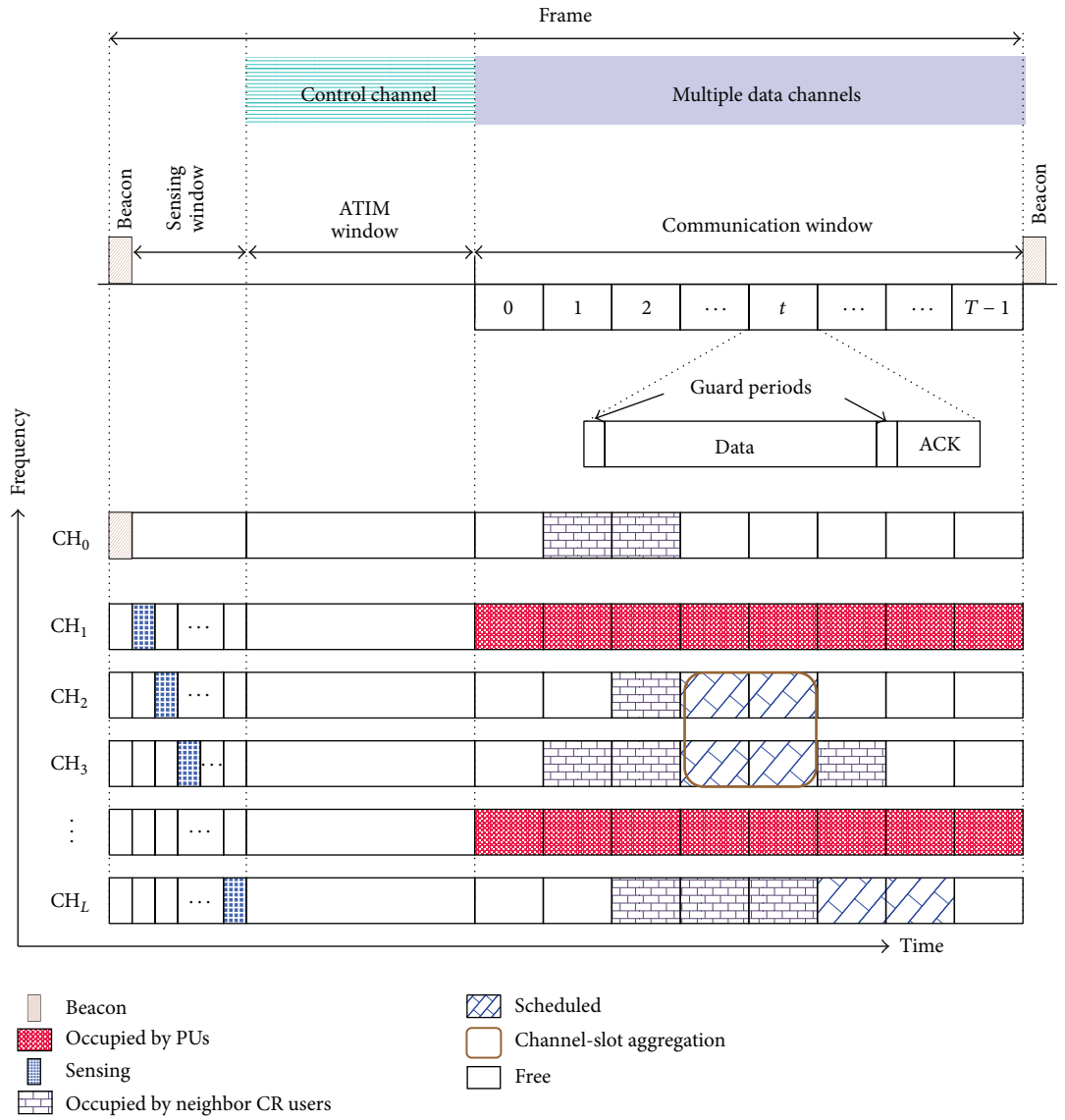

Figure 1: Frame structure and channel access mechanism of the proposed CADSR scheme for CR ad hoc networks.

the first node in the network. The beacon signal is carrying the local time of a node. Similar to the timer synchronization function (TSF) of the IEEE 802.11 MAC protocol [29], a node only updates its time if the time carried in a received beacon signal is faster than its own local time.

A channel-slot pair is defined as the "communication segment". The communication segment (we can say segment later on for simplicity) for timeslot t ($t = 0, 1, \ldots, T-1$) on channel l is denoted by the pair (l, t). A communication segment can be in one of the following three states (see Figure 1).

(i) Occupied: the segment is being used by other transmissions (PUs or other CR users).

(ii) Free: the segment is unassigned and idle.

(iii) Scheduled: the segment is selected by the source-destination pair for packet transmission in a particular link. This state might become the occupied state after a confirmation process.

A PU randomly selects the channel; therefore, a PU can choose an unused channel or the channel occupied by a CR user. However, a CR user randomly selects the channel from among those which are free from PU activities. A forced termination occurs whenever a PU preempts a CR user. Force termination depends on the number of users and the number of remaining channels. If there are fewer channels than required, CR users will be blocked whenever they arrive. However, PU will be blocked only when all the channels are fully used by other PUs. If channel handovers are allowed, a preempted CR user will immediately move to an unused

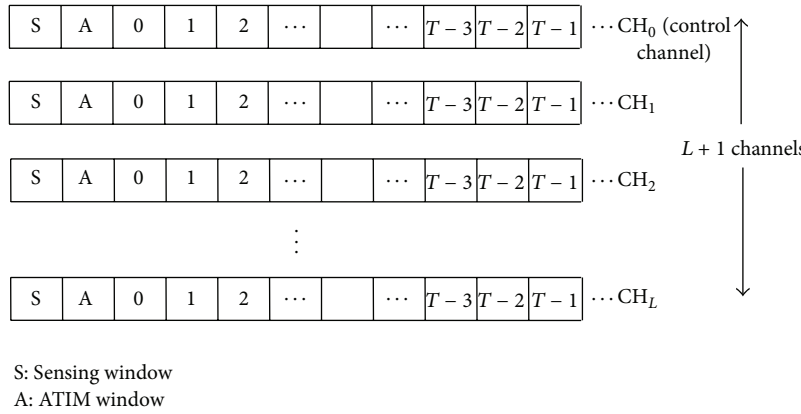

Figure 2: Frame format of the proposed CADSR scheme.

channel. Hence, a forced termination occurs in case there is no channel to handover.

4.1. Frame Structure. The frame of the proposed CADSR scheme has three parts: a sensing window, an ad hoc traffic indication messages (ATIM) window, and a communication widow. As CADSR scheme follows slotted mechanism, clock synchronization is needed among CR users, which is done with the help of periodic beaconing. Sensing part is using to get the spectrum opportunity through spectrum sensing. ATIM part is used for resource reservation through exchanging control packets. Finally, CR users exchange their data packets by using reserved segments in the communication part. Communication window is time slotted with T slots in each frame, which is dynamically adjusted when the frame does not have enough channel-slots to support new neighboring connections or there are too many empty channel-slots. The proposed scheme controls the expansion and recovery of unassigned channel-slots by dynamically changing the frame length according to the traffic load and the number of CR users in the contention area. Here, the contention area is defined for each CR user as the set of CR users that can cause collisions by sending packets to another, that is, CR users within two hops away from the host. The detailed frame and slot structures of the scheme are shown in Figures 1 and 2.

4.2. Channel-Slot Aggregation Diversity. Diversity technique has been widely used in wireless ad hoc networks to improve the network throughput. There are three main diversity techniques available in the literature: channel diversity, link diversity, and multiradio diversity, respectively, that can efficiently improve the network throughput [30–32]. However, some drawbacks in these diversity techniques prevent the network throughput from being further improved. In particular, channel diversity and link diversity only use one channel for packet transmissions, and thus they cannot sufficiently utilize available channel resources. Although multi-radio diversity can use multiple channels simultaneously, mobile nodes need to be equipped with multiple radios, which will increase the implementation cost and power consumption.

The goal of this paper is to develop an efficient scheme to improve the network performances in terms of throughput, spectrum efficiency and energy efficiency, for energy-constraint CRANs. In order to achieve this goal, we adopted channel aggregation technique in time-slotted channel access mechanism, which we termed as channel-slot aggregation, and propose a diversity technique, called channel-slot aggregation diversity. The proposed diversity technique allows CR node to select a group of channels from multiple available channels, which are free from PUs activity, and allocate the upper-bounded transmit power for the selected channels based on the channel qualities and suffered interferences. The CR node then can use the CA technology to utilize the selected group of channels simultaneously and reserve multiple slots based on the traffic demand for data transmission and transmit multiple data packets during one transmission process. Compared with the existing diversity schemes, our proposed channel-slot aggregation diversity based slot reservation scheme can efficiently utilize multiple channel-slots simultaneously with limited energy, which can improve the network performance and reduce the implementation cost as well as the power consumption.

4.3. Operation of the CADSR Scheme. In the CADSR scheme, each node maintains one data structure named list of usage segment (LUS), which will be dynamically updated in order to maximize each node's throughput subject to the ongoing transmissions of other CR nodes cannot be interfered. The LUS records six entries for each channel: (i) "Channel Index l"; (ii) "Frame Length"; (iii) "PU Status"; (iv) "Neighbor Status"; (v) "Received Interference $P_{\text{inf}}(l)$"; and (vi) "Maximal Allowed Transmit Power $P_{\max-u}(l)$". "PU Status" represents whether the lth channel is occupied by PUs and "Neighbor Status" shows the information of the segment used by neighbor CR users.

Traffic is indicated with three-way handshakes. Nodes that have packets to transmit indicate traffic by sending ATIM packets on the control channel in the ATIM window. For transmitting packets, a CR user should first reserve segments. The segment reservation is achieved by exchanging control packets between the sender and the receiver. The control

packet exchange mechanism is based on a kind of CSMA/CA protocol. There are three control packets, namely ATIM, ATIM-ACK, and ATIM-RES, that are used for segment reservation. After successful three-way handshakes, a group of segments and transmission rate can be determined. Then, the source and destination node pair can finish their data transmissions on the selected segments. The transmission process of the control message exchange is described as follows, where U and V represent the source and destination node.

(1) Sending ATIM Packet. U first overhears on the CCC. If the CCC is busy, then U chooses a back-off time and defers its transmission. Otherwise, if the CCC is idle for a duration of one distributed inter-frame space (DIFS) after the backoff time, an ATIM packet that contains the LUS of U will be sent to V.

(2) Sending ATIM-ACK Packet. If V successfully receives the ATIM packet, then it compares its LUS with that of U by performing an OR operation to generate a combined LUS for the link between nodes U and V. If common available channels exist that can be used by the node pairs, the channel power gain of the node pairs on the CCC is represented by g_{UV}^0 and will be determined as

$$g_{UV}^0 = \frac{P_r^{\text{ATIM}}}{P_{\max}}, \tag{5}$$

where P_r^{ATIM} is the received power of the ATIM packet and $P_{\max}$ denotes the maximum transmit power, which was considered for exchanging all control packets. We suppose that all control packets are transmitted with $P_{\max}$. Now, from (3) and (4), the channel power gain of a given channel with the central frequency f between nodes U and V, denoted by $g_{UV}(f)$, can be expressed as

$$\begin{aligned} g_{UV}(f) &= G_t(f)\, G_r(f)\, \frac{h_t^2 h_r^2}{{d_{UV}}^{\alpha} K} \\ &= \frac{16\pi^2 h_t^2 h_r^2 f^4 A_e^t A_e^r}{{d_{UV}}^4 K c^2}, \end{aligned} \tag{6}$$

where d_{UV} is the distance between U and V and we consider the path loss coefficient $\alpha = 4$. Now, consider that there are J common available channels with central frequencies $\{f_1, \ldots, f_J\}$ between U and V. From (5) and (6), the channel gain of the jth common available channel, denoted by g_{UV}^j, can be calculated by

$$g_{UV}^j = g_{UV}^0 \left(\frac{f_0}{f_j}\right)^4, \quad j = 1, 2, \ldots, J. \tag{7}$$

Then V performs the power and channel-slot assignment and determines the number of data packets that can be transmitted in the following transmission process according to the traffic demand. Finally, an ATIM-ACK packet is sent to U, which contains the above information.

(3) Sending ATIM-RES Packet. If node U successfully receives the ATIM-ACK packet, then an ATIM-RES packet that contains the same information with the ATIM-ACK packet is sent to node V. The purposes of sending the ATIM-RES packet are twofold: it can be used to confirm the successful reception of the ATIM-ACK packet and it can also notify the neighbor nodes of U to update the information recorded in their LUSs.

(4) Transmitting Data Packets. After exchanging control packets, U and V switch to the corresponding channels and finish their packet transmission according to the power and segment allocated for them. During the data transmission phase, a CR user, which has successfully reserved a (group of) specific timeslot on a (group of) specific channel to send or receive a packet, first switches to the decided channel and transmits or waits for the data packet in that slot(s). If a user receives a unicast packet, it sends back an ACK in the same timeslot. A CR user that does not send (or receive) a data packet in a specific timeslot can go to doze mode for power saving. If the source node does not receive ACK, it will consider the packet transmission unsuccessful. When a packet transmission is unsuccessful, the packet can be retransmitted after random backoff time. If the number of retransmissions exceeds the predefined limit, the packet is dropped.

(5) Overhearing of ATIM-ACK or ATIM-RES Packets. CR nodes that overheard ATIM-ACK or ATIM-RES packets need to update their LUSs. Suppose node pairs U and V will transmit Q packets with the transmission rate R, and the power allocations are $\{P_{UV}^1, \ldots, P_{UV}^J\}$. If node Y overhears the ATIM-ACK (ATIM-RES) packet sent by $V(U)$, node Y first computes the channel gains $g_{YV}^0(g_{YU}^0)$ and $\{g_{YV}^1, \ldots, g_{YV}^J\}(\{g_{YU}^1, \ldots, g_{YU}^J\})$. Then for each channel j ($j = 1, \ldots, J$), node Y computes the interference caused by the ATIM-ACK (ATIM-RES) packets sent by node $V(U)$ and updates the total interference according to

$$\begin{aligned} P_{\text{inf}}^Y(j) &= P_{UV}^j g_{YV(U)}^j, \\ P_{\text{inf}}(j) &= P_{\text{inf}}(j) + P_{\text{inf}}^Y(j), \end{aligned} \tag{8}$$

where $P_{\text{inf}}^Y(j)$ is the received interference power on the jth channel caused by the ATIM-ACK (ATIM-RES) packet transmission of node $V(U)$, P_{UV}^j represents the transmit power of node $V(U)$ on the jth channel, and $g_{YV(U)}^j$ denotes the channel gain of the jth channel between nodes Y and $V(U)$. Then, the maximum allowed transmit power of node Y on the jth channel, denoted by $P_{\max-u}(j)$, can be expressed as

$$P_{\max-u}(j) = \frac{P_{\min}^{\text{inf}}}{g_{YV(U)}^j}, \quad j = 1, 2, \ldots, J, \tag{9}$$

(1) w listens to the LUS transmitted from other CR users in its contention area.
(2) w sets its frame length as the maximum frame length among its neighbors.
(3) w updates its LUS information by listening to the LUS transmitted from its neighbors.
(4) **if** $\forall l \forall t \in [0, L]\ [0, T-1]$, a group of (l, t) segments are assigned in the frame that will be used by node pairs using channel-slot aggregation diversity technique.
(5) **if** there is no free channel-slot **then**
(6) m = the CR user using the highest number of slots among the neighbors of w.
(7) **if** m is using more than one channel-slot **then**
(8) w requests m to release one channel-slot.
(9) **else**
(10) w doubles its frame length, and the copies information from the former frame to the latter part of the doubled frame and using the empty channel-slot created.
(11) **end if**
(12) **end if**
(13) **end if**

Algorithm 1: Selection of channel-slot by a CR user, w.

where $P_{\min}^{\inf}$ is the maximum interference power that neighbor CR nodes can tolerate.

4.4. Dynamic Channel-Slot Assignment. We have developed an efficient scheme for dynamic channel-slot assignment for CRANs. Our proposed scheme controls the number of unassigned slots by dynamically changing the frame length according to the traffic loads and the number of CR users in the contention area. When a new CR user detects a conflict, it solves the conflict by listening and collecting assigned channel-slot information of the CR users in the contention area. Our proposed scheme improves the channel spatial reuse and maximizes the network throughput. The channel-slots assignment of CADSR scheme is performed according to Algorithm 1.

Let us consider the (communication) segment, that is, channel-slot pair (l, t), assignment for the link between an upstream (source-side) node A and a downstream (destination-side) node B. If node A wants to send a set of packets to node B, node A first sends an ATIM packet to node B containing its LUS and the number of packets it wants to send. After receiving the ATIM packet, node B compares its own states of LUS with that of A and identifies the segments free from the viewpoints of both nodes. If there are sufficient free segments, node B selects the required number of segments for allowing them to aggregate through channel-slot aggregation diversity technique and marks their states as Scheduled. In addition, node B sends the identification of selected segments to node A by using ATIM-ACK packet to node A.

The neighboring nodes of node B update their states by overhearing the ATIM-ACK message and obtain the current segment usage information. After receiving the ATIM-ACK packet from node B, node A updates its states based on the selected segments and changes the segment states from Scheduled to Occupied. Finally node A sends an ATIM-RES packet containing the same list of selected segments to node B. By overhearing the ATIM-RES packet, neighboring nodes of node A update their states to obtain the current segment usage information.

4.5. Frame Recovery. A limitation in most of the slot allocation protocol is that the frame length, set as a power of 2, may expand very quickly when there are many users in the network. Some nodes may be disconnected from the network for a number of reasons such as turning their radio transceiver off, energy exhaustion, and moving away. In order to handle this situation the proposed scheme treated a node to be "disconnected" if it is not exchanging any message for a number of contiguous frames. When many connections end their transmissions and corresponding slots are released, some users in the network are likely to contain long frames with many unused slots.

The frame recovery method in the CADSR scheme improves the efficiency of the frame. When a channel-slot in the frame is released after not receiving anything for a duration of time, the CR user checks its channel-slots assignment information to see if half or more of the slots in the frame are unreserved. If this situation occurs, the CR user immediately releases the unused slots. Then, it sends a request control packet for frame recovery to the neighbors. The neighbors try to assign slots for it after they receive this type of request packet, and they confirm the accepted request made by the recovery requesting CR user. Then, they send a response control packet to their neighbors notifying them of their update. This method significantly increases the frame efficiency. The frame recovery of CADSR scheme is performed according to Algorithm 2.

5. Performance Evaluation

The effectiveness of the proposed CADSR scheme is validated through simulations. This section describes the simulation environment, performance metrics, and experimental results. To evaluate CADSR scheme, we developed a packet-level

(1) **if** the number of unused slots > frame length/2 **then**
(2) w sends a request packet for frame recovery to its neighbors.
(3) The receiving neighboring CR users try to update their channel-slots information and reschedule the channel-slots they were using previously.
(4) The neighboring CR users send a confirmation packet.

Algorithm 2: Frame recovery by a CR user, w.

discrete-event simulator written in C++ programming language, which implements the features of the protocol stack described in this paper. We have evaluated the performance of the CADSR scheme in comparison with T-MAC [27] and F-DSA [23].

5.1. Simulation Setting. We consider a circular area with radius of 500 m. There are M stationary PUs being distributed uniformly within the circle. The PUs operate on L channels according to their own multichannel protocol. The details of PU operation are beyond the scope of this paper. We just model the PU activity as an ON/OFF process. A PU in ON state occupies a channel and it does not use any channel in OFF state. The ON and OFF durations of a PU are exponentially distributed with the mean of 100 s, respectively (i.e., the activity factor is 0.5), unless noted otherwise. A newly activated PU randomly chooses a channel among channels that are not used by other PUs. The sensing range of a PU is set to 250 m. An active PU is assumed to be perfectly detected by a CR user within the sensing range. Moreover, it is also assumed that the CR user being out of sensing range does not disturb the active PU. Thus, all CR users in the sensing range of an active PU cannot exploit the channel occupied by the PU. When a PU activates newly on a channel, the CR users exploiting the channel switch the communication segments on the channel to other free segments. This channel switching delay is set to 80 μs. The summary of simulation parameters is listed in Table 1 whereas Table 2 shows the various timings of the MAC frame usage in the simulation.

The CR network is composed of 100 users (denoted by N), unless noted otherwise. In a simulation run, their initial locations are uniformly distributed within the circle. An example of random deployment scenario of PUs and CR users is shown in Figure 3. A CR user moves to a random direction selected in $[0, 2\pi]$, with a speed distributed uniformly in [0, 10] km/h. The moving speed and the direction of a CR user are updated after a random duration distributed in [0, 10] s. When a CR user reaches the boundary of the circular area, it is bounced in. The CR network utilizes one dedicated control channel as well as L channels (licensed to PU) for data transmission. Each CR node supports three different data rates, which are 2, 4, and 8 Mbps, respectively. The corresponding transmission ranges are 250, 200, and 100 m, respectively. Data rate supported by CCC is 2 Mbps. Assume that frame length is dynamically changing with 4, 8, 16, or 32 slots in communication window and the duration of each slot is 4.25 ms, which is calculated for a 1000-byte packet

Table 1: Summary of simulation parameters.

Parameters	Nominal values
Terrain size	Circular with radius 500 m
Number of mobile CR nodes (N)	100
Number of PUs (M)	10
Initial placement of nodes	Random (uniformly distributed)
Number of channels ($L + 1$)	4, 8, 12
Data rates	2, 4, and 8 Mbps
Transmission range	250, 200, and 100 m
ON and OFF duration of a PU	Exp. Dist. with the mean of 100 s, respectively (activity factor is 0.5)
PU sensing range	250 m
Channel switching delay	80 μs
Mobility model	Random walk
Pause time	0 s (a highly dynamic scenario)
$SINR_{th}$ (control packet exch.)	−28 dB
SNR_{th} (data communication)	−25 dB
Data packet size	1000 bytes
Control packet (ATIM, ATIM-ACK, ATIM-RES, etc.) size	112 bytes
ACK size	100 bits
Simulation time	600 s

Table 2: Various timings of the MAC frame.

Parameters	Values
Frame length	28 ms, 45 ms, 79 ms, 147 ms
Communication window	17 ms, 34 ms, 68 ms, 136 ms
Number of timeslots in communication window	4, 8, 16, 32
Timeslot duration	4.25 ms
ATIM window	5.5 ms
Sensing window	3 ms
Beacon period	2.5 ms
SIFS duration	10 μs
DIFS duration	50 μs

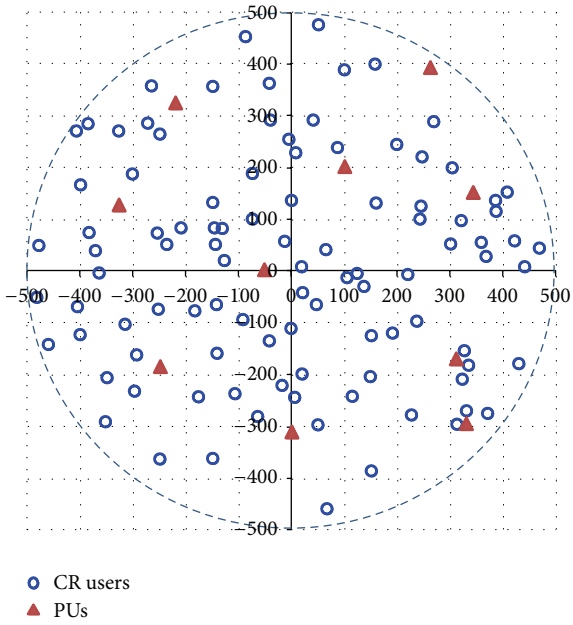

Figure 3: Example of random deployment scenario: 100 CR users and 10 PUs within a circular area with a radius of 500 m.

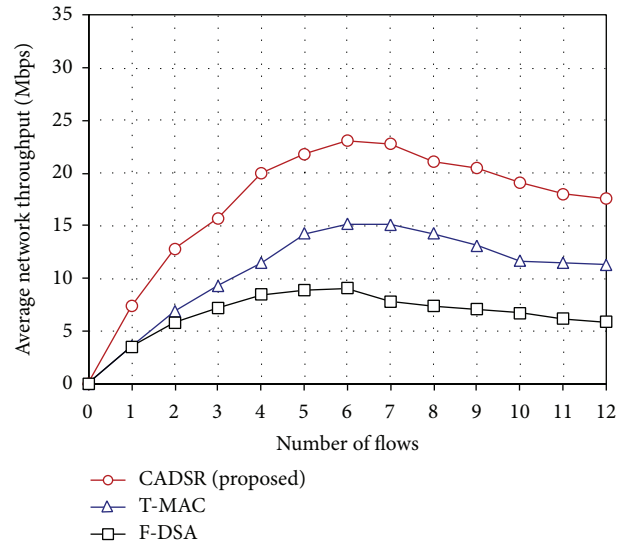

Figure 4: Comparison of average network throughput of CADSR scheme with other protocols.

to be sent through the channel of data rate 2 Mbps. We vary the number of channels from 4 to 12 among them; one channel is CCC and the others are data channels. Based on our simulation experience, we set the beacon period to 2.5 ms and the sensing window is 3 ms. Length of the ATIM window is 5.5 ms. Moreover, the durations of SIFS and DIFS are 10 μs and 50 μs, respectively.

The maximum transmission power of a CR user is set to 100 mW. We consider the path loss and shadowing as the propagation model. The channel gain is calculated by $\gamma \times d^{-4}$, where d is the distance between the transmitter and the receiver, and the constant γ is set to -66.08 dB. The shadowing effect is modeled as a log normal shadowing with zero mean and standard deviation 5 dB. The thermal noise power is set to −103 dBm. Furthermore, the minimum required SINR for control packet exchange is set to −28 dB and the minimum required SNR for data communication is set to −25 dB. If the received SINR or SNR of a packet is higher than the minimum required value, the packet is assumed to be decoded correctly. The retransmission of erroneous packets is tried at maximum three times. The simulation time of each run corresponds to 600 s in reality. Each data point on the graphs is obtained by averaging the results from 10 simulation runs with random initial positioning of PUs and CR users.

5.2. Performance Metrics. The following performance metrics are used to evaluate the proposed scheme.

(i) *Network Throughput.* It is the total number of successfully received bits per second by all destinations in the CRANs.

(ii) *Average End-to-End Packet Delay.* It is average latency incurred by the data packets between their generation time and their arrival time at the destinations.

(iii) *Energy Efficiency.* It is the total number of bits transmitted per unit of power consumption. The larger the value is, the more efficient the transmit power is.

(iv) *Blocking Probability of CR Users.* It is the probability of blocking CR users by PUs whenever they arrive because of the insufficient spectrum resources.

5.3. Simulation Results. Figure 4 shows the comparison results of the network throughput of CADSR scheme with other protocols as a function of the number of flows. We can see that, when the number of flows increases, CADSR offers significantly better performance than all other protocols. When the network is saturated, CADSR achieves about 52% more throughput than T-MAC and about 154% more than F-DSA protocol. The main reason of the higher throughput is that the CADSR scheme uses the channel-slot aggregation diversity technique, which can help CR nodes efficiently and sufficiently utilize available resources opportunistically for data transmissions. Moreover, the appropriate number of channel-slots that the CR nodes use and the corresponding power allocations can be dynamically adjusted by the proposed power and channel-slot allocation scheme. Moreover, CADSR scheme dynamically adjusted the frame length when needed and can efficiently increase the data transmission rate and thus improve the average network throughput. Furthermore, because of the power control mechanism of our proposed scheme, the mutual interference among neighbor CR nodes is reduced and the channel spatial reuse efficiency is improved, which are also promoting the improvement of the network throughput.

Figure 5(a) presents the comparison of average end-to-end packet delay of the protocols by varying the number of flows. When network load increases, there are many requests for slot allocation; our proposed CADSR scheme dynamically enlarges the frame size to accommodate more CR users'

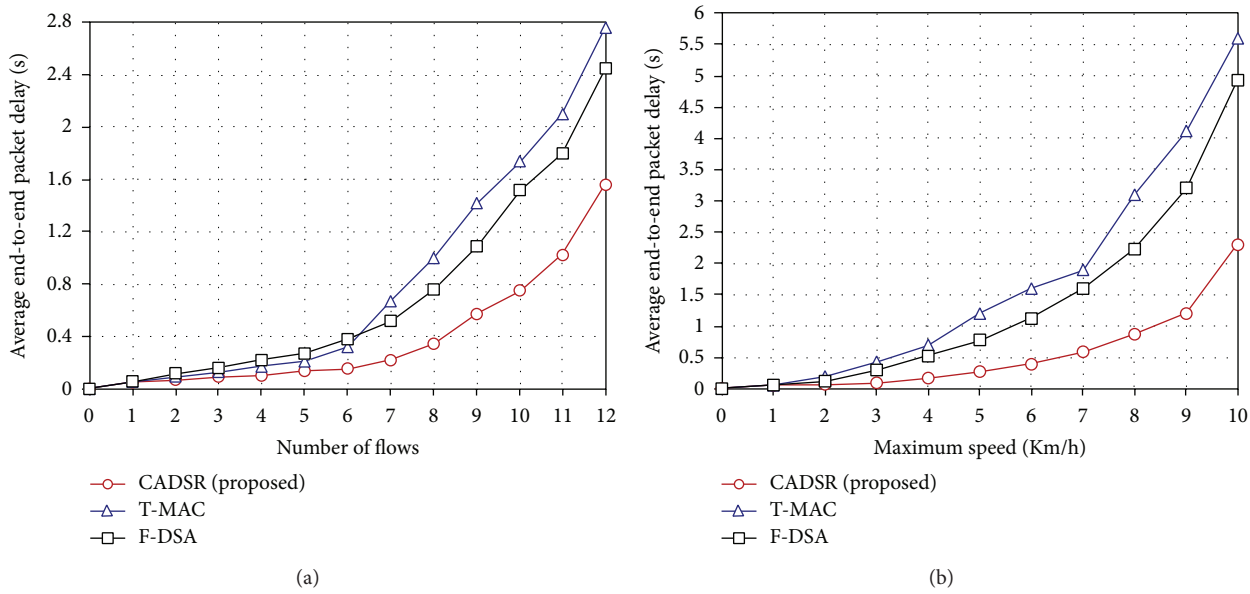

Figure 5: (a) Comparison of average end-to-end delay of CADSR scheme with other protocols as a function of the number of flows. (b) Comparison of average end-to-end delay of CADSR scheme with other protocols as a function of the maximum speed.

request. CADSR assigns contention-free multiple channel-slots to CR users that achieve higher throughput and lower delay as well. When the load increases, queuing delay is raised. The queuing delay makes the performance of each protocol worse. However, the data traffic is split into multiple channel-slots in the case of CADSR scheme. Therefore, the average end-to-end packet transmission delay of CADSR is increased slowly according to the increment of the number of flows.

Figure 5(b) shows that the average end-to-end packet delay increases by the increase of speeds of the mobile CR nodes. However, the proposed CADSR scheme faces significantly lower delay as compared to other protocols.

Figure 6 shows the comparison of average network energy efficiency of CADSR scheme with other protocols in terms of the number of flows. From this plot, we can observe that the network energy efficiency of the proposed CADSR scheme outperforms the other protocols, although the energy efficiency of our proposed scheme reduces when the number of flows is larger than six. The reason of the improvement of energy efficiency in the proposed scheme is because of the utilization of diversity technique along with multiple power control mechanisms. With this proposed approach, multiple channel-slots can be sufficiently utilized with appropriate data transmission rate. Moreover, mutual interference among CR neighbor nodes can be restrained. Furthermore, adapting doze mode operation is also promoted to improve energy efficiency.

Figure 7 shows the blocking probability of CR users in terms of the arrival rate of PUs. From this figure, we can observe that blocking probability of CR users is increasing with the increasing value of arrival rate of PUs, which is justified. When the arrival rate of PUs is high, more channels are used by PUs and remaining resources for CR users are

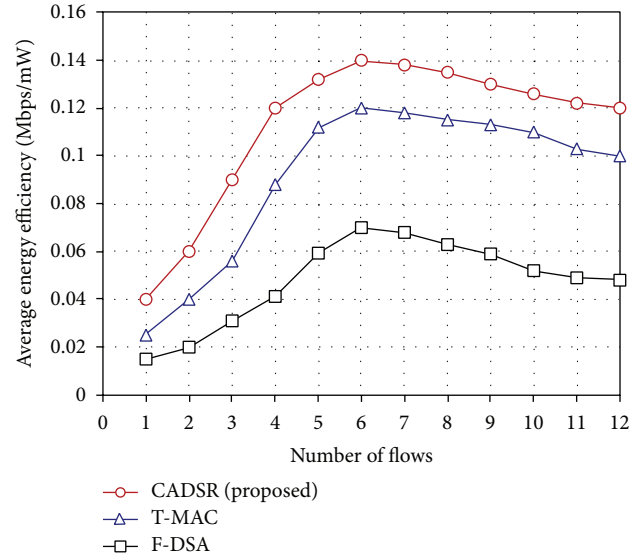

Figure 6: Comparison of average network energy efficiency of CADSR scheme with other protocols.

getting low and, consequently, blocking probability is getting high. The effect of the tolerance level, $e(< 1)$, which adjusts the number of channels reserved for future arrival users is also shown in this figure. As the value of e increases, the blocking probability decreases because the system reserves more resources (channel-slots) with the larger value of e.

Figure 8 shows the impact of channel-slot aggregation on network throughput. From this figure, it has been observed that network throughput is increasing when the number of channel-slot aggregation is getting high. However, the rate of

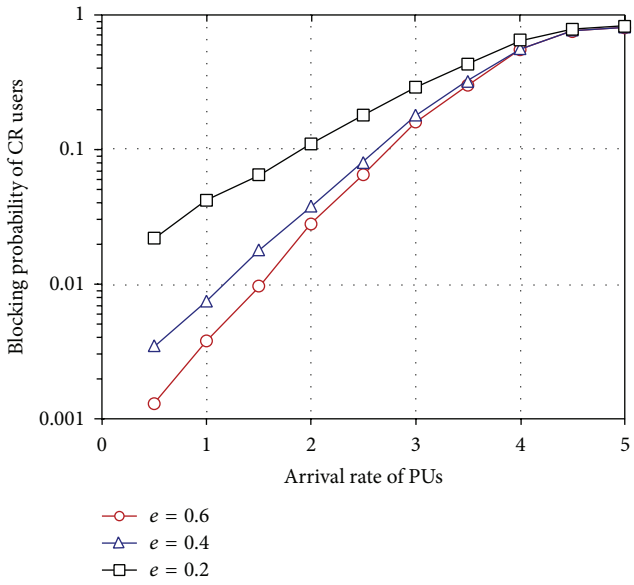

Figure 7: Blocking probability of CR users in terms of arrival rate of PUs.

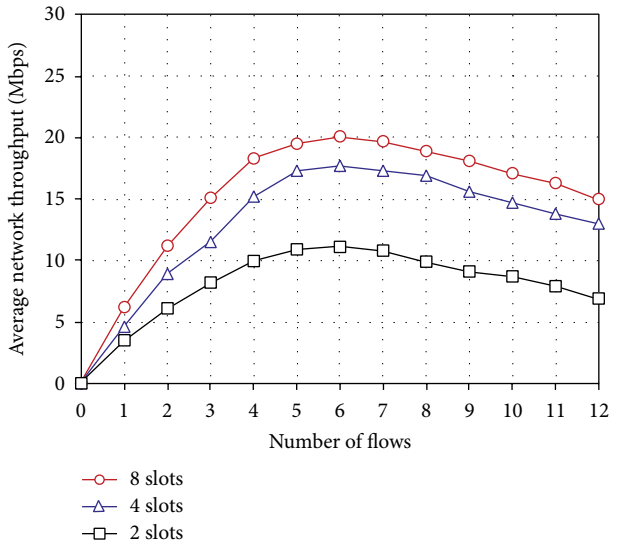

Figure 8: Impact of channel-slot aggregation on network throughput.

increasing is not the same. For example, the throughput of the 4-slot case is about 60% higher than 2-slot case. On the other hand, the throughput of the 8-slot case is only about 14% higher than the 4-slot case. This is because of the impact of PUs and the shortage of available resources, which is insufficient to aggregate the required number of channel-slots.

6. Conclusion

In this paper, we have proposed a channel-slot aggregation diversity based slot reservation scheme, called CADSR, for cognitive radio ad hoc networks. The proposed scheme can change the frame length and the transmission schedule dynamically according to the number of CR users and the bandwidth requirement for the contention area. This method utilizes the channel-slots in an efficient way through the proposed diversity technique and thus increases the channel utilization. Our scheme can effectively assign slots to CR users when a CR user joins and leaves the network. When a connection is released in the network, the frames in many of the CR users may contain a large number of unassigned slots. In such cases, our frame recovery method decreases the amount of unused slots by allowing the CR users to release the unused slots and shrink their frames.

CADSR scheme can efficiently increase the data transmission rate and thus improve the average network throughput. The proposed scheme achieves aggressive energy savings through multiple power saving mechanisms that give higher-energy efficiency. Moreover, because of the power control mechanism of our proposed scheme, the mutual interference among neighbor CR nodes is reduced and the channel spatial reuse efficiency is improved, which are also promoting the improvement of the network throughput, energy efficiency, and spectrum efficiency. Furthermore, through the dynamic frame size and the efficient allocation of channel-slots, CADSR shows low end-to-end packet delay. Extensive simulations confirm the efficiency of the CADSR scheme compared to other protocols and demonstrate its capability to provide high throughput, low end-to-end delay, and high energy efficiency.

In this study, we have considered the fixed length of ATIM window in reservation phase that may limit the channel utilization. The frame length (including the ATIM window) can be dynamically adjusted with smart window size adjusted rule. In future, CADSR scheme can be extended with dynamic ATIM window along with dynamic communication window based upon the network traffic load to achieve higher system throughput. Furthermore, we have considered a single CRAN exploiting the spectrum of PU opportunistically. However, two or more CRANs can simultaneously use a spectrum. The slot reservation problem for the coexistence environment of multiple CRANs can be another future research issue.

Conflict of Interests

The authors declare that there is no conflict of interests regarding the publication of this paper.

Acknowledgment

The authors would like to extend their sincere appreciation to the Deanship of Scientific Research at King Saud University for its funding of this research through the Research Group Project no. RGP-VPP-281.

References

[1] I. F. Akyildiz, W. Y. Lee, and K. R. Chowdhury, "CRAHNs: cognitive radio ad hoc networks," *Ad Hoc Networks*, vol. 7, no. 5, pp. 810–836, 2009.

[2] A. D. Domenico, E. Calvanese Strinati, and M.-G. di Benedetto, "A survey on MAC strategies for cognitive radio networks," *IEEE Communications Surveys and Tutorials*, vol. 14, no. 1, pp. 21–44, 2012.

[3] C. Cordeiro, K. Challapali, D. Birru, and N. S. Shankar, "IEEE 802.22: the first worldwide wireless standard based on cognitive radios," in *Proceedings of the IEEE International Symposium on New Frontiers in Dynamic Spectrum Access Networks (DySPAN '05)*, pp. 328–337, Baltimore, Md, USA, November 2005.

[4] L. Li, W. Zhangy, S. Zhang, M. Zhao, and W. Zhou, "Energy-efficient channel aggregation in cognitive radio networks with imperfect sensing," in *Proceedings of the IEEE Wireless Communications and Networking Conference (WCNC '13)*, pp. 2810–2822, Shanghai, China, April 2013.

[5] IEEE P202.22 Draft Standard for Wireless Regional Area Networks: Channel Bonding versus Channel Aggregation.

[6] IEEE P202.22 Draft Standard for Wireless Regional Area Networks: Channel Aggregation Summary.

[7] S. M. Kamruzzaman, E. Kim, D. G. Jeong, and W. S. Jeon, "Energy-aware routing protocol for cognitive radio ad hoc networks," *IET Communications*, vol. 6, no. 14, pp. 2159–2168, 2012.

[8] S. Sorooshyari, C. W. Tan, and M. Chiang, "Power control for cognitive radio networks: axioms, algorithms, and analysis," *IEEE/ACM Transactions on Networking*, vol. 20, no. 3, pp. 878–891, 2012.

[9] S. Kumar, V. S. Raghavan, and J. Deng, "Medium access control protocols for ad hoc wireless networks: a survey," *Ad Hoc Networks*, vol. 4, no. 3, pp. 326–358, 2006.

[10] C. Cormio and K. R. Chowdhury, "A survey on MAC protocols for cognitive radio networks," *Ad Hoc Networks*, vol. 7, no. 7, pp. 1315–1329, 2009.

[11] G. P. Joshi, S. Y. Nam, and S. W. Kim, "Decentralized predictive MAC protocol for ad hoc cognitive radio networks," *Wireless Personal Communications*, vol. 74, no. 2, pp. 803–821, 2014.

[12] Z. M. Liu, N. Nasser, and H. S. Hassanein, "Intelligent spectrum assignment and migration in cognitive radio network," *EURASIP Journal on Wireless Communications and Networking*, vol. 2013, no. 200, 2013.

[13] S. Aslam and K.-G. Lee, "CSPA: channel selection and parameter adaptation scheme based on genetic algorithm for cognitive radio ad hoc networks," *EURASIP Journal on Wireless Communications and Networking*, vol. 2012, no. 349, 2012.

[14] S. Aslam, A. Shahid, and K.-G. Lee, "Joint sensor-node selection and channel allocation scheme for cognitive radio sensor networks," *Journal of Internet Technology*, vol. 14, no. 3, pp. 453–466, 2013.

[15] M. H. Rehmani, S. Lohier, and A. Rachedi, "Channel bonding in cognitive radio wireless sensor networks," in *Proceedings of the International Conference on Selected Topics in Mobile and Wireless Networking (iCOST '12)*, pp. 72–76, Avignon, France, July 2012.

[16] L. Jiao, V. Pla, and F. Y. Li, "Analysis on channel bonding/aggregation for multi-channel cognitive radio networks," in *Proceedings of the European Wireless Conference (EW '10)*, pp. 468–474, Lucca, Italy, April 2010.

[17] C. D. Young, "USAP: a unifying dynamic distributed multichannel TDMA slot assignment protocol," in *Proceedings of the IEEE Military Communications Conference (MILCOM '96)*, pp. 235–239, Washington, DC, USA, October 1996.

[18] C. D. Young, "USAP multiple access: dynamic resource allocation for mobile multihop multichannel wireless networking," in *Proceedings of the IEEE Military Communications Conference (MILCOM '99)*, pp. 271–275, Atlantic City, NJ, USA, November 1999.

[19] A. Kanzaki, T. Uemukai, T. Hara, and S. Nishio, "Dynamic TDMA slot assignment in ad hoc networks," in *Proceedings of the IEEE International Conference on Advanced Information Networking and Applications (AINA '03)*, pp. 330–335, Xi'an, China, March 2003.

[20] W. Li, J.-B. Wei, and S. Wang, "An evolutionary-dynamic TDMA slot assignment protocol for ad hoc networks," in *Proceedings of the IEEE Wireless Communications and Networking Conference (WCNC '07)*, pp. 138–142, Hong Kong, March 2007.

[21] C.-M. Wu, "Dynamic frame length channel assignment in wireless multihop ad hoc networks," *Computer Communications*, vol. 30, no. 18, pp. 3832–3840, 2007.

[22] B. Bruhadeshwar, K. Kothapalli, and I. R. Pulla, "A fully dynamic and self-stabilizing TDMA scheme for wireless ad-hoc networks," in *Proceedings of the IEEE International Conference on Advanced Information Networking and Applications (AINA '10)*, pp. 511–518, Perth, Australia, April 2010.

[23] J. K. Lee, K. M. Lee, and J. S. Lim, "Distributed dynamic slot assignment scheme for fast broadcast transmission in tactical ad hoc networks," in *Proceedings of the IEEE Military Communications Conference (MILCOM '12)*, pp. 1–6, Orlando, Fla, USA, October 2012.

[24] Y. Wei-dong, L. Pan, L. Yan, and Z. Hong-song, "Adaptive TDMA slot assignment protocol for vehicular ad-hoc networks," *The Journal of China Universities of Posts and Telecommunications*, vol. 20, no. 1, pp. 11–18, 2013.

[25] S. M. Kamruzzaman and M. S. Alam, "Dynamic TDMA slot reservation protocol for cognitive radio ad hoc networks," in *Proceedings of the IEEE International Conference on Computer and Information Technology (ICCIT '10)*, pp. 142–147, Dhaka, Bangladesh, December 2010.

[26] M. Timmers, S. Pollin, and A. Dejonghe, "A distributed multichannel MAC protocol for multihop cognitive radio networks," *IEEE Transactions on Vehicular Technology*, vol. 59, no. 1, pp. 446–459, 2010.

[27] Y. Wang, P. Ren, and G. Wu, "A throughput-aimed MAC protocol with QoS provision for cognitive ad hoc networks," *IEICE Transactions on Communications*, vol. E93-B, no. 6, pp. 1426–1429, 2010.

[28] T. S. Rappaport, *Wireless Communications: Principles and Practices*, Prentice Hall, Upper Saddle River, NJ, USA, 2nd edition, 2002.

[29] IEEE 802.11, IEEE standard for wireless LAN medium access control (MAC) and physical layer (PHY) specifications (revised), 2007.

[30] A. Sabharwal, A. Khoshnevis, and E. Knightly, "Opportunistic spectral usage: bounds and a multi-band CSMA/CA protocol," *IEEE/ACM Transactions on Networking*, vol. 15, no. 3, pp. 533–545, 2007.

[31] J. Wang, H. Zhai, Y. Fang, J. M. Shea, and D. Wu, "OMAR: utilizing multiuser diversity in wireless ad hoc networks," *IEEE Transactions on Mobile Computing*, vol. 5, no. 12, pp. 1764–1778, 2006.

[32] F. Chen, H. Zhai, and Y. Fang, "An opportunistic multiradio MAC protocol in multirate wireless ad hoc networks," *IEEE Transactions on Wireless Communications*, vol. 8, no. 5, pp. 2642–2651, 2009.

Hindawi Publishing Corporation
International Journal of Distributed Sensor Networks
Volume 2014, Article ID 315874, 10 pages
http://dx.doi.org/10.1155/2014/315874

Research Article

A Rendezvous Scheme for Self-Organizing Cognitive Radio Sensor Networks

Junhyung Kim, Gisu Park, and Kijun Han

School of Computer Science and Engineering, Kyungpook National University, Daegu 702-701, Republic of Korea

Correspondence should be addressed to Junhyung Kim; jhkim@netopia.knu.ac.kr

Received 4 October 2013; Revised 14 December 2013; Accepted 19 December 2013; Published 30 January 2014

Academic Editor: Waleed Ejaz

Two or more nodes need to establish a link on an available channel in a cognitive radio (CR) sensor network when they want to transmit data. Rendezvous is the process by which the nodes explore the available channels to establish a link when they want to communicate with each other. The method of finding a common channel is a challenging problem. A dedicated common control channel simplifies the rendezvous process, but it may create a single point of failure. In this paper, we propose a hopping sequence algorithm to provide an effective method to implement a rendezvous without relying on a dedicated control channel. Our scheme achieves a successful rendezvous within a single period in a CR sensor network. Analytical and simulation results show that our proposed scheme outperforms the existing schemes in terms of time to rendezvous, fairness, degree of overlapping, and the effect by primary user appearance.

1. Introduction

Wireless sensor networks (WSNs) have been used in many applications, including home automation, personal health care, and surveillance [1]. They usually utilize the license-exempt industrial, scientific, and medical (ISM) band, but the ISM band is very crowded, since many other communication systems are already operating on it [2, 3]. The concept of self-organization is used to manage resources and guarantee users quality of service with communication networks like ad hoc and sensor networks [4]. It does not require any central coordination to establish a link. Instead, the nodes on the link interact directly with each other. As a solution to overcome the lack of available radio spectrum for wireless sensor networks, the cognitive radio (CR) technology can be considered [5]. A cognitive radio sensor network senses event signals and collaboratively transmits data dynamically over available spectrum bands in a multihop manner to ultimately satisfy application-specific requirements [5]. The communication architecture of a cognitive radio sensor network with self-organization is illustrated in Figure 1.

In CR sensor networks, CR users are secondary users (SUs) that coexist with primary users (PUs), and they continuously sense the radio environment for vacant frequency bands. When two nodes want to communicate with each other, they must exchange a control message on an unoccupied channel in CR sensor networks. Two nodes rendezvous on an available common channel to enable reliable exchange of control messages. Two nodes access a common channel for a certain period of time that is sufficiently long to establish a reliable link; this is referred to as rendezvous [4–6].

In recent years, many works have addressed the rendezvous problem and have tried to simplify it in different ways. The study of rendezvous problems categorize the existing solutions into two major groups based on their operations [7]. These are required and can be achieved by either a centralized approach using a dedicated control channel as a common control channel (CCC) or a distributed approach without using a CCC [7].

The use of a dedicated control channel (or CCC) simplifies the rendezvous process, as well as other medium access issues. However, a dedicated control channel has a number of important disadvantages. A dedicated control channel may become a bottleneck or may create a single point of failure. In addition, the dynamically changing availability of spectrum may make it impossible to maintain a dedicated control channel [8]. The availability of any one channel cannot be guaranteed in a CR network, because SUs must vacate any

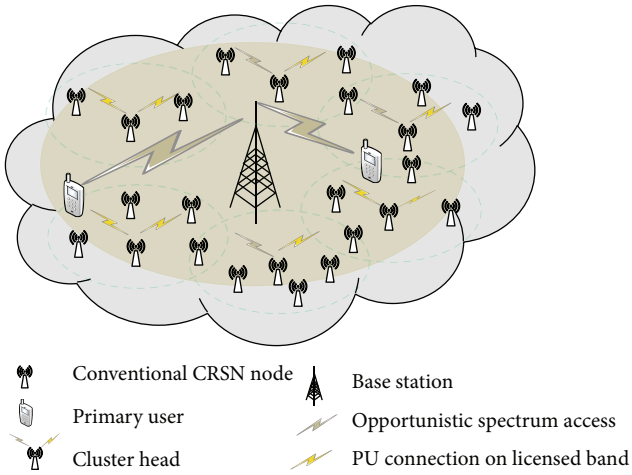

Figure 1: Cognitive radio sensor network with self-organization.

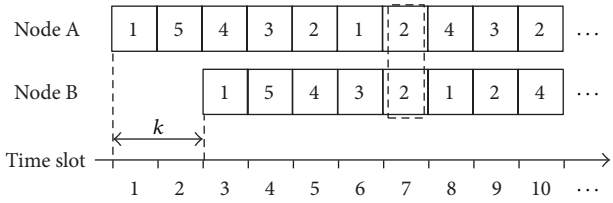

Figure 2: Rendezvous system model.

channel as soon as incumbent signals appear in the channel, thus making it impossible to guarantee the availability of the CCC [9].

We focus on a distributed approach where each node visits all channels in a redefined order using a sequence to guarantee successful rendezvous if there is an available channel. This can provide an effective method to implement a rendezvous without relying on a dedicated control channel. In this paper, we propose a hopping sequence algorithm to achieve a successful rendezvous within a single period in a CR network. With the proposed algorithm, called a hopping sequence guaranteeing rendezvous within a single period (HS-GRSP), CR nodes can rendezvous in a single period and reliably exchange control messages with each other.

2. Background and Related Works

2.1. Background. Figure 2 shows a model for the rendezvous of two nodes in a CR sensor network. For the rendezvous, node A starts first, and node B starts k slots later than node A (i.e., the time lag is k). Assuming that time slots of the sequence are synchronized, two nodes can visit the same channel using the sequence S simultaneously. In Figure 2, two nodes can successfully rendezvous at the seventh time slot.

2.2. Related Works

2.2.1. Quorum-Based Asynchronous Maximum Overlapping Channel Hopping (A-MOCH). The quorum-based scheme was proposed for CCC establishment in CR networks [10].

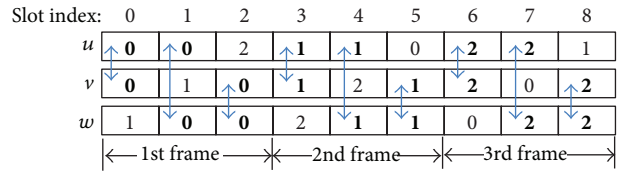

Figure 3: Quorum-based CH system [10].

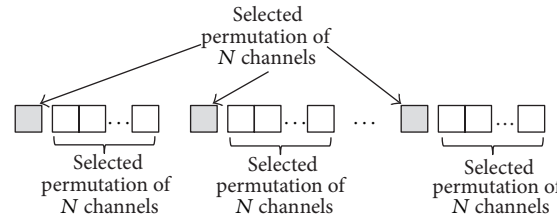

Figure 4: Building a sequence for sequence-based rendezvous [11].

The channel hopping sequence (CHS) is constructed from quorum systems which satisfy the intersection property and increase the degree of overlap between sequences. The A-MOCH system assumes at least one commonly available channel utilizing the rotation closure property of quorum systems to enable at least one rendezvous in N^2 time slots, where N is the total number of channels.

In an A-MOCH system, the pairwise rendezvous over N channels may occur during the last N time slots of a CH period, and thus the maximum time to rendezvous (MTTR) equals $N^2 - N + 1$. If a PU returns to the CCC used for the rendezvous, all quorum-based CH systems (Figure 3) simply replace the CCC with a randomly selected available channel to avoid interfering with the PU. While this may increase the time to rendezvous (TTR) by a factor of N for synchronous quorum systems, it preserves the desired properties of quorum systems in the hopping sequences.

2.2.2. Sequence-Based Rendezvous. Sequence-based rendezvous (SBR) [11] is an asynchronous CH system in which CR users construct nonorthogonal CHS's by using a permutation of available channels. The sequence is built as illustrated in Figure 4. The rendezvous sequence is made from a combination of permutations. The first step in building such a rendezvous sequence is to select a permutation of N channels (there are $N!$ such permutations). The selected permutation is interspersed with each element in the selected permutation. Therefore the selected permutation appears $(N + 1)$ times in the rendezvous sequence. For example, if we select $\{1, 3, 2\}$ as a permutation when $N = 3$, the rendezvous sequence will be $\{1, 1, 3, 2, 3, 1, 3, 2, 2, 1, 3, 2\}$. The sequence generated by the SBR scheme in a CR network with N channels has a period of $N(N + 1)$ slots. The expected TTR is $N^2 + N$, and the maximum TTR is bounded by $N(N + 1)$ time slots.

2.2.3. Channel Rendezvous Sequence. The channel rendezvous sequence (CRSEQ) is based on the properties of triangular numbers and the Chinese Remainder Theorem [12]. In

this algorithm, nodes A and B visit channels according to the rendezvous sequence, a_i, made by

$$a_i = \begin{cases} z \bmod N + 1, & \text{for } 0 \le y < 2N - 1, \\ x \bmod N + 1, & \text{for } 2N \le y < 3N - 1, \end{cases} \quad (1)$$

where $z = ((x(x+1) + y)/2) \bmod N$, $x = \lfloor i/(3N-1) \rfloor$, $y = i \bmod (3N-1)$, and $0 \le i < N(3N-1)$. For example, the channel rendezvous sequence when $N = 3$ is $\{1, 2, 3, 1, 2, 1, 1, 1, 2, 3, 1, 2, 3, 2, 2, 2, 1, 2, 3, 1, 2, 3, 3, 3\}$. The channel rendezvous sequence has a period of $N(3N-1)$ slots, and the MTTR is $N(3N-1)$ slots.

2.2.4. Asynchronous Efficient Channel Hopping. In [13], asynchronous efficient channel hopping (ASYNC-ETCH) protocol was proposed. ASYNC-ETCH first constructs a set of CHSs when a CR node joins the network. It starts the CHS process immediately after construction of the CHS is done. Within a hopping period, a pair of nodes using ASYNC-ETCH that select the same CHS is guaranteed to rendezvous in one slot. In cases where they select two different CHSs, they are guaranteed to rendezvous within N time slots, no matter how their hopping processes are misaligned.

3. Hopping Sequence Guaranteeing Rendezvous within a Single Period

In this section, we propose an algorithm to generate a sequence for a rendezvous in CR networks. The sequence is used by each node to decide the order in which the available channels are to be visited. This sequence should guarantee a successful rendezvous, even when each node has joined the CR network at different times [14]. In the HS-GRSP, each node uses a rendezvous sequence to visit the available channels to search for each other, when each node starts to look for another node at different times.

3.1. Definitions. We assume that time slot T is divided into a number of slots with the same time interval, t, and we are given N channels denoted by $\{CH_1, CH_2, CH_3, \ldots, CH_N\}$.

Rendezvous sequence is defined as the order of the channels that each node visits for the rendezvous. For example, *a rendezvous sequence* $\{CH_1, CH_3, CH_5, CH_6\}$ means that each node should sequentially visit CH_1, CH_3, CH_5, and CH_6. Each element in the sequence is called *a term*.

Time lag, denoted by k, is the difference between the visiting times of the nodes for the rendezvous. The time lag k is a nonnegative integer expressed as the number of time slots.

Center channel means the channel located at the center position of the available channel list. If we are given N available channels, then the center channel is given by $CH_{N/2}$.

Subsequence is a sequence that can be derived from another sequence by choosing some contiguous terms without changing the order. For example, from the sequence $\{CH_1, CH_2, CH_3, CH_4, CH_5\}$, we can get two subsequences with a length of 4: $\{CH_1, CH_2, CH_3, CH_4\}$ and $\{CH_2, CH_3, CH_4, CH_5\}$.

Group sequence is defined by a subsequence that has a certain local regularity when the sequence is partitioned into specific groups. For example, the sequence $\{CH_1, CH_4, CH_3, CH_2, CH_1, CH_2, CH_3, CH_2, CH_1, CH_3, CH_2, CH_1, CH_4, CH_1\}$ consists of four group sequences $\{CH_1, CH_4, CH_3, CH_2, CH_1\}$, $\{CH_2, CH_3, CH_2, CH_1\}$, $\{CH_3, CH_2, CH_1\}$, and $\{CH_4, CH_1\}$.

3.2. Algorithm. Suppose there are N available channels in a cognitive radio network, where N is a prime number. The proposed rendezvous sequence consists of two parts: group sequence and guard sequence. First, we generate a chain sequence by catenating N group sequences. The first term of each group sequence is given by the group index, and the remaining terms (from the second to the last) are given by the arithmetic sequence in reverse order. For example, if there are three available channels ($N = 3$), then we generate three group sequences $\{\mathbf{CH_1}, CH_3, CH_2, CH_1\}$, $\{\mathbf{CH_2}, CH_2, CH_1\}$, and $\{\mathbf{CH_3}, CH_1\}$ (the first term is marked in bold for easier visualization). So, its chain sequence will be $\{\mathbf{CH_1}, CH_3, CH_2, CH_1, \mathbf{CH_2}, CH_2, CH_1, \mathbf{CH_3}, CH_1\}$ by catenating the three group sequences.

Next, we generate a guard sequence to guarantee rendezvous within the bounded time by repeating the center channels. The length of the guard sequence is given by the number of channels from the last center channel to the end of the chain sequence. For the channel list $\{CH_1, CH_2, CH_3\}$, for example, the guard sequence becomes $\{CH_2, CH_2, CH_2, CH_2\}$ since the distance from last center channel to the end of the chain sequence is 4 as illustrated below:

$$\{\mathbf{CH_1}, CH_3, CH_2, CH_1, \mathbf{CH_2}, CH_2, CH_1, \mathbf{CH_3}, CH_1\}. \quad (2)$$

Last, the rendezvous sequence is made by merging the chain sequence and the guard sequence. As a result, the rendezvous sequence consists of one or more group sequences following a guard sequence. This rendezvous sequence can be used by each node for visiting channels to rendezvous (Table 1).

In general, when there are N available channels, the rendezvous sequence S is given by

$$\begin{aligned} S = \{&CH_1, CH_N, CH_{N-1}, \ldots, CH_2, CH_{N-1}, CH_{N-2}, \ldots, \\ &CH_{N-1}, CH_2, CH_1, CH_N, CH_1, CH_{N/2}, \\ &CH_{N/2}, \ldots, CH_{N/2}\}. \end{aligned} \quad (3)$$

As shown in Figure 5, the length of the guard sequence of a channel list $\{CH_1, CH_2, CH_3, \ldots, CH_N\}$ is given by

$$T_{\text{guard}} = \frac{N^2 + 6N - 8}{8}. \quad (4)$$

So, the length of our proposed sequence is given by

$$T = \frac{5N^2 + 18N - 8}{8}. \quad (5)$$

Table 1: Generation of the group sequences, the guard sequence, and the rendezvous sequence.

Number of available channels	Group sequence	Guard sequence	Rendezvous sequence
1	$\{CH_1, CH_1, CH_1\}$	$\{CH_1, CH_1\}$	$\{CH_1, CH_1, CH_1\}$
2	$\{CH_1, CH_2, CH_1\}, \{CH_2, CH_1\}$	$\{CH_1, CH_1\}$	$\{CH_1, CH_2, CH_1, CH_2, CH_1, CH_1, CH_1\}$
3	$\{CH_1, CH_3, CH_2, CH_1\}, \{CH_2, CH_2, CH_1\}, \{CH_3, CH_1\}$	$\{CH_2, CH_2, CH_2, CH_2\}$	$\{CH_1, CH_3, CH_2, CH_1, CH_2, CH_2, CH_1, CH_3, CH_1, CH_2, CH_2, CH_2, CH_2\}$
4	$\{CH_1, CH_4, CH_3, CH_2, CH_1\}, \{CH_2, CH_3, CH_2, CH_1\}, \{CH_3, CH_2, CH_1\}, \{CH_4, CH_1\}$	$\{CH_2, CH_2, CH_2, CH_2\}$	$\{CH_1, CH_4, CH_3, CH_2, CH_1, CH_2, CH_3, CH_2, CH_1, CH_3, CH_2, CH_1, CH_4, CH_1, CH_2, CH_2, CH_2, CH_2\}$
⋮	⋮	⋮	⋮
N	$\{CH_1, CH_N, CH_{N-1}, \ldots, CH_1\}, \{CH_2, CH_{N-1}, CH_{N-2}, \ldots, CH_1\}, \ldots, \{CH_{N-1}, CH_2, CH_1\}, \{CH_N, CH_1\}$	$\{CH_{N/2}, CH_{N/2}, CH_{N/2}, \ldots, CH_{N/2}\}$	$\{CH_1, CH_N, CH_{N-1}, \ldots, CH_1, CH_2, CH_{N-1}, CH_{N-2}, \ldots, CH_1, \ldots, CH_{N-1}, CH_2, CH_1, CH_N, CH_1, CH_{N/2}, CH_{N/2}, CH_{N/2}, \ldots, CH_{N/2}\}$

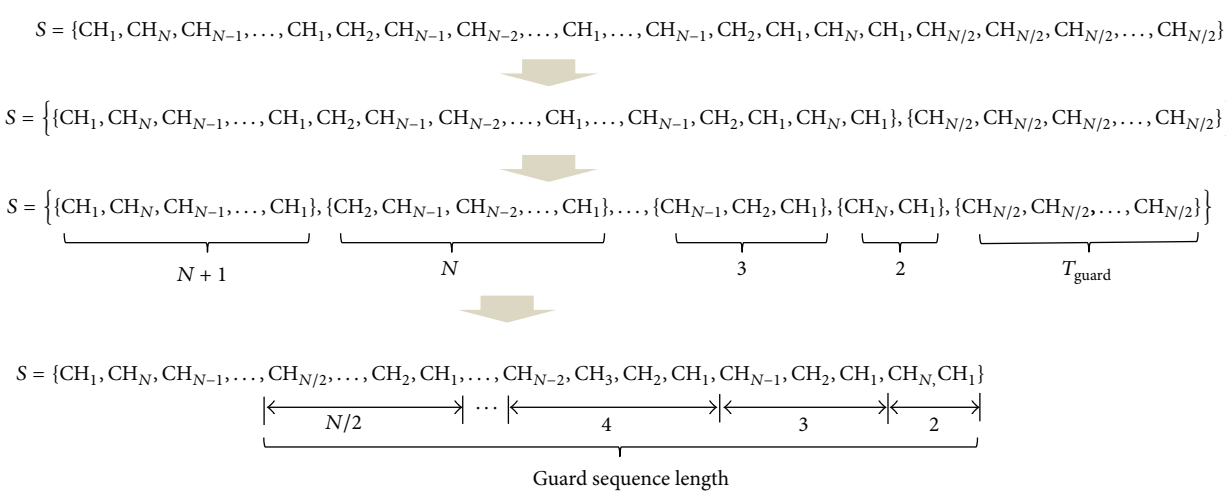

Figure 5: Length of a rendezvous sequence by HS-GRSP.

3.3. Mechanism for PU Appearance. Unlike an SU, a PU is a licensed user who can arrive unexpectedly at any time and on any channel, including a rendezvous channel. The appearance of a PU disturbs SU's activity and may lead to link breakage. The appearance of a PU significantly degrades performance of the rendezvous since the channel(s) occupied by the PU must not be used for rendezvous until the PU leaves the channel. So CR users need to have a mechanism by which they sense and handle PU's appearance. The easiest way is preventing CR users from hopping to that particular channel until the PU leaves.

Figure 6 is the rendezvous mechanism for PU appearance in our scheme.

4. Performance Evaluation

We evaluated the HS-GRSP scheme in terms of four performance criteria, including TTR (ATTR and MTTR), effect of PU appearance, fairness of channel utilization, and degree of overlapping. And we compared their performance with the existing schemes available in the current literature. Comparison targets were SBR, CRSEQ, ASYNC-ETCH, and A-MOCH.

Performance evaluation was done by theoretical analysis and simulation. The CR sensor network is assumed to have 2 to 30 rendezvous channels, each of which could be occupied by a PU at any time. All SUs are supposed to be within communication range of the PU. In the simulation, we first randomly decide whether the PU is detected or not using a Poisson distribution. If the PU appears, we disable the rendezvous channel during a random period of time. Otherwise, all rendezvous channels are made available to the nodes during a random period of time. Every node randomly picks one sequence and performs channel hopping according to the sequence to exchange data packets after acquiring the common channel. The sender follows the receiver's sequences. We repeated this process during the entire simulation. Table 2 shows the simulation parameters.

4.1. TTR Performance. We studied the performance of the HS-GRSP scheme in terms of TTR. TTR is the time needed for any two CR devices to rendezvous using hopping

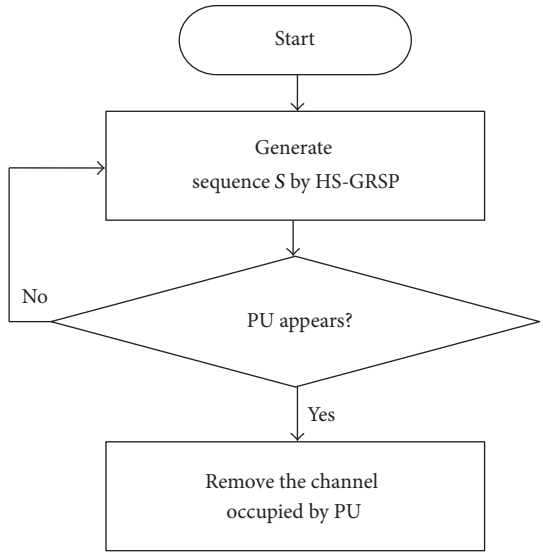

Figure 6: Rendezvous mechanism for PU appearance.

Table 2: Parameters used for simulation.

Parameters	Values
Number of channels	2~30
PU appearance pattern	Poisson distribution
Duration of PU activity	Exponential distribution
Number of CR nodes	2~10
Number of PU nodes	One PU per channel

sequences and is measured by the number of time slots elapsed from the reference time to the rendezvous time. First, we show that our algorithm can guarantee a successful rendezvous of two nodes within a bounded time in a CR sensor network. That is, we show that at least one time slot exists in which nodes A and B both visit the same channel simultaneously within a single period in the worst case (Figure 7).

When $N = 1$ and $k = 0$, they certainly rendezvous in the first time slot, since they start searching simultaneously.

(a) When $N = 1$ and $k = 1$, we get rendezvous sequences for nodes A and B as follows:

$$S_A = \{\mathrm{CH}_1, \mathrm{CH}_1, \mathrm{CH}_1\},$$
$$S_B = \{0, \mathrm{CH}_1, \mathrm{CH}_1, \mathrm{CH}_1\}, \quad (6)$$

where the term "0" indicates no action. This signifies that node B starts the search process in the second time slot. The subsequences of S_A and S_B are $S'_A = \{\mathrm{CH}_1, \mathrm{CH}_1\}$, $\{\mathrm{CH}_1, \mathrm{CH}_1\}$ and $S'_B = \{0, \mathrm{CH}_1\}$, $\{\mathrm{CH}_1, \mathrm{CH}_1\}$, $\{\mathrm{CH}_1, \mathrm{CH}_1\}$, respectively (Table 3). All subsequences with a length of 2 have at least 1 center channel ($\mathrm{CH}_{N/2}$) in common. In this case, two nodes rendezvous two time slots after node A begins the search process, as illustrated in Figure 8.

(b) When $N = 3$ and $k = 2$, nodes A and B can rendezvous in the fifth slot using rendezvous sequences generated by our algorithm.

(c) Assuming that node A starts first, and node B starts four time slots later (i.e., $k = 7$), they can rendezvous at the tenth time slot by generated sequence S, as depicted in Figure 8.

In general, the MTTR with the HS-GRSP scheme is the same as the length of the rendezvous sequence. This means that HS-GRSP guarantees successful rendezvous within a single period. We have

$$\mathrm{MTTR} = \frac{5N^2 + 18N - 8}{8}. \quad (7)$$

In HS-GRSP, we can get ATTR by averaging TTR values for all possible time drifts with a simple calculation:

$$\mathrm{ATTR} = E[\mathrm{TTR}] = \frac{N^2 - 2N + 6}{2}. \quad (8)$$

We compare the TTR performance of the HS-GRSP, together with SBR, CRSEQ, ASYNC-ETCH, and A-MOCH. Figure 9 shows ATTR and MTTR achieved with those five channel hopping protocols. Figure 9(b) indicates that the maximum rendezvous time linearly grows as the number of channels increases. As seen from this figure, HS-GRSP provides the best performance of the five CH protocols in terms of MTTR for all values of N. Also, we can see that our algorithm offers a shorter average rendezvous time than SBR and CRSEQ. So, HS-GRSP can be used to reduce the delay of medium access control (MAC) protocols for a CR sensor network. In CRSEQ, it may take a long time to find a neighboring node on a channel to exchange control information, especially when the number of available channels is large.

4.2. Effect of PU Appearance on TTR. The appearance of a PU highly affects TTR of the hopping sequence since the channel occupied by the PU cannot be used anymore for conducting the rendezvous until the PU leaves the channel.

Assuming the PU appears on the channel for a time slot with a probability of p, then the probability that a given channel is occupied by the PU (i.e., the PU appears on a given channel at least one time) during a of hopping sequence period will be

$$P_{\mathrm{PU}} = 1 - (1 - \rho)^T, \quad (9)$$

where T is the period of the hopping sequence.

As described earlier, the hopping sequence period with HS-GRSP is $(5N^2 + 18N - 8)/8$. Thus, during a hopping sequence period (denoted by M), the average number of channels occupied by a PU during will be

$$M = N \cdot P_{\mathrm{PU}} = N\left(1 - (1 - \rho)^{(5N^2+18N-8)/8}\right). \quad (10)$$

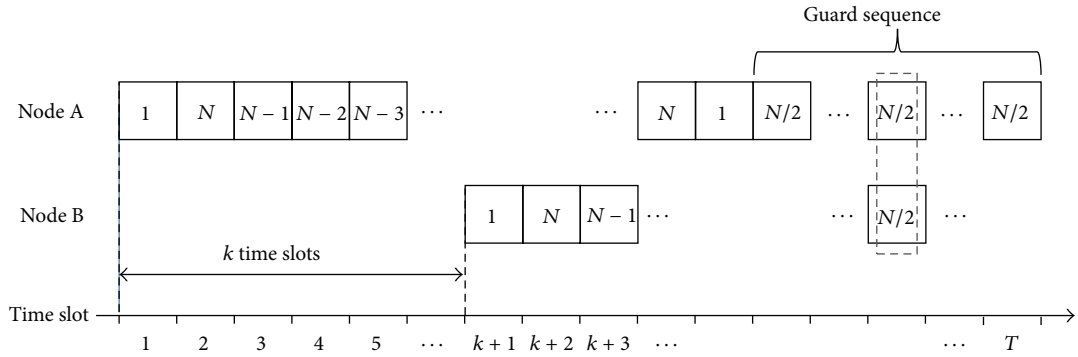

Figure 7: Rendezvous of nodes A and B when there are N channels.

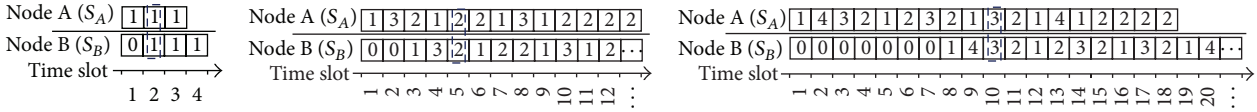

(a) The rendezvous process when $N = 1$ and $k = 1$

(b) The rendezvous process when $N = 3$ and $k = 2$

(c) The rendezvous process when $N = 4$ and $k = 7$

Figure 8: Examples of the rendezvous process.

Now, we can get ATTR under the impact of PU activity in a CR network with N channels as follows:

$$\mathrm{ATTR}' = \frac{N\left(\left(N^2 - 2N + 6\right)/2\right)}{N - M} = \frac{(1/2)\left(N^2 - 2N + 6\right)}{(1-\rho)^{(5N^2+18N-8)/8}}. \tag{11}$$

From (8) and (11), we can express the effect of the PU appearance on ATTR performance with HS-GRSP with the following impact factor, f:

$$f = \frac{\mathrm{ATTR}'}{\mathrm{ATTR}} = \frac{N}{N - M} = \frac{1}{(1-\rho)^{(5N^2+18N-8)/8}}. \tag{12}$$

The impact factor indicates the increasing ratio of ATTR when the PU appears on its own channel for a time slot with probability p.

As seen in Figure 10(a), our scheme is not significantly affected by the appearance of the PU regardless of the number of available channels. We can see that ATTR with our scheme does not rise meaningfully for all values of N, although the probability of a PU appearance increases. This means that our scheme provides a very stable performance in ATTR under the impact of the PU appearance.

4.3. Fairness of Channel Utilization and Degree of Overlapping Performance. Fairness of channel utilization can be expressed by a reciprocal value of the normalized standard deviation of the number of channels used for rendezvous by CR nodes. Even distribution of rendezvous channels over different time slots is an important requirement in order to overcome the rendezvous convergence problem. If a large proportion of neighboring nodes rendezvous on the same channel, then channel congestion can occur and lead to a control channel bottleneck problem [12]. Therefore, the rendezvous should spread out evenly over all channels. As the fairness of channel utilization increases, network capacity at the communication setup stage becomes proportionally large.

Figure 11 shows that in CRSEQ and SBR, fairness of channel utilization is inversely proportional to the number of channels, whereas fairness with HS-GRSP is not significantly affected by the number of channels, although it shows a small fluctuation. In CRSEQ, the rendezvous channels are not found with equal probability in a given period. Such unfair distributions may result in traffic load on certain channels over more than others. On the other hand, with HS-GRSP and SBR, the possibility of rendezvous convergence is low because different pairs of sender and receiver are likely to construct different pairs of alternative and default hopping sequences, and thus, the rendezvous points (in terms of frequency and time) of those hopping sequence pairs are different.

Degree of overlap refers to the number of time slots in which any two sequences can overlap within one sequence period, or can intersect, to ensure any one pair of nodes is able to communicate. If two ith slots are the same for two CH sequences S_A and S_B (i.e., $S_{A[i]} = S_{B[i]}$), then this slot is called an overlapping or rendezvous slot between S_A and S_B. Figure 12 shows that CRSEQ offers the highest degree of overlap, whereas SBR only overlaps at a single rendezvous point per channel between any two given sequences. In HS-GRSP, the degree of overlapping linearly increases as the number of available channels increases above 5. This contributes to achieving a very short MTTR with HS-GRSP.

4.4. Comparison Summary. Finally, we compared HS-GRSP using five metrics: ATTR, MTTR, PU impact factor, fairness

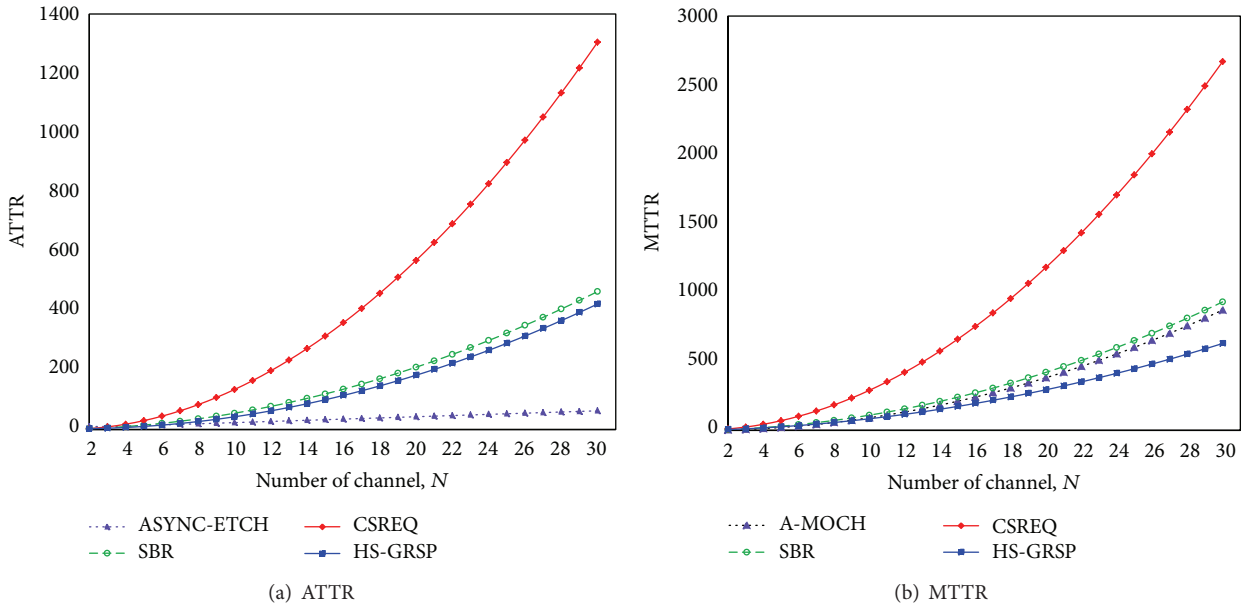

(a) ATTR (b) MTTR

Figure 9: TTR performance of channel hopping protocols.

Table 3: Subsequences S'.

Number of available channels	Subsequence S'
1	$\{CH_1, CH_1\}, \{CH_1, CH_1\}$
2	$\{CH_1, CH_2\}, \{CH_2, CH_1\}, \{CH_1, CH_2\}, \{CH_2, CH_1\}, \{CH_1, CH_1\}, \{CH_1, CH_1\}$
3	$\{CH_1, CH_3, CH_2, CH_1\}, \{CH_3, CH_2, CH_1, CH_2\}, \{CH_2, CH_1, CH_2, CH_1\}, \{CH_1, CH_2, CH_2, CH_1\}, \{CH_2, CH_2, CH_3, CH_1\}, \{CH_2, CH_1, CH_3, CH_1\}, \{CH_1, CH_3, CH_1, CH_2\}, \{CH_3, CH_1, CH_2, CH_2\}, \{CH_1, CH_2, CH_2, CH_2\}, \{CH_2, CH_2, CH_2, CH_2\}$
4	$\{CH_1, CH_4, CH_3, CH_2\}, \{CH_4, CH_3, CH_2, CH_1\}, \{CH_3, CH_2, CH_1, CH_2\}, \{CH_2, CH_1, CH_2, CH_3\}, \{CH_1, CH_2, CH_3, CH_2\}, \{CH_2, CH_3, CH_2, CH_1\}, \{CH_3, CH_2, CH_1, CH_3\}, \{CH_2, CH_1, CH_3, CH_2\}, \{CH_1, CH_3, CH_2, CH_1\}, \{CH_3, CH_2, CH_1, CH_4\}, \{CH_2, CH_1, CH_4, CH_1\}, \{CH_1, CH_4, CH_1, CH_2\}, \{CH_4, CH_1, CH_2, CH_2\}, \{CH_1, CH_2, CH_2, CH_2\}, \{CH_2, CH_2, CH_2, CH_2\}$
⋮	⋮
N	$\{CH_1, CH_N, CH_{N-1}, \ldots, CH_{N/2}, \ldots, CH_2\}, \{CH_N, CH_{N-1}, CH_{N-2}, \ldots, CH_{N/2}, \ldots, CH_1\}, \{CH_{N-1}, CH_{N-2}, CH_{N-3}, \ldots, CH_{N/2}, \ldots, CH_{N-1}\}, \ldots, \{CH_{N/2}, CH_{N/2}, CH_{N/2}, \ldots, CH_{N/2}\}$

Table 4: Comparison of channel hopping schemes.

CH protocol	ATTR	MTTR	PU impact factor	Fairness of rendezvous channel utilization	Degree of overlapping
ASYNC-ETCH	$\frac{2N^2+N}{N-1}$	—	$\frac{1}{(1-\rho)^{2N-1}}$	High	At least 1
A-MOCH	—	N^2-N+1	$\frac{1}{(1-\rho)^{N^2}}$	High	High
SBR	$\frac{N^2+N}{2}$	N^2+N	$\frac{1}{(1-\rho)^{N(N+1)}}$	High	At least 1
CRSEQ	$\frac{3N^2-3N}{2}$	$N(3N-1)$	$\frac{1}{(1-\rho)^{N(3N-1)}}$	Low	High
HS-GRSP	$\frac{N^2-2N+6}{2}$	$\frac{5N^2+18N-8}{8}$	$\frac{1}{(1-\rho)^{(5N^2+18N-8)/8}}$	High	At least 1

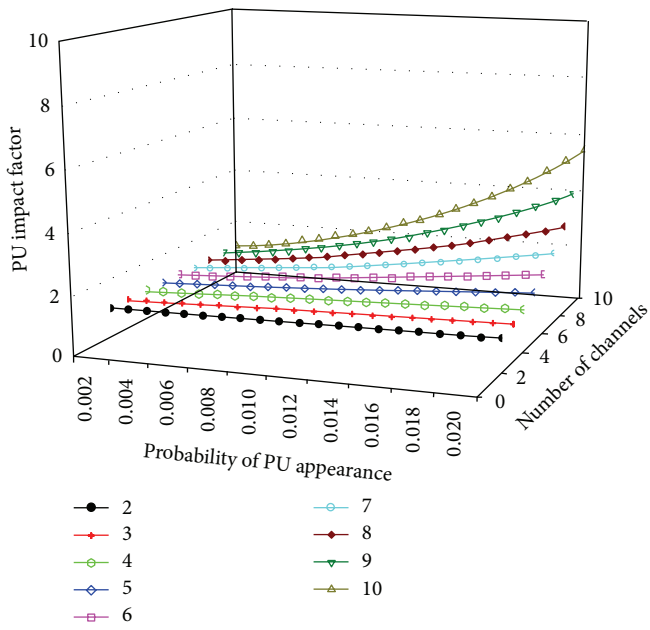

(a) PU impact factor with HS-GRSP (as N and P are varied)

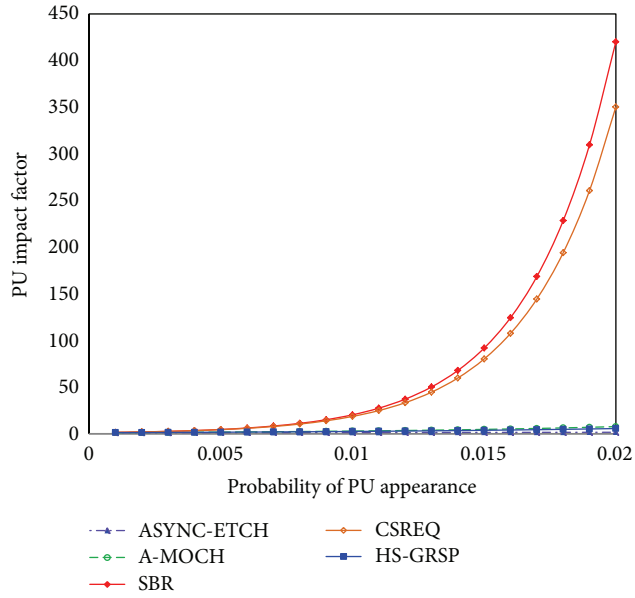

(b) PU impact factor (when $N = 10$)

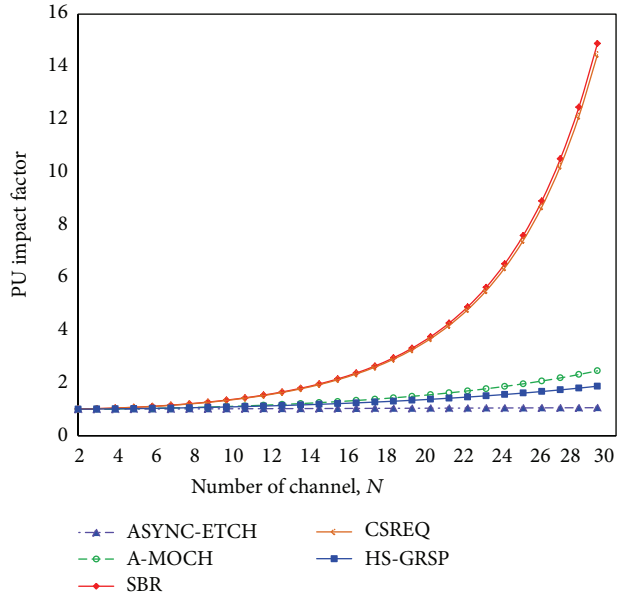

(c) PU impact factor (when $P = 0.001$)

Figure 10: PU impact factor.

of channel utilization, and degree of overlapping. Table 4 summarizes the comparison results, where N is the number of channels used in the CR network and p is the probability that a PU appears on the channel in a time slot.

5. Conclusion

In this paper, we propose an asynchronous channel hopping mechanism, called HS-GRSP, to establish a control channel in self-organizing CR sensor networks. We illustrate how two nodes wishing to communicate perform channel hopping in order to form a rendezvous point within an upper bound using our algorithm. We evaluated the performance of HS-GRSP and compared it with other schemes in the literature. Theoretical and simulation results showed that HS-GRSP provides successful communication rendezvous within a single period. HS-GRSP provides superior performance in terms of MTTR and shows very stable performance in ATTR under the effects of PU appearance, even when the number of channels increases. Thus, HS-GRSP can be used to successfully reduce delay of MAC protocols. Moreover,

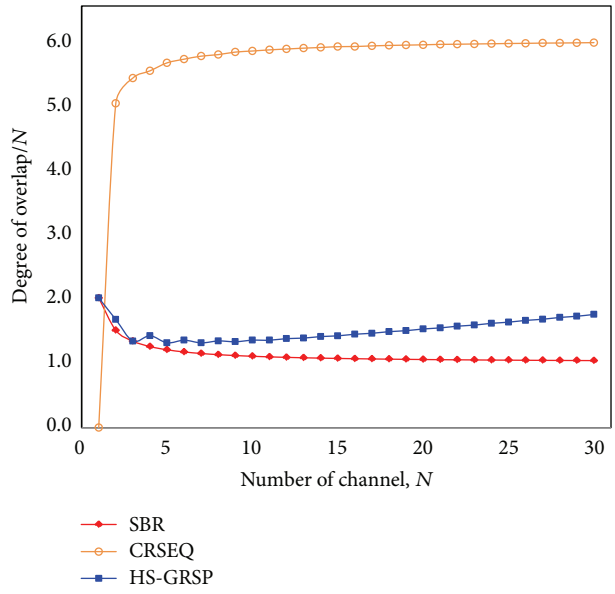

Figure 11: Fairness of channel utilization with channel hopping protocols.

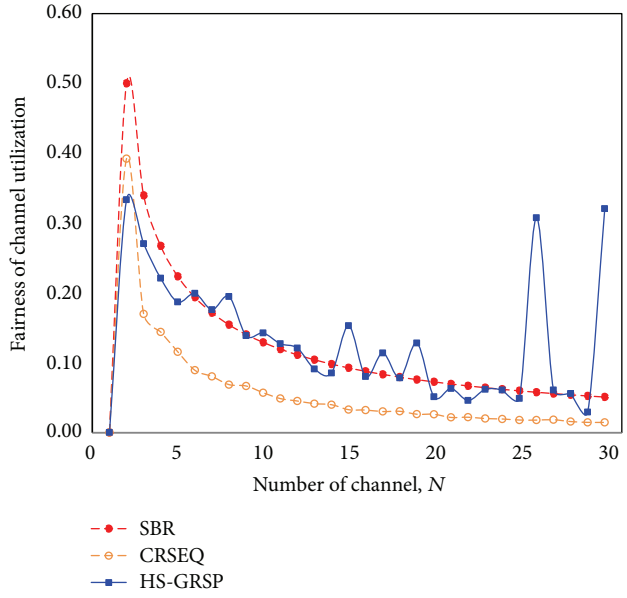

Figure 12: Degrees of overlap.

the possibility of rendezvous convergence is low with HS-GRSP because its fairness is not significantly affected by the number of channels. In HS-GRSP, the degree of overlapping linearly increases as the number of available channels increases above 5. This contributes to achieving a very short MTTR with HS-GRSP.

Conflict of Interests

The authors declare that they have no conflict of interests regarding the publication of this paper.

Acknowledgments

This work was supported by the National Research Foundation of Korea (NRF) Grant funded by the Korea government (MSIP) (2011-0029034). This work was supported by the IT R&D Program of MSIP/KEIT. [10041145, Self-Organized Software platform (SoSp) for Welfare Devices]. This research was supported by the MSIP (Ministry of Science, ICT and Future Planning), Korea, under the IT/SW Creative Research Program supervised by the NIPA (National IT Industry Promotion Agency) (NIPA-2013-H0502-13-1122). This work was supported by the Brain Korea 21+ Program.

References

[1] D. Puccinelli and M. Haenggi, "Wireless sensor networks: applications and challenges of ubiquitous sensing," *IEEE Circuits and Systems Magazine*, vol. 5, no. 3, pp. 19–31, 2005.

[2] G. Zhou, J. A. Stankovic, and S. H. Son, "Crowded spectrum in wireless sensor networks," in *Proceedings of the 3rd Workshop on Embedded Networked Sensors (EmNets '06)*, pp. 1–5, Cambridge, Mass, USA, May 2006.

[3] C. H. M. de Lima, M. Bennis, and M. Latva-aho, "Statistical analysis of self-organizing networks with biased cell association and interference avoidance," *IEEE Transactions on Vehicular Technology*, vol. 62, no. 5, pp. 1950–1961, 2013.

[4] C. Cormio and K. R. Chowdhury, "Common control channel design for cognitive radio wireless ad hoc networks using adaptive frequency hopping," *Ad Hoc Networks*, vol. 8, no. 4, pp. 430–438, 2010.

[5] D. M. Yang, J. M. Shin, and C. H. Kim, "Deterministic rendezvous scheme in multi-channel access networks," *Electronics Letters*, vol. 46, no. 20, pp. 1402–1404, 2010.

[6] O. B. Akan, O. B. Karli, and O. Ergul, "Cognitive radio sensor networks," *IEEE Network*, vol. 23, no. 4, pp. 34–40, 2009.

[7] Z. Htike, C. S. Hong, and S. Lee, "The life cycle of the rendezvous problem of cognitive radio ad hoc networks: a survey," *Journal of Computing Science and Engineering*, vol. 7, no. 2, pp. 81–88, 2013.

[8] T. Chen, H. Zhang, G. M. Maggio, and I. Chlamtac, "CogMesh: a cluster-based cognitive radio network," in *Proceedings of the 2nd IEEE International Symposium on New Frontiers in Dynamic Spectrum Access Networks (DySPAN '07)*, pp. 168–178, Dublin, Ireland, April 2007.

[9] K. Bian, J.-M. Park, and R. Chen, "Control channel establishment in cognitive radio networks using channel hopping," *IEEE Journal on Selected Areas in Communications*, vol. 29, no. 4, pp. 689–703, 2011.

[10] K. Bian, J.-M. Park, and R. Chen, "A quorum-based framework for establishing control channels in dynamic spectrum access networks," in *Proceedings of the 15th Annual International Conference on Mobile Computing and Networking (MobiCom '09)*, pp. 25–36, Beijing, China, September 2009.

[11] L. A. DaSilva and I. Guerreiro, "Sequence-based rendezvous for dynamic spectrum access," in *Proceedings of the 3rd IEEE Symposium on New Frontiers in Dynamic Spectrum Access Networks (DySPAN '08)*, pp. 1–7, Chicago, Ill, USA, October 2008.

[12] J. Shin, D. Yang, and C. Kim, "A channel rendezvous scheme for cognitive radio networks," *IEEE Communications Letters*, vol. 14, no. 10, pp. 954–956, 2010.

[13] Y. Zhang, Q. Li, G. Yu, and B. Wang, "ETCH: efficient channel hopping for communication rendezvous in dynamic spectrum access networks," in *Proceedings of the IEEE INFOCOM*, pp. 2471–2479, Shanghai, China, April 2011.

[14] J. Kim, Y. Baek, J. Yun et al., "A repeated group sequence rendezvous scheme for cognitive radio networks," in *Proceedings of the Spring Congress on Engineering and Technology (S-CET '12)*, pp. 1–4, Xian, China, 2012.

Hindawi Publishing Corporation
International Journal of Distributed Sensor Networks
Volume 2014, Article ID 965495, 9 pages
http://dx.doi.org/10.1155/2014/965495

Research Article

A Game Theory Based Strategy for Reducing Energy Consumption in Cognitive WSN

Elena Romero, Javier Blesa, Alvaro Araujo, and Octavio Nieto-Taladriz

ETSI Telecomunicación, Universidad Politécnica de Madrid, 28040 Madrid, Spain

Correspondence should be addressed to Elena Romero; elena@die.upm.es

Received 6 September 2013; Revised 28 November 2013; Accepted 19 December 2013; Published 28 January 2014

Academic Editor: Al-Sakib Khan Pathan

Wireless sensor networks (WSNs) are one of the most important users of wireless communication technologies in the coming years and some challenges in this area must be addressed for their complete development. Energy consumption and spectrum availability are two of the most severe constraints of WSNs due to their intrinsic nature. The introduction of cognitive capabilities into these networks has arisen to face the issue of spectrum scarcity but could be used to face energy challenges too due to their new range of communication possibilities. In this paper a new strategy based on game theory for cognitive WSNs is discussed. The presented strategy improves energy consumption by taking advantage of the new change-communication-channel capability. Based on game theory, the strategy decides when to change the transmission channel depending on the behavior of the rest of the network nodes. The strategy presented is lightweight but still has higher energy saving rates as compared to noncognitive networks and even to other strategies based on scheduled spectrum sensing. Simulations are presented for several scenarios that demonstrate energy saving rates of around 65% as compared to WSNs without cognitive techniques.

1. Introduction

Global data traffic in telecommunications grows annually at a rate of 70%. The increasing number of wireless devices that are accessing mobile networks worldwide is one of the primary contributors to traffic growth. The number of mobile-connected devices will exceed the world's population in 2013 according to the CISCO report [1]. One of the main causes of this spectacular growth of mobile traffic is the increase in mobile-connected laptops and tablets and the emergence of smartphones whose use has increased by 82% in 2012. Handsets will exceed 50% of mobile data traffic in 2013. All of these devices (smartphones, tablets, and laptops) are usually connected via Wi-Fi or Bluetooth, which work on a 2.4 GHz unlicensed band.

Reexamining the CISCO report, machine to machine (M2M) communications are shown as one of the most important trends with a 90% annual growth between 2012 and 2017. Typical M2M applications include security and surveillance, health, or monitoring. These applications are usually supported by wireless sensor networks (WSNs) providing a wireless and flexible structure for the transmission of the data acquired by sensors to the rest of the network.

One of the problems with WSNs is certainly spectral coexistence. Regarding spectrum scarcity, most WSN solutions operate on unlicensed frequency bands. In general they use the industrial, scientific, and medical (ISM) bands like the worldwide available 2.4 GHz band. This band is also used by a large number of popular wireless applications, as mentioned before, or wireless networks based on IEEE 802.15.4. As a result, coexistence issues on unlicensed bands have been the subject of extensive research showing that IEEE 802.11 networks can significantly degrade the performance of 802.15.4 networks when operating on overlapping frequency bands [2]. To address the efficient spectrum utilization problem, cognitive radio (CR) [3] has emerged as the key technology, which enables opportunistic access to the spectrum.

One of the most important challenges with WSNs is energy consumption. Due to the number of nodes, their wireless nature, and, sometimes, their deployment in difficult access areas, nodes should not require any maintenance. In terms of consumption this means that the sensors must be energetically autonomous, the networks should not require human intervention, and therefore the batteries cannot be changed or recharged. In these kinds of scenarios, node

lifetime should last for years, making energy consumption a dramatic requirement to establish. If energy consumption has not been taken into account, nodes will eventually shut down.

The introduction of CR capabilities in WSNs provides a new paradigm for power consumption reduction offering new opportunities to improve it, but this also implies some challenges [4]. Specifically, sensing state, collaboration among devices—which requires communication, and changes in transmission parameters all increase the total energy consumption.

When designing WSN optimization strategies, the fact that WSN nodes are very limited in terms of memory, computational power, or energy consumption is not insignificant. Thus, light strategies that require low computing capacity must be found. In this way, different previous works, shown in Section 2, have demonstrated the feasibility and effectiveness of implementing game-theory-based strategies to optimize limited resources on WSNs. Since the field of energy conservation in WSNs has been widely explored, we assumed that new strategies should emerge from the new opportunities presented by cognitive networks.

In this paper a new game-theory-based strategy to optimize energy consumption in WSNs is presented. This strategy takes advantage of a new opportunity offered by cognitive wireless sensor networks (CWSNs): the ability to change the transmission and reception channel.

The organization of the paper is as follows. Section 2 presents the review of the state of the art. Assumptions about the network are exposed in Section 3. The game-theory-based strategy is presented in Section 4. Section 5 describes the baseline scenario and tools used in the simulations and the results are presented and discussed. Finally, Section 6 presents the conclusions from this work.

2. Related Work

CWSNs are a young technology and there is not a wide range of contributions in this area. Most works found in the literature on CWSNs introduce the general idea and promote research in this field. Zahmati et al. present in [4] an overview of CWSNs, discussing the emerging topics and the potential challenges in the area. Moving on to energy efficiency, there are several approaches to reduce power consumption for CNs but not specifically for CWSNs. Most of the research work focuses on achieving power-efficient spectrum use. In [5] a transmission power management is proposed to minimize interference with primary users and to guarantee an acceptable quality of service (QoS) level for cognitive transmission. In [6] the power constraint is integrated into the objective function which is a combination of the main system parameters of the cognitive network.

If we move to the specific area of consumption reduction in CWSNs, there is still much work to do. Focusing on low-power networks that exploit CR features, [7] notes the importance of CR features to improve power consumption, as in [8] where it is noted that CR could be able to adapt to varying channel conditions, which would increase transmission efficiency and hence help reduce power used for transmission and reception. These papers address the new opportunities offered but lack in specific solutions. In [9] two main problems related to energy consumption are listed: network lifetime maximization and energy efficient routing.

Specific solutions are given in [10] where authors propose a routing scheme optimizing the size of transmitted data and the transmission distance. Also, Stabellini and Zander center their work on reducing power consumption in the sensing step [11]. They use an energy constrained system comprising of two sensor nodes that avoid interference by exploiting spectrum holes in the time domain to prove its algorithm.

Given that the contributions in the field of reducing energy consumption in CWSNs are still scarce, it is possible to use the advances in WSNs to inspire new strategies for CWSNs. This way, it is possible to find a wide range of previous works in the area of algorithms based on game theory seeking energy optimizations in sensor networks. As stated in [12], more than 330 research articles related to game theory and WSNs were published from 2003 to 2011. Modeled games range from routing, task scheduling, or MAC energy efficient implementations.

Moreover, the use of game theory based algorithms is suited well to the characteristics of CNs. There are several studies based on game theory that model CN resources, from an overview presented in 2010 by [13] to models of channel selection [14], power allocation [15], or the mixture of both [16].

However, the introduction of intrinsic characteristics of WSNSs makes it essential to model energy consumption games. In addition, games designed for CWSNs should be lighter in terms of processing and energy consumption. In this area, a game-theory-based energy-efficient approach to power allocation in CWSNs is presented in [17]. Even if the approach takes energy efficiency into account, the game models power allocation instead of energy consumption.

Even though the research in this area looks to be very interesting, the use of CR to improve energy consumption in WSNs is not a mature research area. Some ideas are given but real proposals outside of the efficient sensing area or routing protocols are missing.

3. Assumptions and CWSNS Scenario

CWSNs are based on typical WSNs, improved with several features provided by cognitive networks. Thus, typical CWSNs are similar in components, distribution, and behavior to WSNs.

In this model, a CWSNS consists of a set $N = \{1, 2, \ldots, n\}$ of n cognitive wireless sensor nodes which could implement different final applications. Each node can communicate with others depending on their position and the transmission range. A typical CWSN consists of a number of nodes which can vary from tens to thousands of devices. These nodes are battery powered. CWSNS communicate over IEEE 802.15.4 specification with rates of up to 250 Kbps. However, typical CWSN rates are lower. Transmission power is limited due to energy consumption constraints. Nodes could perform in transmission mode, reception mode, or standby mode.

Typical current consumptions are 20 mA in transmission or reception mode and below 1 mA in standby mode [18]. Moreover, the mode usually described as sensing refers to a long-lasting reception mode.

As mentioned before, CWSN nodes communicate on an ISM band in coexistence with Wi-Fi or Bluetooth devices. Due to their bandwidth and their transmission power, each Wi-Fi channel can mask up to four 802.15.4 channels when both technologies coexist on the 2.4 GHz band.

Even if one of the main characteristics of CR is the existence of primary users (PUs) and secondary users (SUs), in this scenario no distinction shall be made between them. According to their formal definition, PUs are the "owner" of the spectrum band with right to communicate without restrictions, while SUs can use the spectrum if they do not jam PUs. Because of the CWSN use of unlicensed bands, the definition in this case refers to the information importance or relevance. Moreover, the strategy could apply to PUs and SUs improving their energy consumption in both cases.

4. Game Theory Strategy

As mentioned in Section 1, constrained resources are an intrinsic challenge related to WSNs. The additional complexity added to the nodes to enable cognitive capabilities makes nodes have higher energy consumption. Moreover, processing capability of WSN nodes is limited; thus, the strategies implemented should have low complexity.

There are many new different opportunities for reducing energy consumption in CWSNs. The proposal presented is to divide the opportunities for energy consumption optimization into three groups, namely, those that are obtained through spectrum sensing, those related to the capability to change transmission parameters, and those that depend on the ability to share network knowledge. The first two groups are directly derived from the cognitive capabilities added to the WSN nodes. However, the third one, related to the cooperation between devices, is one of the basic characteristics of WSNs, now enriched with cognitive information.

The proposed strategy addressed in this paper focuses on the ability to change transmission parameters based on sensed information. In addition, this strategy takes advantage of the cooperation in the network to share the information. In this work, a channel shift strategy to prevent unnecessary retransmissions has been selected. The use of less noisy channels avoids extra retransmissions and makes the global consumption reduction of the network possible.

As shown in Section 2, game theory is widely accepted for resource optimization in cooperative WSNs, and, now, with cognitive capabilities, it could fit even more. Although other approaches to optimize energy consumption such as genetic algorithms have been explored, their implementation in WSN nodes is expensive in terms of cost in computational resources and energy consumption [19, 20].

By its intrinsic nature, a sensor-network resource problem can be easily modeled like a game. In addition, games can be simplified enough without losing functionality to make them supported by a WSNS node, even if its processing capability is limited.

Table 1: Payoff matrix for player n.

Payoff for node n	m changes channel	m does not change channel
n changes channel	$-C_{ch}$	$-C_{ch} - C_n$
n does not change channel	$-C_n$	$-C_o$

A game is defined by several characteristics. The *resource* being modeled, the *players*, their *strategies,* and the *actions* they can take. Thereon, *costs* associated with each *action* will be defined, and, by combining this with the *odds* (suspected or known) of such *actions* occurring, the *payoff matrix and function* will be obtained.

In the approach described in this paper, the game is modeled as a finite resource game due to the battery-powered nodes, which provide them with a finite energy. The *resource* is the energy available in each node. *Players* are CWSN nodes $N = \{1, 2, \ldots, n\}$ and the *strategies* are those relating to the selection of the communication channel $S = \{s_1, s_2, \ldots, s_i\}$. The feasible *actions* that each one of the *players* can carry out are to change or not change the transmission channel. This *action* can arise from themselves or after a *move*—request—from another *player*. Energy consumption is modeled as the *resource* for which players compete. Thus, the *payoffs* and *costs* are those energy expenses associated with the *actions* taken. $P_n(s)$ where $n \in N$ is the nth payoff function.

This game can be described as a hybrid game because although it is noncooperative in game theory terminology, communication between nodes can lead to the common good. It is a non-zero-sum game, in which there is no correlation between one player's payoffs and another player's losses. In fact, there may be values that maximize the payoffs of every player. The game is sequential because actions are performed sequentially. This game is asymmetrical since payoffs are different depending on the players. In this case this dependence refers to the position of the players and the traffic between them. It is also an evolutionary game, since players can learn, adapt, and evolve their actions based on the information shared and the odds perceived from the rest of the nodes.

For the calculation of the *payoff* matrix of this game, the resulting *payoffs* coming from the combination of the *actions* taken by the *players* (to change or not to change the transmission channel) are taken into account.

The *payoff* matrix for *player n* that communicates with *player m* is shown in Table 1.

And the *payoff* matrix for node n could be expressed as

$$P_n = \begin{pmatrix} -C_{ch} & -C_{ch} - C_n \\ -C_n & -C_o \end{pmatrix}, \quad (1)$$

where C_{ch} is defined as the energy cost associated with a change of the communication channel. It is calculated as the addition of the extra energy cost associated with the sensing mode (C_{sensing}) and the cost of the transmission (C_{tx}) and reception (C_{rx}) caused by the agreement messages needed to

negotiate the channel change (n_msg). Thus, the energy cost of the action of change in this case is

$$C_{ch} = C_{\text{sensing}} + (C_{tx} + C_{tx}) \cdot n\_\text{msg}. \quad (2)$$

C_o is the energy cost of transmission in noisy channels. It is calculated as the cost of a packet transmission taking into account that it requires a number of retransmissions named n_rtx. This n_rtx depends on the observed and stored number of retransmissions needed by previous packets and is calculated as the average of the needed message retransmissions for the previous k (parameterizable) messages:

$$C_o = C_{tx} \cdot n\_rtx. \quad (3)$$

C_n is the energy cost associated to communications in a channel not shared with the receiver. Even though this situation is not very common, it could happen if several CWSNs perform the strategy without agreement. C_n is calculated as the cost of transmission when the number of retransmission has run out and consequently the maximum allowed has been reached (max $\_rtx$):

$$C_n = C_{tx} \cdot \max\_rtx. \quad (4)$$

Naming x the odds of node n and y the supposed probability of node m to take the action to change the communication channel and calculating the total *payoff* of node n result in

$$\begin{aligned} P_n = &- C_{ch} \cdot x \cdot y - (C_{ch} + C_n) \cdot x \cdot (1 - y) \\ &- C_n \cdot (1 - x) \cdot y - C_o \cdot (1 - x) \cdot (1 - y), \\ P_n = &(2 \cdot C_n - C_o) \cdot x \cdot y + (C_o - C_{ch} - C_n) \cdot x \\ &+ (C_o - C_n) \cdot y - C_o. \end{aligned} \quad (5)$$

To determine the optimal value of x, each node n stores the observed number of accepted and sent requests from its neighbor nodes. From this stored data it is possible to extract the supposed probability of change y. Evaluating C_{ch}, C_n, and C_o at the time of the channel change request, the optimal value of x that maximizes the payoff can be obtained.

Applying the maximization criterion of this simple algorithm in every device, it is possible to optimize the consumption of each node without impacting the breakdown of other nodes in the network. Thus, by maximizing the lifetime of each network node, the lifetime of the network as a whole is prolonged. Although this statement is not always true, the energy saved in each node has a positive effect on the overall operation of the network.

For the implementation of this strategy, it could be possible to always run the maximization of the payoff in the background, but in terms of energy conservation and computing capabilities it is more efficient to optimize only when the transmission channel is noisy enough. In this way, the strategy considers that the optimization will be triggered, taking into account other parameters such as the RSSI received in the communication channel, which is related to noise presence.

Optimization strategy performs as follows.

(1) Every node in the CWSN receives messages by the assigned channel and saves RSSI samples from each message received.

(2) If the RSSI value saved in node n is above a certain threshold (in a certain number of samples), node N activates the optimization algorithm that evaluates the payoff function to decide if changing the channel is interesting at that moment or not.

(3) If the result of this evaluation is a change, node N senses the spectrum and chooses the least noisy channel.

(4) Node N communicates its decision to the rest of the network nodes and the new chosen channel according to its sensing values.

(5) The rest of nodes evaluate this change and decide whether to change the channel depending on its payoff function. This decision is communicated back to other nodes in the network.

(6) The value of the stored accepted channel change requests is updated in order to calculate y in future situations.

Although in this work the sensing state only involves one node, this approach could be adapted to any type of sensing depending on the network features. To demonstrate the validity of this algorithm, only the triggered node is responsible for sensing. However, new collaborative techniques or channel negotiation in clusters could be included according to the location of the nodes.

5. Experimental Results

In this section results of different simulations are presented. First, the simulation tool used to perform them is presented. The baseline scenario and the different scenario configurations are shown. Finally, the simulations performed and the results obtained are presented and discussed.

5.1. Simulation Tools. In this work the architecture of cognitivity brokerage framework [21] is used. For simulation results the framework used is composed of two fundamental elements: a CWSN simulator and low power cognitive radio real devices. This framework [22] has been tested and referenced in previous works. Both the simulator (based on Castalia) and real nodes implement the cognitivity brokerage architecture mentioned.

The structure of Castalia simulator has been enhanced to provide cognitive features. The simulator can carry out sensing tasks in order to acquire and share spectrum information. This information may include received signal power, noise power, or time between packets. The information is processed, stored, and shared according to the implemented strategy. A virtual control channel (VCC) also exists to share sensed information, with no extra overhead over regular communications.

The simulator is also responsible for the scenario definition, the simulation of the spectrum state, and the communication between nodes from the physical to the application layer.

Real nodes are used just to confirm, as empirical testing, results for small-scale networks. So that all the results presented in this paper are extracted from the simulator.

5.2. Cognitive Baseline Scenario. The baseline scenario which carries out the simulation tests is deployed in a 100 m × 10 m area, such as an example of a WSN scenario. It contains two coexisting networks, a CWSN and a Wi-Fi network. In the baseline scenario 100 Wi-Fi nodes are assumed, but a simulation with a varying number of Wi-Fi nodes is performed (from 50 to 200 devices). CWSN results show the energy consumption of a cognitive device which communicates only with the network coordinator (as a WSN star topology).

CWSNs are modeled with a Texas Instrument CC2420 transceiver. Values of energy consumption are extracted from datasheet (for transmission, reception and idle modes, and energy costs of transitions between modes) and verified through experimental measurement. Sensing stage is modeled as a reception mode lasting for 200 ms.

CWSN nodes transmit common WSN packets of 50 bytes at −5 dBm while Wi-Fi network transmits the usual Wi-Fi packets of 2000 bytes at −3 dBm. Both networks use ISM band at 2.4 GHz. A maximum number of 20 retransmissions are set for CWSN and Wi-Fi nodes in the baseline scenario. However, it is interesting to check the behavior by varying the maximum number of retransmissions allowed. Therefore, a simulation for this is included.

For the baseline scenario, a RSSI threshold of −150 dBm taking into account 5 samples is assumed. Nevertheless, a simulation with a different number of samples and a variable threshold is also considered.

In order to facilitate simulations of different configurations, a reduction in simulation 10 times lower in every magnitude is assumed. For this assumption, a long-term simulation is performed, showing similar results to those presented in the paper. Thus, simulation time is 300 s, and network rates of 1 packet per second on CWSNs and 50 packets per second on Wi-Fi are chosen. The spectrum sensing period for CWSNs is 2 s.

In order to simulate new Wi-Fi configurations or the appearance of new Wi-Fi networks or nodes in the area, these simulated nodes change their communication channel every 30 s.

In all the results shown, figures show the energy consumption in accumulated Joules over time. For a real reference, typical batteries for CWSNs have a total energy of 18,000 J.

5.3. Results and Discussion. In this section results of different simulations are discussed. Even if the simulations do not last as long as the battery life, energy consumption reduction can be appreciated for enhancing the network lifetime. Presented results always show the energy consumption for a CWSN node.

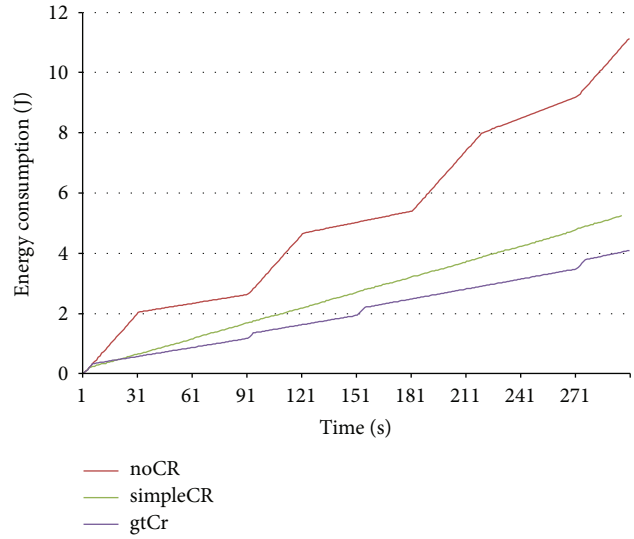

Figure 1: Baseline scenario.

For the first simulation, the baseline scenario is simulated with three different CWSN optimization strategies. The first one, marked in red, is a typical WSN without cognitive capabilities—noCR, which must remain on their initial channel even if this channel becomes very noisy. Green line—simpleCR, shows a first strategy approach to the CWSN, where cognitive nodes are able to sense the spectrum and change their transmission parameters accordingly. This first approach to the CWSN senses the spectrum every 2 s and changes the transmission and reception channel for the whole network. In this way, the least noisy channel is assured each 2 s. In the third CWSN strategy—gtCR, the proposed optimization strategy based on game theory explained in Section 4 is shown in purple. In order to compare energy consumption, the chosen sensing period is 2 s as well.

Figure 1 shows that even in the first 300 s gtCR strategy provides energy consumption savings of around 65% compared to the noCR scenario. Furthermore, these savings will increase over time as both noCR and simpleCR have steeper slopes in energy consumption. In relation to simpleCR, gtCR saves energy consumption by approximately 30% in the first 300 s. As in the previous case, these energy savings are increasing over time.

Figure 2 shows the energy consumed each second instead of the accumulated consumption over time for the baseline scenario. This figure shows the detailed energy consumption of the algorithm each time it is triggered.

Looking at the noCR line, energy consumption is lower than simpleCR when Wi-Fi channel does not overlap with the CWSN one. However, when the channel does coincide (0–30 or 90–120 seconds) energy consumption spikes.

Focusing on simpleCR energy consumption is almost regular throughout the simulation. This is due to the fact that energy consumption imposed by the sensing state is much higher than the energy consumption in transmission and reception modes in an ideal situation (without coexistence Wi-Fi) so the biggest amount of energy consumed comes from the sensing state.

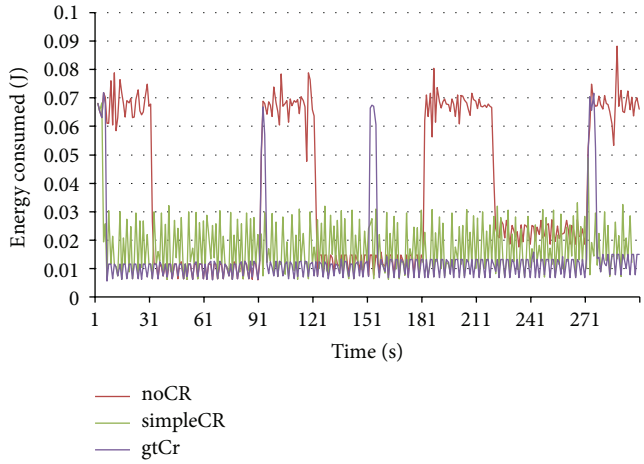

Figure 2: Instantaneous energy consumption for the baseline scenario.

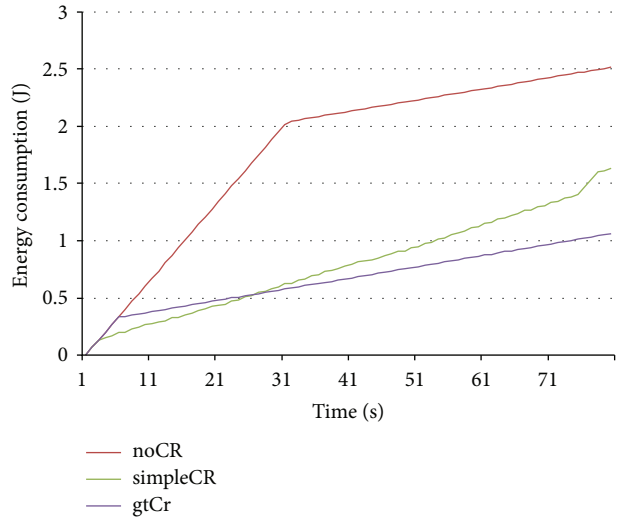

Figure 3: Baseline scenario with 50 Wi-Fi nodes.

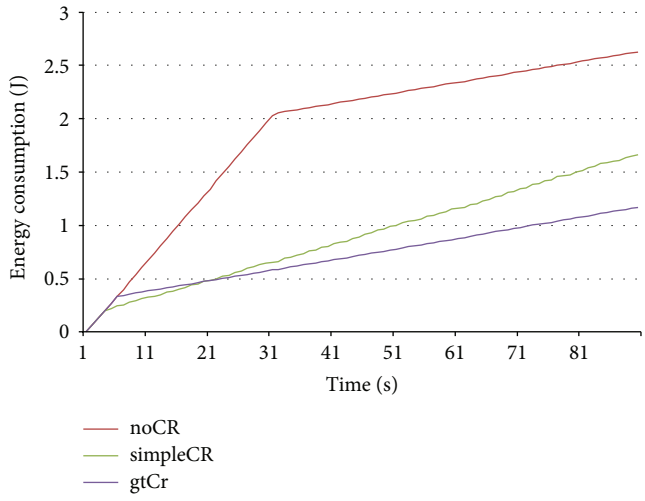

Figure 4: Baseline scenario with 200 Wi-Fi nodes.

Even though in some cases gtCR increases node processing consumption, for the strategy calculation, this energy cost is offset by the energy consumption savings by avoiding noisy channels.

The next simulations show the results of varying the number of Wi-Fi nodes on the baseline scenario in order to change noise in the area. These results can be seen in Figure 3, which uses 50 Wi-Fi nodes instead of 100 in the baseline scenario, and Figure 4, with 200 Wi-Fi nodes for a very noisy ambience.

As can be seen, both simulations are similar in shape and values as baseline scenario, so it can be concluded that the proposed algorithm is not influenced by the amount of noise present in the scenario.

The next scenario modifies the RSSI threshold used by the gtCR strategy as a first decision mechanism to show if this threshold influences the behavior of the strategy. In Figure 5, the behavior of the algorithm for different decision thresholds in dBm is shown.

As shown, algorithm performance is also not greatly influenced by the chosen threshold. This is because of the game-theory-based strategy design which takes into account subsequent corrections such as the number of retransmissions used to calculate the best moment to change the channel.

Small changes that are seen in the center values of the figure are due to the random character of the channel chosen by the Wi-Fi nodes, which makes CWSN nodes take the decision of change at 90 s or at 180 s depending on the existing noise in the channel. But energy consumption at 300 s is similar for every chosen threshold.

The next scenario changes the number of RSSI samples taken into account in order to calculate the RSSI value. The intention of these different values is to probe the strength of the strategy employed against anomalous measures of RSSI. For the simulation shown in Figure 6, different numbers of samples are taken.

The increased value of energy consumption shown in Figure 6 for 10 samples is due to the time waste produced by the sampling RSSI with every received packet. As the packet rate for the CWSN is 1 packet per second, it must wait longer to obtain more samples, thereby making the algorithm take longer to react to changes and trigger the game-theory-based strategy. Although increasing the number of samples protects the algorithm from possible erroneous samples, it is shown that the reaction time makes the CWSN node remain on a noisy channel longer; thus, the number of retransmissions increases, raising its consumption. The number of samples must be chosen depending on the WSN application scenario and the randomness of the noise.

For the next scenario it is interesting to vary the maximum number of retransmissions allowed by the CWSN nodes, as it is a parameter that depends directly on the decision to change the channel or not in the game-theory-based strategy design. Figure 7 shows the results.

As can be seen, the greater the maximum number of retransmissions set, the higher the energy consumption produced. In this case, it should reach a compromise between consumption and network reliability depending on the final

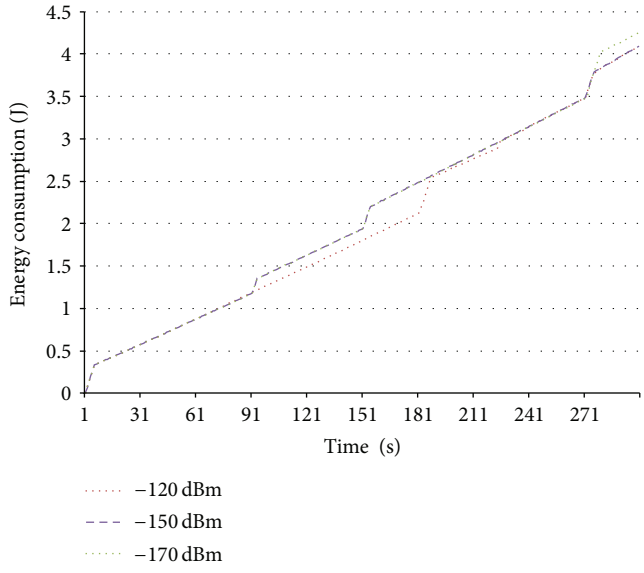

Figure 5: Scenario varying RSSI threshold.

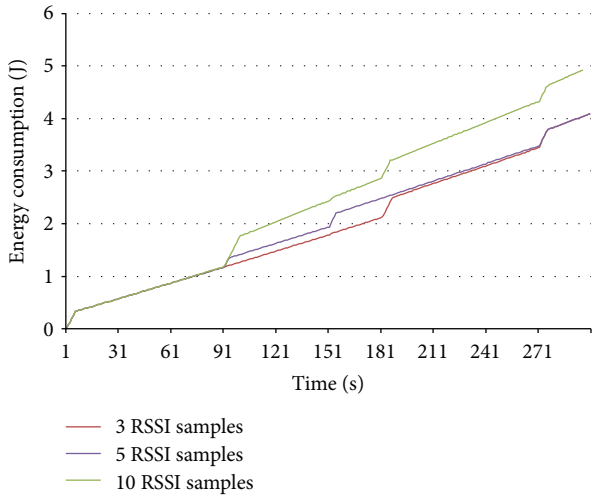

Figure 6: Scenario varying number of RSSI samples.

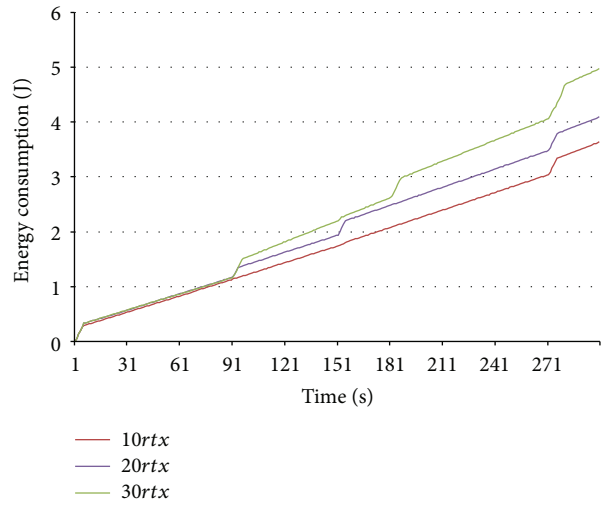

Figure 7: Scenario varying number of *rtx*.

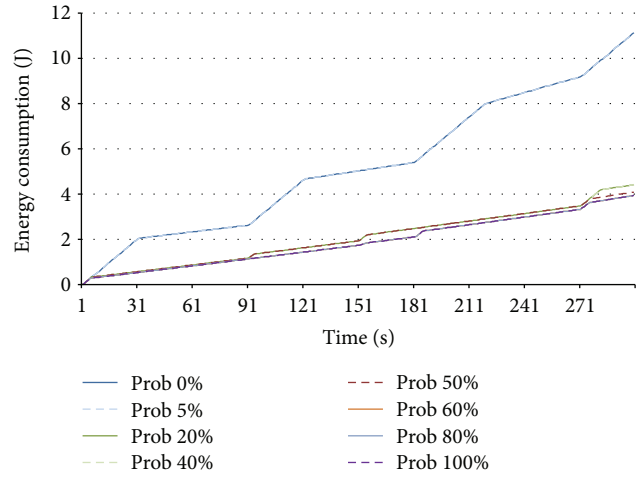

Figure 8: Scenario varying init probY.

application of the WSN or the importance of the data transmitted by the nodes.

One of the most interesting questions is how this strategy evolves depending on the initialization values of the probability of accepting the changes request y stored for the rest of the network nodes. This evolution could show if the strategy could adapt to real behavior or, instead, relies heavily on initialization values. In this case several experiments that include initialization values from 0 to 100% of change requests accepted are performed showing the following results.

Figure 8 shows that values from 0 to 5% demonstrate values similar to noCR techniques in energy consumption, shown in Figure 1. Moreover, 80% to 100% values are exactly the same, as are 50% to 60% and 20% to 40%.

In any case, it is shown that initialization values between 20% and 100% are quite similar in terms of long-term power consumption, indicating that the algorithm, regardless of its initialization, moves rapidly toward a stationary situation based on the sensed spectrum around the node and the behavior of the rest of the devices.

To summarize results, the algorithm shows improvement rates of over 65% compared to WSNs without cognitive techniques and over 30% compared to sensing strategies for changing channels based on a decision threshold. For the dependence of the values used in the payoff function, results are shown in Table 2.

6. Conclusions

WSNs are shown as one of the most important trends in wireless communication. Energy consumption became

Table 2: Results summary.

Parameter	Dependence	Factors
Number of nodes	No	
RSSI threshold	No	
RSSI samples	Yes	Application Data rate Sensing period
Number of *rtx*	Yes	Network reliability
Init probY	No (above 20%)	

an important problem to face in typical WSN application because of the use of batteries. The introduction of CN features opens up new interesting research challenges ranging from CR capabilities to WSN intrinsic features.

In this paper, a new strategy based on game theory for reducing energy consumption in CWSNs has been presented. This is a light optimization algorithm that enables its implementation in CWSNs although the nodes computing resources are limited. The strategy is applicable in conjunction with other energy consumption optimizations. This way the results can be further improved by incorporating routing protocols that have been proven efficient or MAC implementations for low consumption.

The developed algorithm has been tested on a framework based on Castalia adapted to incorporate cognitive capabilities. As seen in the results section, the algorithm shows improvement rates of over 65% compared to WSNs without cognitive techniques and over 30% compared to sensing strategies for changing channels based on a decision threshold.

It can also be seen that the algorithm behaves similarly even with significant variations in the number of noisy nodes. Likewise, RSSI decision threshold and the number of samples taken into account for their calculation do not influence the operation of the algorithm. In regard to the number of samples, the only relationship arises from taking a large number of samples, which increases the consumption as the node keeps in the noisy channel for too long.

Concerning the maximum number of retransmissions allowed for CWSN nodes, energy consumption increases along with them but is caused by the retransmissions itself and completely unrelated to the algorithm. In this case, a compromise should be reached between consumption and network reliability. The initialization value of the odds of change from other nodes does not significantly affect the performance of the algorithm for values above 20%, since this probability evolves based on the noise and not on its initialization.

Reducing energy consumption in WSNs is an interesting field in which there is much work to be done. CWSNs introduce new features to take advantage of and also new challenges to face. It would be interesting to see how this algorithm behaves on a larger network or a comparison with other game models.

Conflict of Interests

The authors declare that there is no conflict of interests regarding the publication of this paper.

Acknowledgment

This work was funded by the Spanish Ministry of Economy and Competitiveness, under INNPACTO Program (Reference Grant IPT-2011-1197-370000, PRECOIL; IPT-2011-1241-390000, LINEO; IPT-2011-0782-900000, S2S).

References

[1] Cisco Systems Inc., "Cisco visual networking index: global mobile data traffic forecast update, 2012–2017," Tech. Rep., 2013.

[2] I. Howitt and J. A. Gutierrez, "IEEE 802.15.4 low rate—wireless personal area network coexistence issues," in *Proceedings of the IEEE Wireless Communications and Networking (WCNC '03)*, vol. 3, pp. 1481–1486, New Orleans, La, USA, 2003.

[3] J. Mitola, *Cognitive radio: an integrated agent architecture for software defined radio [Ph.D. thesis]*, Royal Institute of Technology, Stockholm, Sweden, 2000.

[4] A. S. Zahmati, S. Hussain, X. Fernando, and A. Grami, "Cognitive wireless sensor networks: emerging topics and recent challenges," in *Proceedings of the IEEE Toronto International Conference—Science and Technology for Humanity (TIC-STH '09)*, pp. 593–596, Ontario, Canada, September 2009.

[5] D. J. Kadhim, S. Gong, W. Xia, W. Liu, and W. Cheng, "Power efficiency maximization in cognitive radio networks," in *Proceedings of the IEEE Wireless Communications and Networking Conference (WCNC '09)*, pp. 1–6, Budapest, Hungary, April 2009.

[6] I. Aissa, M. Frikha, and S. Tabbane, "A dynamic power management procedure in cognitive radio," in *Proceedings of the IFIP Wireless Days (WD '10)*, pp. 1–5, Venice, Italy, October 2010.

[7] G. Gür and F. Alagoüz, "Green wireless communications via cognitive dimension: an overview," *IEEE Network*, vol. 25, no. 2, pp. 50–56, 2011.

[8] O. B. Akan, O. B. Karli, and O. Ergul, "Cognitive radio sensor networks," *IEEE Network*, vol. 23, no. 4, pp. 34–40, 2009.

[9] G. Vijay, E. B. A. Bdira, and M. Ibnkahla, "Cognition in wireless sensor networks: a perspective," *IEEE Sensors Journal*, vol. 11, no. 3, pp. 582–592, 2011.

[10] I. Glaropoulos, V. Fodor, L. Pescosolido, and C. Petrioli, "Cognitive WSN transmission control for energy efficiency under WLAN coexistence," in *Proceedings of the 6th International ICST Conference on Cognitive Radio Oriented Wireless Networks and Communications (CROWNCOM '11)*, pp. 261–265, Yokohama, Japan, June 2011.

[11] L. Stabellini and J. Zander, "Energy-aware spectrum sensing in cognitive wireless sensor networks: a cross layer approach," in *Proceedings of the IEEE Wireless Communications and Networking Conference (WCNC '10)*, pp. 1–6, Sydney, Australia, April 2010.

[12] H. Y. Shi, W. L. Wang, N. M. Kwok, and S. Y. Chen, "Game theory for wireless sensor networks: a survey," *Sensors*, vol. 12, no. 7, pp. 9055–9097, 2012.

[13] B. Wang, Y. Wu, and K. J. R. Liu, "Game theory for cognitive radio networks: an overview," *Computer Networks*, vol. 54, no. 14, pp. 2537–2561, 2010.

[14] N. Tang, J. Sun, S. Shao, L. Yang, and H. Zhu, "An improved spectrum sharing algorithm in cognitive radio based on game theory," in *Proceedings of the 12th IEEE International Conference on Communication Technology (ICCT '10)*, pp. 504–507, Nanjing, China, November 2010.

[15] E. del Re, R. Pucci, and L. S. Ronga, "Energy efficient non-cooperative methods for resource allocation in cognitive radio networks," *Communications and Network*, vol. 4, pp. 1–7, 2012.

[16] J. D. Deaton, S. A. Ahmad, U. Shukla, R. E. Irwin, L. A. Dasilva, and A. B. MacKenzie, "Evaluation of dynamic channel and power assignment for cognitive networks," *Wireless Personal Communications*, vol. 57, no. 1, pp. 5–18, 2011.

[17] B. Chai, R. Deng, P. Cheng, and J. Chen, "Energy-efficient power allocation in cognitive sensor networks: a game theoretic approach," in *Proceedings of the of IEEE Global Communications Conference (GLOBECOM '12)*, pp. 416–421, Anaheim, Calif, USA, 2012.

[18] CC2530 Datasheet. Texas instruments, http://www.ti.com/lit/ds/symlink/cc2530.pdf.

[19] J. Cooper and C. Hinde, "Improving genetic algorithms' efficiency using intelligent fitness functions," in *Developments in Applied Artificial Intelligence*, vol. 2718 of *Lecture Notes in Computer Science*, pp. 636–643, Springer, Berlin, Germany, 2003.

[20] A. E. Ohazulike and T. Brands, "Multi-objective optimization of traffic externalities using tolls. A comparison of genetic algorithm and game theoretical approach," in *Proceedings of the IEEE Congress on Evolutionary Computation (CEC '13)*, pp. 2465–2472, Cancun, Mexico, 2013.

[21] J. Rabaey, A. Wolisz, A. Ercan et al., "Connectivity brokerage—enabling seamless cooperation in wireless networks," Tech. Rep., Berkeley Wireless Research Center, Berkeley, Calif, USA, 2010.

[22] A. Araujo, E. Romero, J. Blesa, and O. Nieto-Taladriz, "Cognitive wireless sensor networks framework for green communications design," in *Proceedings of the 2nd International Conference on Advances in Cognitive Radio (COCORA '12)*, pp. 34–40, Chamonix, France, 2012.

Hindawi Publishing Corporation
International Journal of Distributed Sensor Networks
Volume 2014, Article ID 453248, 9 pages
http://dx.doi.org/10.1155/2014/453248

Research Article

Energy Detection in Multihop Cooperative Diversity Networks: An Analytical Study

M. O. Mughal, L. Marcenaro, and C. S. Regazzoni

Department of Electrical, Electronic, Telecommunications Engineering and Naval Architecture, DITEN, University of Genova, Via Opera Pia 11A, 16145 Genova, Italy

Correspondence should be addressed to M. O. Mughal; ozairmughal@ginevra.dibe.unige.it

Received 6 September 2013; Revised 4 December 2013; Accepted 11 December 2013; Published 27 January 2014

Academic Editor: Khalid Al-Begain

This work presents a study of detection performance of energy detector in relay-based multihop cooperative diversity networks operating over independent Rayleigh fading channels. In particular, upper bound average detection probability expressions are obtained for three scenarios: (i) multihop cooperative relay communication; (ii) multi-hop cooperative relay communication with direct link and maximum ratio combiner (MRC) at destination; and (iii) multi-hop cooperative relay communication with direct link and selection combiner (SC) at destination. Classical method of performance evaluation based on probability density function (PDF) of received signal-to-noise ratio (SNR) is used. Furthermore, an alternative series form representation of generalized Marcum-Q function is employed in order to simplify the ensuing mathematical derivations. Because the obtained detection probability expressions are in the form of infinite summation series, their respective truncation error bounds are also derived. In the end, analyses are validated with the help of simulations and several observations regarding the impact of different parameters on detector's performance are outlined.

1. Introduction

Recently, a plethora of new wireless services are being introduced, which has in turn increased the demand for radio spectrum. As a result, radio spectrum is facing scarcity problem since most portions of the available spectrum are already allocated for different uses. However, it was reported in [1] that some frequency bands in the spectrum are largely underutilized most of the time. Cognitive radio (CR) [2, 3] has emerged as a firm candidate to address this spectrum scarcity problem. CR allows the unlicensed users to use licensed spectrum when it is vacant due to idle licensed users.

Spectrum sensing is the primary task of a CR transceiver and there are different detection methods to achieve it. These methods include matched filter detection, cyclostationary feature detection, and energy detection [4]. Among these, energy detector has the least implementation complexity and it was first analyzed over noisy channels by Urkowitz [5] to give mathematical expressions for false alarm probability (P_f) and detection probability (P_d). Few decades later, [6] revisited the energy detection problem and extended the work of [5] to fading channels. Kostylev [6] analyzed the energy detectors over Rayleigh, Rice, and Nakagami fading channels.

Since the advent of CR, energy detectors have gained enormous attention from researchers due to their simple structure and applicability to CR [7–15]. In particular, [7–9] studied the energy detectors with various diversity combiners over various fading environments. For instance, authors in [7] analyzed the energy detectors with combiners such as equal gain combiner (EGC), selection combiner (SC), and switch-and-stay combiner (SSC) to yield average P_d expressions. Reference [8] further expanded the work of [7] to analyze energy detectors with square-law combiner (SLC) and square-law selection combiner (SLS). Herath et al. [9] considered the same problem for maximum-ratio combiner (MRC) and EGC, using both probability density function (PDF) method and moment generating function (MGF) method. On the other hand, SC was analyzed only with PDF method in [9] because MGF method fails to give complete analytical solution for SC. The motivation for considering diversity combining was to increase the received signal-to-noise ratio (SNR), which in turn improves the detection performance.

Likewise, relay-based cooperative diversity may also improve the detection performance. It was illustrated by [10, 11] that cooperation not only improves the detection performance, but also improves the agility of the overall network. More recently, energy detectors were studied in dual-hop cooperative diversity networks operating over Rayleigh fading channels in [12–15]. Authors in [12] utilized the moment-generating function (MGF) method to derive closed-form upper bound expressions of the average P_d for dual-hop multiple relay cooperative diversity system, utilizing fixed-gain amplify-and-forward (AF) relays. On the other hand, authors in [13, 14] followed the classical probability density function (PDF) method to analyze variable-gain AF relay-based dual-hop three-node cooperative diversity system with MRC and SC at the destination, respectively. In addition, [14] also computed the truncation error bounds for truncating the infinite summation series in the final expressions. Reference [15] considered fixed-gain AF relay-based three-node system to compute exact average P_d expressions, as opposed to the upper-bounds presented in [12–14]. Authors in [15] also calculated the truncation error bounds to truncate infinite summation series in final P_d expressions to finite terms.

Over the past few years, multihop relay communications have gained attention from the radiocommunication research community due to their capability in rendering wider coverage with low transmitting powers. Therefore, in [12], authors briefly outlined the formulation of multihop relaying (without incorporating direct link) for average P_d analysis. An upper-bound on end-to-end SNR was considered in [12], which was further approximated using Padé approximation to find out the MGF of SNR in the multihop relay link. (For details on Padé approximation and ensuing derivations of the MGF, readers are suggested to refer [16].) This MGF was then utilized to obtain an approximate average P_d expression for multihop relay link transmission. It seems that the MGF method of [12] does not grant the analytical solution for average P_d in a multihop cooperative diversity system.

Due to this, we revert back to the classical PDF method of performance analysis in order to obtain analytical average P_d expressions for multihop cooperative diversity network. First, we model an analytical framework to obtain average P_d expression for multihop relay path communication. For this, the PDF of signal's SNR received over the multihop relay path is derived. This PDF is then utilized along with canonical series form representation of generalized Marcum-Q function to obtain average P_d expression of the multihop relay transmission. After that, the PDF of multihop cooperative diversity system is derived where the destination is assumed to combine the received direct and relay path signals using MRC. This PDF is then used to compute the overall average P_d of the multihop cooperative diversity system. In the end, SC is also considered for combining direct and relay path signals. Closed-form PDF expression is obtained for multihop cooperative diversity system with SC, which is then utilized to compute the average P_d of the considered system. Because the obtained analytical expressions were in the form of infinite summation series, their respective truncation error bounds are also calculated. These error bounds can be used to compute the finite number of terms required to achieve a given figure of accuracy. To the best of our knowledge, energy detection problem in multihop cooperative diversity networks is not reported so far in the open literature. It is expected that these analysis will assist in the study of future communication networks such as CRs.

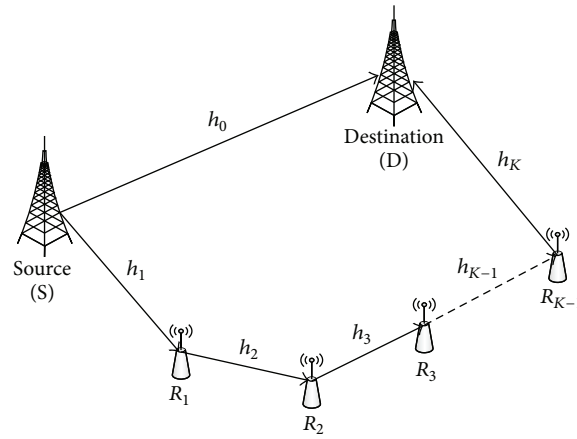

Figure 1: A multihop cooperative network consisting of a source terminal (S), a destination terminal (D), and multiple relay nodes (R_k, $1 \le k \le K-1$).

The paper is structured as follows. Section 2 outlines the channel and system model. Section 3 covers the analysis of energy detection in nonfading and fading environments. Section 4 is dedicated to detail the simulation and analytical results and finally the paper is concluded in Section 5.

2. Channel and System Model

A cooperative network is assumed where the source terminal (S) communicates with the destination terminal (D) with the help of $K-1$ relays (R_k, $1 \le k \le K-1$), as shown in Figure 1. Each relay amplifies the signal it receives either from source or from the previous relay and forwards the amplified signal only from previous hop to the next hop neighbour. The system is assumed to be operating over independent and identically distributed (IID), slowly varying, and flat Rayleigh fading channels, where h_0 is the channel gain of the direct path and h_k ($1 \le k \le K$) corresponds to the channel gain for each link in the multihop relay path. Total communication time is divided into K time slots such that each transmitting terminal uses only one time slot to communicate with the next terminal (as in time division multiple access systems). Therefore, the signals received at the destination side from the direct link and multihop relay link [17, equation (1)], over different time-slots can be, respectively, expressed as

$$x_0(t) = h_0 s_p(t) + n_0(t),$$
$$x_K(t) = h_K \prod_{k=1}^{K-1} G_k h_k s_p(t) + \sum_{k=1}^{K-1} \prod_{j=k}^{K-1} G_j h_{j+1} n_k(t) + n_K(t), \quad (1)$$

where $s_p(t)$ is the source transmitted unknown deterministic signal and n_0 is the additive white Gaussian noise (AWGN)

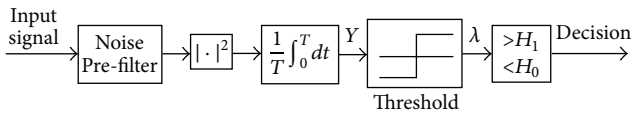

Figure 2: A generic block diagram of an energy detector.

on the direct link. Additionally, h_k and n_k represent the channel gain and AWGN for the kth link while h_K and n_K are the channel gain and noise for the Kth link, in the multihop relay path. We assume that all the AWGNs are modeled as zero mean and $\{N_{0,k}\}_{k=0}^{K}$ variance. For our system model, we choose the relay-gain G_k as $G_k^2 = 1/(|h_{k-1}|^2 + N_{0,k})$. Note that the relays employing this kind of relay-gain are referred to as variable-gain relays [13, 14]. They are on the contrary to fixed-gain relays which were assumed in [12, 15] and have gain, $G_k^2 = 1/(\mathbf{E}(|h_{k-1}|^2) + N_{0,k})$, where $\mathbf{E}(\cdot)$ is the mathematical expectation operator. An advantage of variable-gain relays over fixed-gain relays is a slightly better performance of the former, which comes at a cost of additional processing overhead. It is because variable-gain relays require the instantaneous channel state information of the preceding hop to produce their gain while forwarding received signals over the next hop. The total end-to-end SNR for the multihop relay path is expressed as [18]

$$\gamma_{\text{rel}} = \left[\prod_{k=1}^{K-1}\left(1 + \frac{1}{\gamma_k}\right) - 1\right]^{-1}, \tag{2}$$

where $\gamma_k = |h_k|^2/N_{0,k}$ is the instantaneous SNR of the kth hop. Because channels are assumed to follow Rayleigh distribution, the instantaneous SNR (γ_k) follows exponential distribution, with cumulative distribution function (CDF) and PDF, respectively, expressed as

$$\begin{aligned} F_{\gamma_k}(\gamma) &= 1 - \exp\left(-\frac{\gamma}{\overline{\gamma_k}}\right), \\ f_{\gamma_k}(\gamma) &= \frac{1}{\overline{\gamma_k}}\exp\left(-\frac{\gamma}{\overline{\gamma_k}}\right), \end{aligned} \tag{3}$$

where $\overline{\gamma_k} = \mathbf{E}(\gamma_k)$ is the average SNR of the kth link and $\mathbf{E}(\cdot)$ is the mathematical expectation operator.

It is well known that the performance of the multihop relay path is dominated by that of the weakest hop or link [18], because outage in the single hop can cause the entire relay path to fail. Therefore, γ_{rel} can be tightly upper-bounded as follows:

$$\gamma_{\text{rel}} \leq \gamma_{\min} = \min\left(\{\gamma_k\}_{k=1}^{K}\right). \tag{4}$$

This bound is common for the asymptotic analysis of dual-hop relay links; for example, see [12–14]. Furthermore, using the above bound greatly simplifies the ensuing mathematical analysis because of the convenience in finding the associated CDF and PDF statistics, as will become clear in the next section.

3. Mathematical Analysis

In what follows, formulation of energy detection in nonfading environment is outlined first, followed by the mathematical analysis of energy detection in fading channels using cooperative diversity technique.

3.1. Energy Detection in Nonfading Environment. It is well known that spectrum sensing task is the decision problem on the following two hypotheses:

$$x(t) = \begin{cases} n(t) & H_0 \\ hs(t) + n(t) & H_1, \end{cases} \tag{5}$$

where H_0 and H_1 are the hypotheses for the absence and presence of signal, respectively. The situation of interest is shown in the block diagram of an energy detector in Figure 2. At the destination, the input signal is fed to the noise prefilter of bandwidth W. The output of this filter is then squared and integrated over the time interval T in order to measure the received energy. Now the output of the integrator, Y, is compared with a predefined threshold, λ, to test the binary hypotheses H_0 and H_1. Although this process is of band-pass type, we can still deal with its low-pass equivalent because it has been proved in [5] that both low-pass and band-pass processes are equivalent from a decision statistics point of view, which is our main point of attention. The PDF of Y, $f_Y(y)$, is expressed as [7, 8]

$$f_Y(y) = \begin{cases} \dfrac{1}{2^u\Gamma(u)}y^{u-1}e^{-y/2} & H_0 \\ \dfrac{1}{2}\left(\dfrac{y}{2\gamma}\right)^{(u-1)/2} e^{-(2\gamma+y)/2}I_{u-1}\left(\sqrt{2\gamma y}\right) & H_1, \end{cases} \tag{6}$$

where $u = \text{TW}$ is restricted to integer values, $\Gamma(\cdot)$ is the gamma function [19, Section 8.31], and $I_v(\cdot)$ is the vth order modified Bessel function of the first kind [19, Section 8.40].

In a nonfading environment, the probabilities of false alarm (P_f) and detection (P_d) are expressed as [8]

$$P_f = \frac{\Gamma(u, \lambda/2)}{\Gamma(u)}, \tag{7}$$

$$P_d = Q_u\left(\sqrt{2\gamma}, \sqrt{\lambda}\right), \tag{8}$$

where $\Gamma(\cdot,\cdot)$ is the upper incomplete gamma function [19, equation (8.350.2)] and $Q_u(\cdot,\cdot)$ is the uth order generalized Marcum Q-function defined as [20]

$$Q_u(a,b) = \int_b^\infty \frac{x^u}{a^{u-1}}\exp\left(-\frac{x^2+a^2}{2}\right)I_{u-1}(ax)\,\mathrm{d}x. \tag{9}$$

An alternate canonical series form representation of the generalized Marcum Q-function is reported in [21, equation (4.74)], which can be further simplified by noting the relationship of finite summation series with upper incomplete gamma function as outlined in [19, Section 8.352] to give

$$Q_u\left(\sqrt{2\gamma}, \sqrt{\lambda}\right) = \sum_{n=0}^{\infty} e^{-\gamma}\frac{\gamma^n}{n!}\frac{\Gamma(n+u, \lambda/2)}{(n+u-1)!}. \tag{10}$$

Although the above expression of $Q_u(\cdot,\cdot)$ requires summation up to infinite terms, we will be using this expression subsequently because it aids in simplifying the involved mathematical analysis. The problem of infinite summation will be dealt with by deriving truncation error bounds when truncating the series to finite terms.

3.2. Energy Detection in Fading Environment: Relay Link Only. It is clearly observable that false alarm probability is independent of γ. Therefore, average P_f for the fading channels can be calculated from (7). On the other hand, the detection probability is *conditioned* on γ. In this case, average P_d may be derived by averaging (8) over the fading statistics:

$$\overline{P_d} = \int_{\gamma} Q_u\left(\sqrt{2\gamma}, \sqrt{\lambda}\right) f_{\gamma}(\gamma)\, \mathrm{d}\gamma. \tag{11}$$

In order to obtain average P_d for the multihop relay path, it is required to obtain the PDF of γ_{rel}. However, a tight upper-bound on γ_{rel}, namely, $\gamma_{\min}$, was noted in previous section to aid in simplification of the involved mathematical derivations. Therefore, we will proceed with the derivation of PDF of $\gamma_{\min}$ in the following to arrive at average P_d expression for the multihop relay communication.

From probability theory, it is well known that if $X_1, \ldots, X_i$ are independent exponential random variables with parameters $\mu_1, \ldots, \mu_i$, then $\min(X_1, \ldots, X_i)$ is also exponential with $\mu = \mu_1 + \cdots + \mu_i$ [22, page 246]. Therefore, PDF of $\gamma_{\min}$ can be expressed as

$$f_{\gamma_{\min}}(\gamma) = \sum_{k=1}^{K} \left(\frac{1}{\overline{\gamma}_k}\right) e^{-\sum_{k=1}^{K}(1/\overline{\gamma}_k)\gamma}. \tag{12}$$

Taking first-order integral of the above with respect to γ, we get the CDF of $\gamma_{\min}$ as shown below:

$$F_{\gamma_{\min}}(\gamma) = 1 - e^{-\sum_{k=1}^{K}(1/\overline{\gamma}_k)\gamma}. \tag{13}$$

Substituting (12) and (10) into (11), average P_d for multihop relay path is expressed in integral form as

$$\overline{P}_{d,\mathrm{rel}} = \sum_{k=1}^{K} \left(\frac{1}{\overline{\gamma}_k}\right) \sum_{n=0}^{\infty} \frac{1}{n!} \int_0^{\infty} \gamma^n e^{-(1+\sum_{k=1}^{K}(1/\overline{\gamma}_k))\gamma} \mathrm{d}\gamma \times \frac{\Gamma(n+u, \lambda/2)}{(n+u-1)!} \tag{14}$$

and the integral in above expression can be solved using the identity reported in [19, equation (3.351.3)] to give $\overline{P}_{d,\mathrm{rel}}$ as follows:

$$\overline{P}_{d,\mathrm{rel}} = \sum_{n=0}^{\infty} \left[\frac{\sum_{k=1}^{K}(1/\overline{\gamma}_k)}{\left(1+\sum_{k=1}^{K}(1/\overline{\gamma}_k)\right)^{n+1}}\right] \frac{\Gamma(n+u, \lambda/2)}{(n+u-1)!}. \tag{15}$$

The above expression gives the average P_d for the multihop relay path but is in the form of infinite summation series.

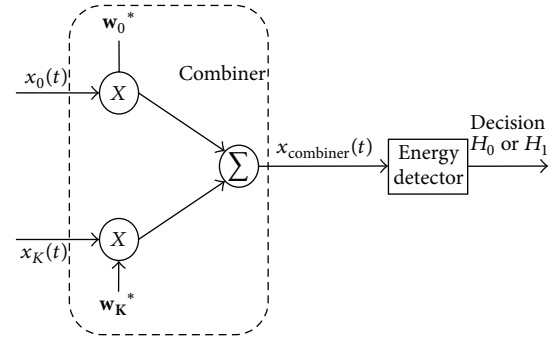

Figure 3: A hypothetical diagram of a dual-branch predetection combiner followed by an energy detector.

The error bound in truncating the infinite summation series in above expression can be obtained as shown in [14]

$$\left|E_{\mathrm{rel}}\right| = \left[\left\{ {}_1F_0\left(1;; \frac{1}{1+\sum_{k=1}^{K}(1/\overline{\gamma}_k)}\right) - \sum_{n=0}^{N}\left(\frac{1}{1+\sum_{k=1}^{K}(1/\overline{\gamma}_k)}\right)^n \right\} \times \frac{\sum_{k=1}^{K}(1/\overline{\gamma}_k)}{1+\sum_{k=1}^{K}(1/\overline{\gamma}_k)}\right] \frac{\Gamma(N+u, \lambda/2)}{(N+u-1)!}, \tag{16}$$

where the function ${}_1F_0(a;;x) = \sum_{n=0}^{\infty}((a)_n/n!)x^n$ is a special case of generalized hypergeometric series [19, equation (9.14.1)] and $(\cdot)_n$ denotes the Pochhammer symbol such that $(a)_n = \Gamma(a+n)/\Gamma(a)$. Finite number of terms required to achieve given figure of accuracy can be easily calculated from the above expression.

3.3. Energy Detection in Fading Environment: Incorporating Direct Link Using MRC. In the preceding subsection, only relay path signals were used for energy detection. Now suppose that direct path signals can also be received at the destination. Then, the destination can combine the direct and relay path signals by means of a predetection diversity combiner as shown in Figure 3, where, $\mathbf{w_0}$ and $\mathbf{w_K}$ are the weight factors which are different for different combining schemes. All predetection combiners such as MRC, EGC and SC require channel state information (CSI) of each branch in order to combine the received signals. This CSI may be available to relays and destination nodes over control channel or over a broadcast channel through an access point in a cognitive radio network [23, 24].

Although the idea of using a predetection combiner with energy detector appears to be contrasting, the main objective of this assumption is to obtain the optimum achievable performance for energy detector. Hence, the analyses presented in this paper clarify the fundamental performance limits of energy detector in a multihop cooperative diversity system. Furthermore, the use of predetection combiners followed by the noncoherent detector have been under investigation by many researches lately. For example, [7, 9, 25] used different

predetection combiners to coherently combine the received signals on multiple diversity branches in conjunction with noncoherent detector (Please note that our system model is different from these references as we consider relay-based cooperative diversity system.).

Among various diversity combiners, MRC is considered the optimum combiner because it maximizes the SNR at its output; that is, $\mathbf{w_0}$ and $\mathbf{w_K}$ correspond to the weights which maximizes the output SNR. Needless to say that the best option for MRC is to choose the weights to be the fading of each branch. The instantaneous SNR at the destination due to MRC combiner can be expressed as

$$\gamma_{\mathrm{MRC}} = \gamma_0 + \gamma_{\min}. \tag{17}$$

Because of the independence of channels, the PDF of γ_{MRC} can be computed by convolving the individual PDFs of γ_0 and $\gamma_{\min}$ as follows:

$$\begin{aligned} f_{\gamma_{\mathrm{MRC}}}(\gamma) &= \int_0^{\gamma} f_{\gamma_0}(\gamma)\, f_{\gamma_{\min}}(\gamma - z)\, \mathrm{d}z \\ &= \frac{1}{\overline{\gamma}_0 - \left(\sum_{k=1}^{K} (1/\overline{\gamma}_k)\right)^{-1}} \left[e^{-\gamma/\overline{\gamma}_0} - e^{-\sum_{k=1}^{K}(1/\overline{\gamma}_k)\gamma}\right]. \end{aligned} \tag{18}$$

Now, using (10), (11), and (18), the overall average P_d for multihop cooperative diversity system can be expressed in integral form as

$$\begin{aligned} \overline{P}_{d,\mathrm{MRC}} = {} & \frac{1}{\overline{\gamma}_0 - \left(\sum_{k=1}^{K} (1/\overline{\gamma}_k)\right)^{-1}} \sum_{n=0}^{\infty} \frac{1}{n!} \\ & \times \int_0^{\infty} \gamma^n \left(e^{-(1+(1/\overline{\gamma}_0))\gamma} - e^{-(1+\sum_{k=1}^{K}(1/\overline{\gamma}_k))\gamma}\right) \mathrm{d}\gamma \\ & \times \frac{\Gamma(n+u, \lambda/2)}{(n+u-1)!}. \end{aligned} \tag{19}$$

Now it is easy to solve the integral in above expression by using [19, equation (3.351.3)] as before. Finally, after some mathematical simplifications, $\overline{P}_{d,\mathrm{MRC}}$ can be expressed as

$$\begin{aligned} \overline{P}_{d,\mathrm{MRC}} = {} & \frac{1}{\overline{\gamma}_0 - \left(\sum_{k=1}^{K} (1/\overline{\gamma}_k)\right)^{-1}} \\ & \times \sum_{n=0}^{\infty} \left[\frac{1}{\left(1 + (1/\overline{\gamma}_0)\right)^{n+1}} - \frac{1}{\left(1 + \sum_{k=1}^{K} (1/\overline{\gamma}_k)\right)^{n+1}}\right] \\ & \times \frac{\Gamma(n+u, \lambda/2)}{(n+u-1)!}. \end{aligned} \tag{20}$$

Note that when $K = 2$ (i.e., dual-hop), (20) reduces to the results presented in [13]. Hence, average P_d expression of multihop cooperative diversity system with MRC at the destination, derived in this work is a generalization of the results presented in [13]. The truncation error bound in this case can be expressed as

$$\begin{aligned} \left|E_{\mathrm{MRC}}\right| = {} & \frac{1}{\overline{\gamma}_0 - \left(\sum_{k=1}^{K} (1/\overline{\gamma}_k)\right)^{-1}} \\ & \times \left[\left\{ {}_1F_0\left(1;; \frac{1}{1 + (1/\overline{\gamma}_0)}\right) - \sum_{n=0}^{N} \left(\frac{1}{1 + (1/\overline{\gamma}_0)}\right)^n \right\} \right. \\ & \quad \times \frac{1}{1 + (1/\overline{\gamma}_0)} \\ & \quad - \left\{ {}_1F_0\left(1;; \frac{1}{1 + \sum_{k=1}^{K} (1/\overline{\gamma}_k)}\right) \right. \\ & \qquad \left. - \sum_{n=0}^{N} \left(\frac{1}{1 + \sum_{k=1}^{K} (1/\overline{\gamma}_k)}\right)^n \right\} \\ & \qquad \left. \times \frac{1}{1 + \sum_{k=1}^{K} (1/\overline{\gamma}_k)} \right] \frac{\Gamma(N+u, \lambda/2)}{(N+u-1)!}. \end{aligned} \tag{21}$$

Using above expression, finite number of terms required to obtain given accuracy figure can be computed.

3.4. Energy Detection in Fading Environment: Incorporating Direct Link Using SC. Although MRC is the optimum combiner for diversity systems, it comes at the cost of increased computational burden on the receiver terminal. SC on the other hand provides comparable performance to that of MRC with less computational burden. It selects the branch with the maximum SNR and performs detection on the signal from the selected path. Therefore, at any instant in SC, the best SNR branch's weight factor will be "1" while the other will be "0." The instantaneous SNR for the SC is expressed as

$$\gamma_{\mathrm{SC}} = \max\left(\gamma_0, \gamma_{\min}\right). \tag{22}$$

Utilizing the CDFs and PDFs of γ_0 and $\gamma_{\min}$, the PDF of γ_{SC} can be computed using the equation reported in [22, Section 6.2] as follows:

$$\begin{aligned} f_{\gamma_{\mathrm{SC}}}(\gamma) &= F_{\gamma_0}(\gamma)\, f_{\gamma_{\min}}(\gamma) + f_{\gamma_0}(\gamma)\, F_{\gamma_{\min}}(\gamma) \\ &= \frac{1}{\overline{\gamma}_0} e^{-\gamma/\overline{\gamma}_0} + \sum_{k=1}^{K} \left(\frac{1}{\overline{\gamma}_k}\right) e^{-\sum_{k=1}^{K}(1/\overline{\gamma}_k)\gamma} \\ &\quad - \sum_{k=0}^{K} \left(\frac{1}{\overline{\gamma}_k}\right) e^{-\sum_{k=0}^{K}(1/\overline{\gamma}_k)\gamma}. \end{aligned} \tag{23}$$

Substituting (10) and (23) into (11), average P_d for multihop cooperative networks with SC at the destination is expressed as

$$\overline{P}_{d,\mathrm{SC}} = \sum_{n=0}^{\infty} \frac{1}{n!} \left[\frac{1}{\overline{\gamma}_0} \int_0^{\infty} \gamma^n e^{-(1+(1/\overline{\gamma}_0))\gamma} \mathrm{d}\gamma + \frac{1}{\sum_{k=1}^{K} (1/\overline{\gamma}_k)} \int_0^{\infty} \gamma^n e^{-(1+\sum_{k=1}^{K}(1/\overline{\gamma}_k))\gamma} \mathrm{d}\gamma - \frac{1}{\sum_{k=0}^{K} (1/\overline{\gamma}_k)} \int_0^{\infty} \gamma^n e^{-(1+\sum_{k=0}^{K}(1/\overline{\gamma}_k))\gamma} \mathrm{d}\gamma \right] \times \frac{\Gamma(n+u, \lambda/2)}{(n+u-1)!}. \tag{24}$$

Now all the integrals in above expression are in such form that they can be solved using [19, equation 3.351.3] as before. Therefore, average P_d in this case is

$$\overline{P}_{d,\mathrm{SC}} = \sum_{n=0}^{\infty} \left[\frac{1/\overline{\gamma}_0}{\left(1+(1/\overline{\gamma}_0)\right)^{n+1}} + \frac{\sum_{k=1}^{K}(1/\overline{\gamma}_k)}{\left(1+\sum_{k=1}^{K}(1/\overline{\gamma}_k)\right)^{n+1}} - \frac{\sum_{k=0}^{K}(1/\overline{\gamma}_k)}{\left(1+\sum_{k=0}^{K}(1/\overline{\gamma}_k)\right)^{n+1}} \right] \frac{\Gamma(n+u, \lambda/2)}{(n+u-1)!}. \tag{25}$$

Interesting to note is that, for dual-hop case, the above expression reduces to the results reported in [14, equation (13)]. Hence average P_d expression of multihop cooperative diversity system with SC at the destination, derived in this work, is a generalization of the results stated in [14]. To the best of our knowledge, no average P_d expression for cooperative multihop diversity system is reported so far in the literature and hence, (20) and (25) are novel.

The truncation error bound while truncating the infinite summation series in above expression is given as

$$\begin{aligned} |E_{\mathrm{SC}}| &= \left[\left({}_1F_0\left(1;; \frac{1}{1+(1/\overline{\gamma}_0)}\right) - \sum_{n=0}^{N} \left(\frac{1}{1+(1/\overline{\gamma}_0)} \right)^n \right) \times \frac{1/\overline{\gamma}_0}{1+(1/\overline{\gamma}_0)} \right. \\ &\quad + \left({}_1F_0\left(1;; \frac{1}{1+\sum_{k=1}^{K}(1/\overline{\gamma}_k)}\right) - \sum_{n=0}^{N} \left(\frac{1}{1+\sum_{k=1}^{K}(1/\overline{\gamma}_k)} \right)^n \right) \times \frac{\sum_{k=1}^{K}(1/\overline{\gamma}_k)}{1+\sum_{k=1}^{K}(1/\overline{\gamma}_k)} \\ &\quad - \left({}_1F_0\left(1;; \frac{1}{1+\sum_{k=0}^{K}(1/\overline{\gamma}_k)}\right) - \sum_{n=0}^{N} \left(\frac{1}{1+\sum_{k=0}^{K}(1/\overline{\gamma}_k)} \right)^n \right) \times \frac{\sum_{k=0}^{K}(1/\overline{\gamma}_k)}{1+\sum_{k=0}^{K}(1/\overline{\gamma}_k)} \left. \right] \\ &\quad \times \frac{\Gamma(N+u, \lambda/2)}{(N+u-1)!}. \end{aligned} \tag{26}$$

In next section, we show the simulation results and outline several observations based on them.

4. Simulation Results

Analyses of the previous sections are validated using the simulations. Receiver operating characteristic (ROC) curves are plotted with the assumption that all channels are under the influence of independent and identically distributed (IID) Rayleigh fading and average SNR on each link is equal, that is, $\overline{\gamma}_0 = \overline{\gamma}_1 = \cdots = \overline{\gamma}_K$. Threshold ($\lambda$) values are computed by varying P_f from 10^{-4} to 10^0, using (7). Several observations are made which are outlined below.

Figure 4 shows the comparison of analytical equation (15) with its simulation counterpart. The curves are plotted against different number of hops (K) on varying values of SNR. Furthermore, the value of u is fixed at $u = 2$. It is clearly observable that the analytical curves of this study lie tightly above their corresponding simulation curves at different values of SNR and K, indicating the accuracy of our analysis. Secondly, it is evident from this figure that, with increasing SNR, the detection performance of energy detector also improves, as expected.

In Figures 5 and 6, the analytical curves for (20) and (25) are plotted against different number of hops at varying values of SNR, respectively. For comparison, analytical results of [13], which considers dual-hop cooperative diversity system with MRC at destination, are also plotted in Figure 5. Likewise, the results of [14] are shown in Figure 6 for comparison with (25) of this study. As was noted in the previous section, the analytical curves of [13, 14] coincide with the analytical curves of (20) and (25), respectively. Hence, it shows that this study is a generalization of the results presented in [13, 14]. Furthermore, from the study of multihop systems [17, 18], it was substantiated that the performance of such systems decrease with the increase in number of hops. This is also consolidated through this study because with increasing number of hops, the detection performance deteriorates, as can be seen in both figures. Moreover, it should be noted that, with increasing number of hops, the ensuing communication delay also increases.

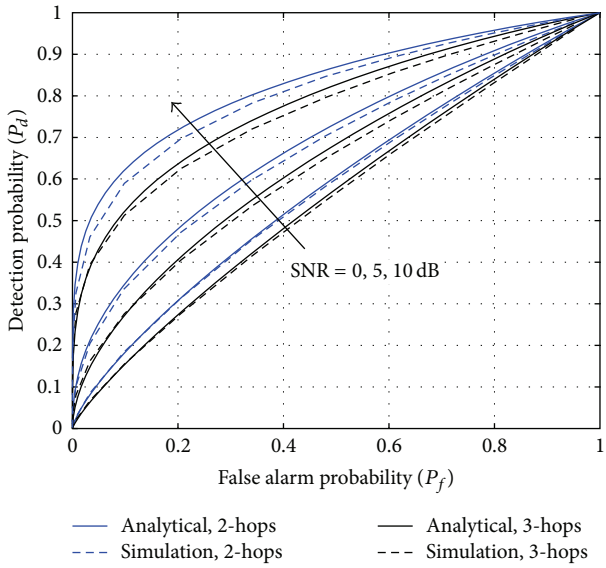

Figure 4: ROC curves comparing analytical $\overline{P}_{d,\text{rel}}$ with its simulation counterpart at different values of SNR and different number of hops (K).

Table 1: Required number of terms for four figure accuracy.

$P_f = 0.01, u = 2$	0 dB	3 dB	5 dB	10 dB
N from (16), $K = 2$	06	09	15	37
N from (16), $K = 3$	03	07	11	26
N from (16), $K = 5$	02	04	06	17
N from (21), $K = 2$	11	18	27	79
N from (21), $K = 3$	10	18	26	76
N from (21), $K = 5$	10	17	25	74
N from (26), $K = 2$	10	17	25	73
N from (26), $K = 3$	09	17	25	72
N from (26), $K = 5$	09	17	24	72

Therefore, it seems optimal to keep the number of hops minimal to ensure signal detection within feasible time.

To see the effect of number of samples (u) on detection performance, ROC curves for $\overline{P}_{d,\text{MRC}}$ and $\overline{P}_{d,\text{SC}}$ are plotted over different SNRs and varying values of u, in Figure 7. At each given SNR value, detection performance deteriorates when u is increased. It is in agreement with various previous studies of the energy detectors because for a same signal energy, energy detector exhibits better performance with fewer number of samples [14]. Finally note that MRC provides slightly better detection performance than SC at each value of SNR and u. However, this performance improvement comes at the cost of increased implementation complexity of MRC over SC. Hence, choice of combiner can be made depending on the flexibility of desired performance matrices.

Required number of terms for a given figure of accuracy, as per (16), (21), and (26), is listed in Table 1. For fixed values of $P_f = 0.01$ and $u = 2$, the table is populated by varying SNRs and number of hops. The number of terms listed in Table 1 is used to simulate the analytical results in Figures 4–7.

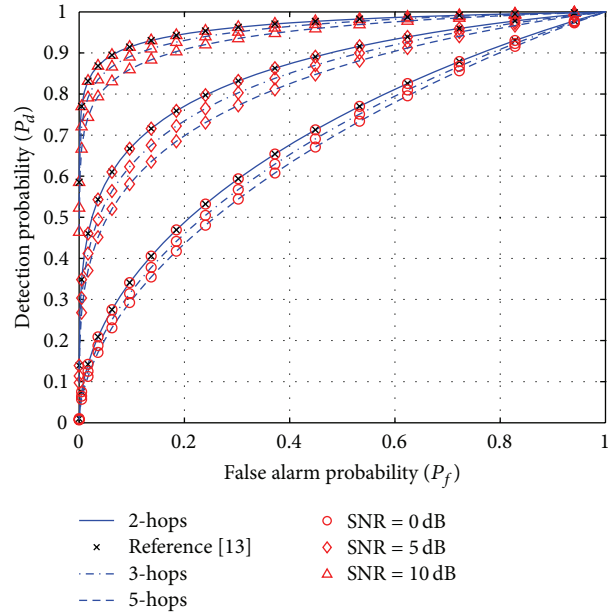

Figure 5: ROC curves of $\overline{P}_{d,\text{MRC}}$ with different number of hops at various SNR values along with the results of [13] for comparison.

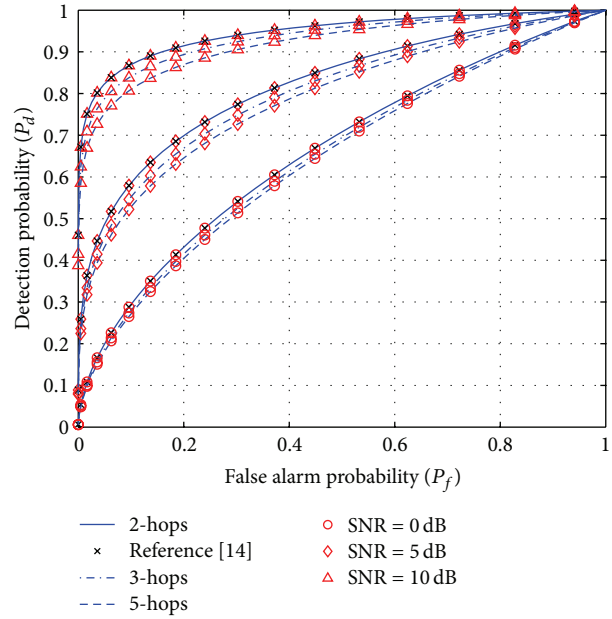

Figure 6: ROC curves of $\overline{P}_{d,\text{SC}}$ with different number of hops at various SNR values along with the results of [14] for comparison.

5. Conclusion

Energy detector appears as a preferred choice for spectrum sensing in cognitive radio-based systems because of its low implementation complexity. Because of this, energy detectors are under investigation by many researches lately. Nevertheless, energy detectors are known for poor performance at low SNR values. Therefore, relay-based cooperative diversity was proposed as one of the solutions to cope with this problem.

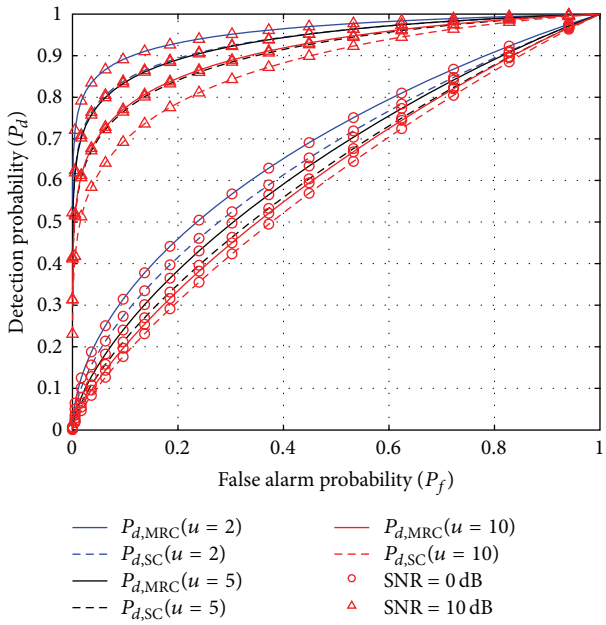

FIGURE 7: ROC curves comparing $\overline{P}_{d,\mathrm{MRC}}$ and $\overline{P}_{d,\mathrm{SC}}$ at various SNR values and different number of samples ($u = 2, 5, 10$).

In this work, detailed mathematical analysis was presented to quantify the energy detector in multihop cooperative relay networks. Average detection probability expressions were derived both for the multihop relay transmission and for the multihop cooperative diversity system where the system was assumed to be operating over IID Rayleigh fading channels. Truncation error bounds were also calculated because the obtained expressions were in the form of infinite summation series. In the end, the derived analytical results were validated with the help of simulations. It is expected that these analyses will turn out to be helpful in the study of future communication technologies such as cognitive radio.

Conflict of Interests

The authors declare that there is no conflict of interests regarding the publication of this paper.

Acknowledgment

This work was developed within nSHIELD project (http://www.newshield.eu/) cofunded by the ARTEMIS JOINT UNDERTAKING (Subprogramme SP6) focused on the research of SPD (Security, Privacy, Dependability) in the context of Embedded Systems.

References

[1] "Spectrum policy task force," Report ET Docket 02-135, Federal Communications Commission, 2002.

[2] J. Mitola III and G. Q. Maguire Jr., "Cognitive radio: making software radios more personal," *IEEE Personal Communications*, vol. 6, no. 4, pp. 13–18, 1999.

[3] S. Haykin, "Cognitive radio: brain-empowered wireless communications," *IEEE Journal on Selected Areas in Communications*, vol. 23, no. 2, pp. 201–220, 2005.

[4] I. F. Akyildiz, W.-Y. Lee, M. C. Vuran, and S. Mohanty, "Next generation/dynamic spectrum access/cognitive radio wireless networks: a survey," *Computer Networks*, vol. 50, no. 13, pp. 2127–2159, 2006.

[5] H. Urkowitz, "Energy detection of unknown deterministic signals," *Proceedings of the IEEE*, vol. 3, no. 4, pp. 523–531, 1967.

[6] V. Kostylev, "Energy detection of a signal with random amplitude," in *Proceedings of the IEEE International Conference on Communications*, vol. 3, pp. 1606–1610, April 2002.

[7] F. F. Digham, M.-S. Alouini, and M. K. Simon, "On the energy detection of unknown signals over fading channels," in *Proceedings of the International Conference on Communications (ICC '03)*, vol. 5, pp. 3575–3579, May 2003.

[8] F. F. Digham, M.-S. Alouini, and M. K. Simon, "On the energy detection of unknown signals over fading channels," *IEEE Transactions on Communications*, vol. 55, no. 1, pp. 21–24, 2007.

[9] S. P. Herath, N. Rajatheva, and C. Tellambura, "Energy detection of unknown signals in fading and diversity reception," *IEEE Transactions on Communications*, vol. 59, no. 9, pp. 2443–2453, 2011.

[10] G. Ganesan and Y. Li, "Cooperative spectrum sensing in cognitive radio, part I: two user networks," *IEEE Transactions on Wireless Communications*, vol. 6, no. 6, pp. 2204–2213, 2007.

[11] G. Ganesan and Y. Li, "Cooperative spectrum sensing in cognitive radio, part II: multiuser networks," *IEEE Transactions on Wireless Communications*, vol. 6, no. 6, pp. 2214–2222, 2007.

[12] S. Atapattu, C. Tellambura, and H. Jiang, "Energy detection based cooperative spectrum sensing in cognitive radio networks," *IEEE Transactions on Wireless Communications*, vol. 10, no. 4, pp. 1232–1241, 2011.

[13] M. O. Mughal, J. Gu, and J. Kim, "Detection probability analysis for AF assisted cooperative spectrum sensing in cognitive radio networks," in *Proceedings of the International Conference on ICT Convergence (ICTC '11)*, pp. 461–464, September 2011.

[14] M. O. Mughal, A. Razi, and J. M. Kim, "Tight upper bounds on average detection probability in cooperative relay networks with selection combiner," *Transactions on Emerging Telecommunications Technologies*, 2013.

[15] M. O. Mughal, A. Razi, S. S. Alam, L. Marcenaro, and C. S. Regazzoni, "Analysis of energy detector in cooperative relay networks for cognitive radios," in *Proceedings of the 7th International Conference on Next Generation Mobile Apps, Services and Technologies (NGMAST '13)*, pp. 220–225, 2013.

[16] G. K. Karagiannidis, "Moments-based approach to the performance analysis of equal gain diversity in Nakagami-m fading," *IEEE Transactions on Communications*, vol. 52, no. 5, pp. 685–690, 2004.

[17] V. Asghari, D. B. da Costa, and S. Aissa, "Performance analysis for multihop relaying channels with nakagami-m fading: ergodic capacity upper-bounds and outage probability," *IEEE Transactions on Communications*, vol. 60, no. 10, pp. 2761–2767, 2012.

[18] M. O. Hasna and M.-S. Alouini, "Outage probability of multihop transmission over Nakagami fading channels," *IEEE Communications Letters*, vol. 7, no. 5, pp. 216–218, 2003.

[19] I. S. Gradshteyn and I. M. Ryzhik, *Table of Integrals, Series, and Products*, Academic Press, 7th edition, 2007.

[20] A. H. Nuttall, "Some integrals involving the q_M function," *IEEE Transactions on Information Theory*, vol. 21, no. 1, pp. 95–96, 1975.

[21] M. K. Simon and M. S. Alouini, *Digital Communications over Fading Channels*, Wiley, 2nd edition, 2005.

[22] A. Papoulis, *Probability, Random Variables, and Stochastic Processes*, McGraw-Hill, New York, NY, USA, 4th edition, 1965.

[23] M. Carlos de Cordeiro, S. Kiran Challapali, D. Birru, and S. N. Shankar, "Ieee 802. 22: an introduction to the first wireless standard based on cognitive radios," *Journal of Clinical Microbiology*, vol. 1, no. 1, pp. 38–47, 2006.

[24] S. M. Almalfouh and G. L. Stüber, "Uplink resource allocation in cognitive radio networks with imperfect spectrum sensing," in *Proceedings of the IEEE 72nd Vehicular Technology Conference Fall (VTC '10)-Fall*, pp. 1–6, September 2010.

[25] J. Ma, G. Zhao, and Y. Li, "Soft combination and detection for cooperative spectrum sensing in cognitive radio networks," *IEEE Transactions on Wireless Communications*, vol. 7, no. 11, pp. 4502–4507, 2008.

Hindawi Publishing Corporation
International Journal of Distributed Sensor Networks
Volume 2013, Article ID 450626, 10 pages
http://dx.doi.org/10.1155/2013/450626

Research Article

Consensus-Based Distributive Cooperative Spectrum Sensing for Mobile Ad Hoc Cognitive Radio Networks

Anam Raza,[1] Waleed Ejaz,[2] Syed Sohail Ahmed,[1] and Hyung Seok Kim[2]

[1] *Department of Computer Engineering, University of Engineering and Technology, Taxila, Pakistan*
[2] *Department of Information and Communication Engineering, Sejong University, Seoul, Republic of Korea*

Correspondence should be addressed to Hyung Seok Kim; hyungkim@sejong.edu

Received 3 September 2013; Accepted 31 October 2013

Academic Editor: Khalid Al-Begain

Cognitive radio network (CRN) is an intelligent network that provides solution to underutilization of spectrum band by detecting spectrum holes. For this purpose, certain important tasks including spectrum sensing, spectrum analysis, and spectrum decision are required to be performed. Spectrum sensing is the crucial step as it is not only responsible for fast and reliable detection of primary users (PU) but also evades disturbance to their transmission. Different methods of enhancements in local sensing scheme have been proposed in the literature. However, cooperative spectrum sensing schemes are preferred as they provide significant gains in CRN performance by countering shading effects. In this paper, an efficient distributed cooperative spectrum sensing scheme is proposed for mobile ad hoc cognitive radio networks. The consensus-based distributed cooperative spectrum sensing (CDCSS) scheme relies on energy detection for local sensing. Random walk mobility model (RWMM) is used for the movement pattern of nodes. Mobility model is employed as movement of nodes results in reduced fading effects and efficient detection. Simulation results were compared with the existing consensus algorithm and equal gain combining (EGC) rule, and the results showed improvement in sensing phenomenon.

1. Introduction

Advancement in wireless communication requires efficient utilization of limited spectrum resources. Recent research shows that this limitation is because of spectrum management policies [1]. To overcome this limitation and for better utilization of spectrum, one requires a new networking standard, which is known as cognitive radio network (CRN) [2–4]. Software defined radio (SDR) is used to build cognitive radio (CR). CR is a smart system that senses the environment called spectrum sensing and adapts to variations in operating parameters. The two prime objectives of spectrum sensing are the efficient detection of spectrum holes and interference avoidance with primary system/licensed system [5–7]. Current research divides spectrum sensing into two branches that are local sensing and cooperative spectrum sensing. In cooperative spectrum sensing, each cognitive radio user (CRU) shares its local observation with the rest of CRUs in the network, which results in improved spectrum sensing.

In cooperative spectrum sensing, the CRUs either forward their sensing information to the central entity or they can exchange sensing information with each other for cooperative decisions. In infrastructure mode shown in Figure 1(a), there is central entity to fuse the sensing results; however, there is no central entity in ad hoc mode also known as cognitive radio ad hoc network (CRAHN) as shown in Figure 1(b). Distinguishing features of CRAHN's are lack of central entity, distributed multihop architecture, dynamic network topology, and time/location-varying spectrum availability [8]. Advancement introduced to the ad hoc network involves mobility and the network is known as mobile ad-hoc network (MANET). In MANETs, devices can move randomly in all directions, and links with other devices are also updated repeatedly. Without utilizing a fixed infrastructure, a dynamic network is established by wireless nodes.

To achieve a common goal, MANET nodes cooperate with each other because of the lack of centralized control in MANETs. In self-organization of nodes, the major responsibilities are topology organization, neighbor discovery, and

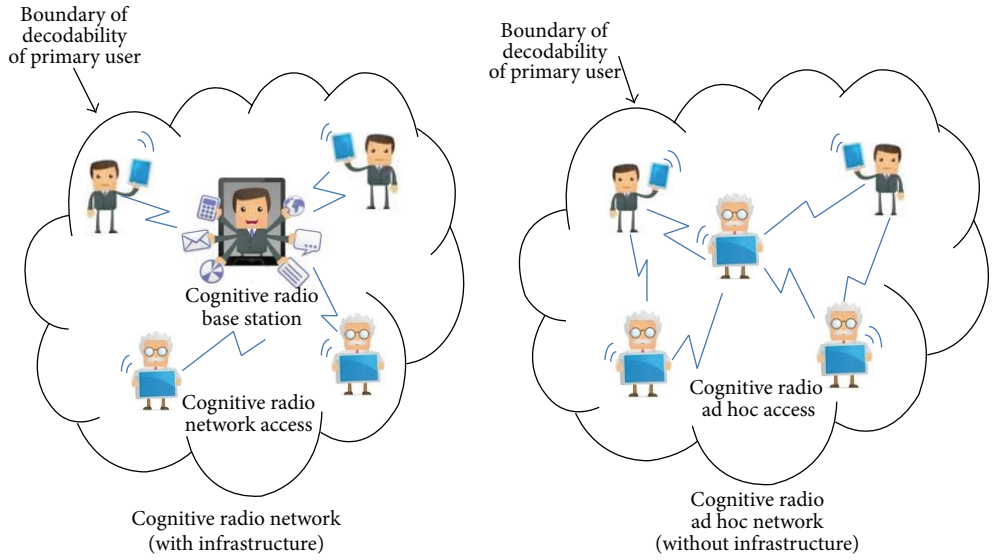

Figure 1: Types of network: (a) infrastructure based CRN and (b) CRAHN.

topology reorganization [9]. Movement patterns of mobile nodes (MNs) are defined using mobility models. It is important to keep track of node movement because nodes in MANETs are free to move. This also includes information about their speed, location, velocity, and acceleration change over time.

In this paper, a consensus-based distributed cooperative spectrum sensing scheme (CDCSS) in CR-MANET is proposed which is inspired by Novel biological mechanisms. These mechanisms have become an important phenomenon in handling intricate communication networks. CDCSS works on MNs in distributive network without using a centralized center to improve the sensing performance in CR-MANETs. The main contributions of this paper are as follows.

(i) A consensus-based distributed spectrum sensing for CR-MANETs is proposed.

(ii) Random walk mobility model (RWMM) is used in CRN for the movement pattern of nodes.

(iii) Through the simulation, the proposed scheme is compared with existing consensus algorithm and EGC-rule scheme.

The rest of the paper is as follows. Section 2 explains work carried out in fields of spectrum sensing and mobility models. Section 3 involves the methodology adopted to develop a scheme for cooperative spectrum sensing among MNs. Section 4 explains implementation process, Section 5 involves analysis, and Section 6 contains conclusion of our work.

2. Background and Related Work

The rapid advancement in wireless applications has resulted in increased usage of unlicensed band, causing a problem of nonuniform spectrum usage [10]. The CR cycle is divided into four broad fields of research to cope with spectrum utilization challenges: (1) the spectrum sensing that determines which portion of the spectrum is available, (2) the spectrum decision that picks the best vacant channel, (3) the spectrum sharing that allows user's coordinated access to channel, and (4) the spectrum mobility that allows vacating the channel when a PU is detected.

2.1. Spectrum Sensing. Spectrum sensing techniques are classified into noncooperative and cooperative spectrum sensing. The three most common schemes for noncooperative transmitter detection are energy detection, matched filter detection, and cyclostationary detection [11–14].

Due to random changing in wireless environment, it is difficult for a single CRU to detect PU signal accurately. To cope with factors such as noise uncertainty, shading, and fading, cooperative spectrum sensing is introduced by researchers. In cooperative spectrum sensing, CRUs cooperate and share their information about PU detection. These methods give more accurate results as uncertainty can be minimized [15].

In decentralized spectrum sensing, there is no requirement of infrastructure and fusion center. Here, the CRUs exchange their information with each other to cooperate. The most well-known decentralized spectrum sensing technique is gossiping algorithm because it performs sensing with a significant low overhead. Other decentralized techniques include clustering schemes which are already known for sensor network architectures. In these schemes, CRUs form clusters, which coordinate among themselves [16].

A gradient based distributed cooperative spectrum sensing method was proposed for CRAHNs [17]. The gradient field changes with the energy sensed by CRU, and the gradient is calculated based on the components, which include energy sensed by CRUs and received from neighbors. The proposed scheme was evaluated on the basis of reliable sensing,

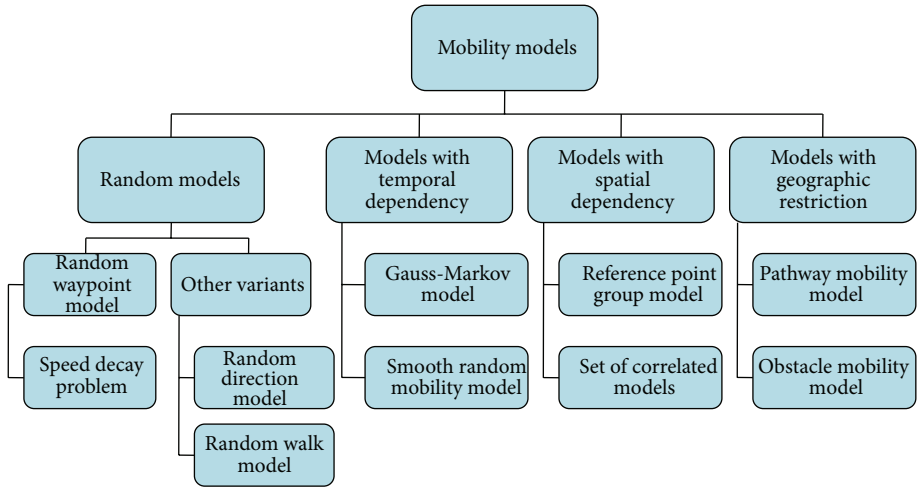

Figure 2: Mobility model classification.

convergence time, and energy consumption. This scheme consumes less energy compared to existing consensus-based approach.

Wu et al. [18] proposed a decentralized clustering consensus algorithm based on two phases. First phase is related to clustering CRU with best detection performance and second phase carries out distributed data fusion of the sensing outcomes of the CRUs in the cluster. Like [18], our proposed scheme is also for distributed network but this former scheme does not take into account parameters related to mobility of nodes which on the other hand are a major concern of our proposed scheme.

Ribeiro et al. [19] presented a two-step adaptive combining based technique for distributive cooperative spectrum sensing. In the first step, an adaptive combiner is used for the fusion of neighborhood nodes, and, in the second step, a consensus decision is made by sharing local decisions within the neighborhoods. Their results showed better performance compared to the optimal linear fusion rule.

In [20], a consensus-based spectrum sensing scheme is presented. This scheme is fully distributive where local sensing information obtained by CRUs is sent to their neighbors. Information from neighbors is used by CRUs, and consensus algorithm is applied for stimulating new state for consensus variable. This process is continued till the individual states converge to a common value. Spectrum sensing data falsification (SSDF) attacks are also dealt with by researchers by excluding those nodes from neighbors list that give very much deviation from mean value.

Like [20], our proposed scheme is also for distributed network. The existing consensus algorithm required each node to have a prior knowledge of the upper bound of the maximum degree of the network. Our proposed algorithm is not only fully distributive and robust against SSDF attacks but also does not require prior knowledge of degree of the network. Further, this new algorithm is applied on mobile nodes. For nodes motion, mobility models are investigated.

2.2. Mobility Models. The movement patterns of MN are defined using mobility models. It is important to keep track of nodes movement as nodes in MANETs are free to move. This also includes information about their speed, location, velocity, and acceleration change over time. Bai and Helmy [21] provided a detailed classification of mobility models according to the mobility characteristics, which is also shown in Figure 2. Some models keep track of their history movements and are referred to as models with temporal dependency, while the others are restricted by geographic bounds. There is also a class of mobility models, known as models with spatial dependency, in which nodes move in a correlated manner. Most of these mobility models are random models.

3. Modeling Philosophy

In this section, we will first discuss the spectrum sensing model of CRU and then illustrate the local sensing model and information sharing with neighboring CRUs using CDCSS. Network topology and consensus notions for CDCSS are also presented along with the movement pattern of CRU/MN using RWMM.

Spectrum sensing process is divided into two phases that are local spectrum sensing and cooperative spectrum sensing. For local spectrum sensing, CRUs use energy detection technique to detect PU and make local decision about presence or absence of PU. Reference [12] shows a block diagram of energy detection.

The basic hypothesis model for local spectrum sensing is given as [1, 14, 16]

$$x(t) = \begin{cases} n(t) & H_0 \\ h * s(t) + n(t) & H_1, \end{cases} \quad (1)$$

where $x(t)$ is the received signal, $n(t)$ is the additive white Gaussian noise (AWGN), $s(t)$ is the PU signal, and h is the amplitude gain of PU signal. H_1 indicates that a PU is present while H_0 represents absence of PU.

Received signal is passed through a band-pass filter of bandwidth W and center frequency f_s. Signal received from filter is further fed to a squaring device and then to an integrator over a time period T. Output from the integrator is

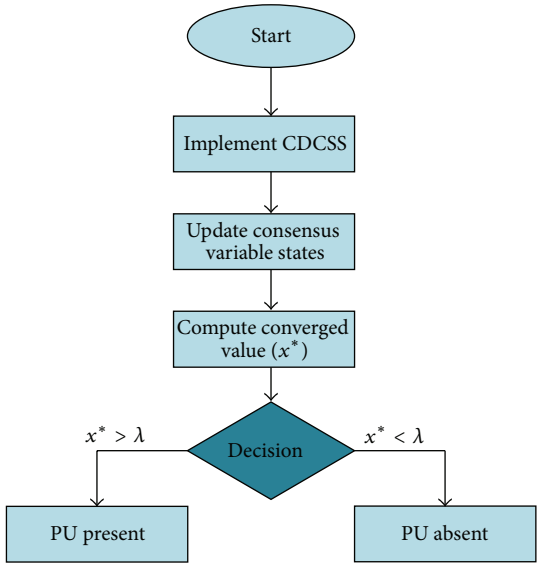

Figure 3: Flow chart for cooperative sensing.

checked against predefined threshold λ and makes a decison about presence or absence of PU and is represented as Y. Local measurement of user i is denoted by Y_i. The output Y of the energy detection has the distribution [22]

$$Y = \begin{cases} \chi^2_{2Z} & H_0 \\ \chi^2_{2Z}(2\gamma) & H_1, \end{cases} \tag{2}$$

where χ^2_{2Z} represents central chi-square distribution and $\chi^2_{2Z}(2\gamma)$ represents noncentral chi-square distribution, each with $2Z$ ($Z = TW$) degree of freedom and a non-centrality parameter of 2γ for the latter distribution. Here, γ represents SNR. So in short in local observation each MN is represented as i will detect the energy after every T seconds and take measurement Y_i.

3.1. Consensus-Based Distributive Cooperative Spectrum Sensing. In this stage, MNs communicates their local information with their neighbors and make a common decision about presence or absence of PU. They share information via common control channel (CCC). The CCC is responsible for transferring control information and CRUs coordinate with each other using this medium. The CCC not only facilitates cooperation among CRUs but also provides several other network operations that include neighbor discovery, topology change, channel access negotiation, and routing information updates. In this algorithm overlay, CCC was used because CRUs temporarily allocated the spectrum not used by PU. Further, in this algorithm, we assumed that the dedicated CCC is predetermined and usually unaffected by PU activity.

Cooperative sensing is an iterative process where each MN sets $x_i(0) = Y_i$ as the starting value of local state variable at time instant $k = 0$. For further time intervals, that is, $k = 1, 2, \ldots$, MNs share their local observation with neighbors and then compute their next state $x_i(k+1)$. This is the basic idea adopted from self-organizing capability of CRAHNs. The maximum degree of the network is defined as the maximum number of neighbors of a node. In the present work, the degree is represented as Δ, and step size is represented as ε' where $0 < \varepsilon' < 1/\Delta$. The state of each MN is obtained by following rule:

$$x_n(k+1) = x_n(k) + \varepsilon' \sum_{m \varepsilon N} \left(x_m(k) - x_n(k)\right), \tag{3}$$

where N represents number of nodes and x_m is the neighbor with which x_n shares information. This process continues until a converged value is achieved by all MNs. This converged value is represented by x^*. This converged value is then compared against a predefined threshold λ and then cooperative decision is made by all MNs about the presence or absence of PU. Figure 3 shows the flow diagram of the proposed consensus algorithm applied on MNs:

$$\text{Decision} = \begin{cases} 1, & x^* > \lambda \\ 0, & x^* \leq \lambda. \end{cases} \tag{4}$$

An average consensus is ensured if $0 < \varepsilon' < 1/\Delta$. If no malicious node is present in the network, then the final converged value x^* will be equal to the average of initial state values. The convergence rate is one of the great concerns in the field of cooperative spectrum sensing. MNs continuously detect the presence of PU and, on identifying its presence, it backs up as soon as possible. For this reason, reaching at consensus, that is, convergence rate, is a significant factor for network topology design and also for analyzing the performance of CDCSS.

Yu et al. [20] proposed (3) in which constant step size ε is used, which appeared as a limitation as it required each node to have a complete knowledge of network topology and maximum degree of the network. Also, it was applied on fixed network with predefined connections. In this new proposed technique, these limitations were overcome by the following.

(1) Employing a variable ε' instead of constant step size: rather than using a predefined constant step size, its value is predicted by following rule [23]:

$$\Delta \sim N^{1/\alpha - 1}, \tag{5}$$

where Δ represents the degree of network, N represents the number of nodes in the network, and α is a constant factor that can have a value between 2 and 3. Using this rule, no knowledge about complete network topology is required except for the number of nodes in the network. Using this rule, the maximum degree of the network (Δ) can also be predicted. The step size is given as $0 < \varepsilon' < 1/\Delta$.

(2) Applying further CDCSS scheme on MNs which are travelling considering RWMM: issues faced in case of fixed graph do not occur here as nodes are mobile and motion of nodes causes small-scale fading [24]. As nodes are mobile, nodes with a distance greater than a certain limit are not considered as neighbors, which changes the degree of node (Δ) and makes step size (ε') a variable factor instead of constant value.

3.2. Network Topology Using Random Graph. As stated earlier, each MN creates links with neighbors and communicates local information with them. Network topology used as reference in this research can be represented as a graph G. The graph consists of nodes $\{i = 1, 2, 3, \ldots, n\}$ and a set of edges, where each edge is denoted by E. When two MNs are connected in an edge, it means that they can send and receive information from each other, and their ordered pair will be (i, j). When nodes are connected through a path, then the graph is said to be connected. A path in a graph consists of sequence of nodes such as $i_1, i_2, i_3, \ldots, i_m$, where $m \geq 2$. In case of fixed graphs, the nodes face certain problems such as fading of signals, which may cause link failures and packet errors, and signal reception may also get affected by moving objects between neighboring nodes. To overcome this problem, we used random graph, in which the link goes down as the nodes move away. Random graph representation of network topology of 10 MNs, which was taken for demonstration in the present work, is shown in Figure 4.

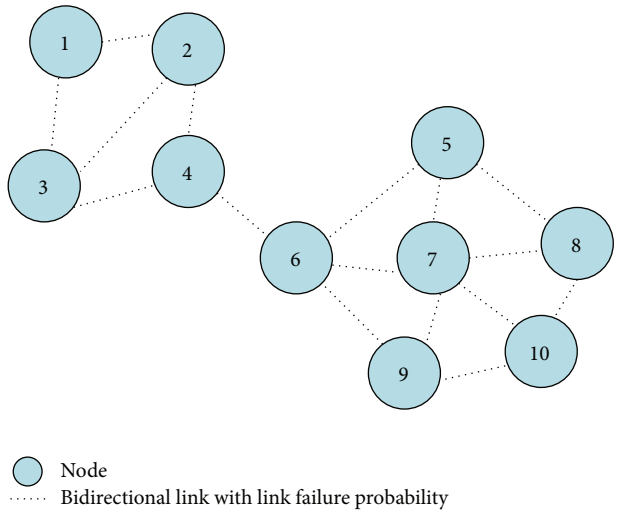

Figure 4: Network topology of 10 MNs.

3.3. Random Walk Mobility Model. The basic idea behind this movement emerged from unexpected movements of particles. It was developed to follow such erratic movement patterns, and hence it became the most widely used mobility model. MN randomly chooses its new speed and direction and then moves from its current location to a new location to which it is to travel. Predefined ranges are used for selecting new speed and direction. For speed, the range can be from minimum speed to maximum speed, and directions can range from 0 to 2π. Either a constant time interval t or a constant distance d is selected for each movement in this model. At the end of each movement, a new direction and speed are selected in a similar manner for the next movement. In this model, when MN reaches simulation boundary, it bounces back from the simulation boundary and comes back at some angle. This angle is determined by incoming direction. The MN then moves along a newly selected path. RWMM is a memoryless model as no knowledge of previous speed and direction is retained, and also these parameters are not used for future decisions. The current direction and speed of MN is independent of both past and future speed and direction.

Different derivates of this model are also developed by researchers. These include 1D, 2D, 3D and d-D walks [25]. Here, we here are concerned with 2D walk, which is also shown in Figure 5. In this example, MN is allowed to choose a speed between 0 and 10 m/s and a direction between 0 and 2π. In this case, fixed time interval is used; that is, MN can move in a direction for 1 sec before changing its direction and choosing a new destination. As time is made constant, the distance to be travelled is not fixed or specified. MN can move in the specified simulation boundary.

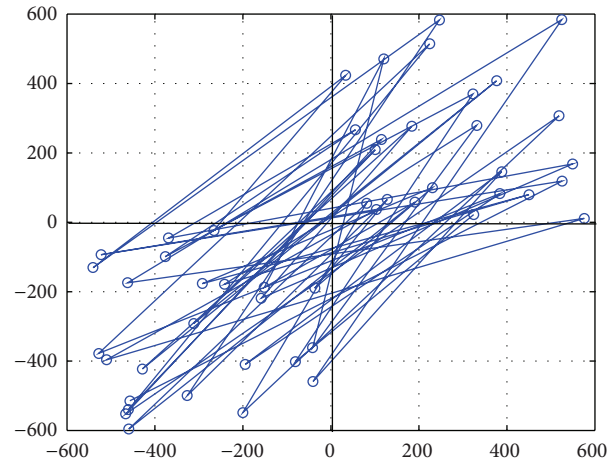

Figure 5: Mobility pattern of MN using RWMM.

4. Simulation Setup

As mentioned earlier, we used random graph of nodes and assumed that nodes were mobile which follow RWMM for movement patterns. Figure 6 shows the simulation result for movement of 10 MNs. The time period for this simulation was 100 seconds. MN took each move in constant time interval of 1 second. The simulation area in which nodes moved was a 20 m × 20 m rectangle with 15 m transmission range.

Such transmission scenario consisting of MNs can be seen in wireless regional area network (WLAN) which has adopted operations of mobile devices [24]. As in RWMM, either a constant time interval or constant speed was used. We considered a constant time interval while speed was variable, which made the distance travelled by MN in each move a variable factor.

4.1. Constraints for Consensus-Based Distributive Cooperative Spectrum Sensing. CDCSS algorithm is based on certain constraints some of which were not considered in [20]. These constraints are as follows:

(1) implementing prediction rule given in (5) to get maximum degree of the network (Δ) which in turn gives

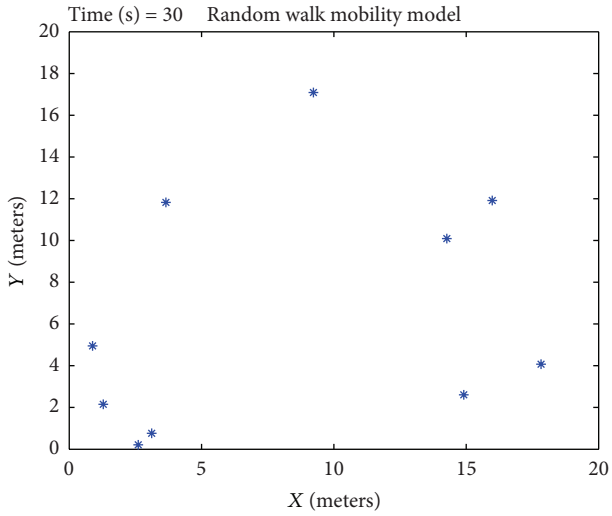

Figure 6: RWMM for 10 MNs.

range for selection of step size (ε'): this prediction will omit the need of knowledge of whole network topology,

(2) sharing local information of MNs with their neighbors,

(3) excluding those MN from neighbor list which give maximum deviation from mean value (calculated by taking the average of all values from MN),

(4) considering distance restriction, that is, if a neighbor MN exceeds a specified distance then exclude it from neighbor list thus making step size variable (ε').

Above given factor affect affect convergence rate, so the aim through their execution is to fasten convergence rate. Implementation of these constraints is explained below. This whole process of CDCSS and RWMM is also shown via flowchart in Figure 7.

4.2. Prediction Rule. The first step for cooperation is to predict maximum degree of the network. Equation (5) gives this prediction rule. Ten-node network is shown in Figure 6; therefore, using prediction rule, the degree of network is calculated as

$$\Delta \sim 10^{1/2.5-1}, \tag{6}$$

where $N = 10$ and α which is a constant factor and can have a value between 2 and 3, so 2.5 is assigned to α. Thus maximum degree of network predicted for 10-node network using (5) is $\Delta = 5$. Thus, the maximum degree of network Δ is 5 for 10-node network. Then $0 < \varepsilon' < 1/5$. We know that the algorithm converges faster when ε' approaches $1/\Delta$, in this case 0.2.

After getting maximum degree of network, all MNs will continue sharing their local information with neighbors and update their states according to (3). Given below is the simulation results obtained by applying prediction rule and

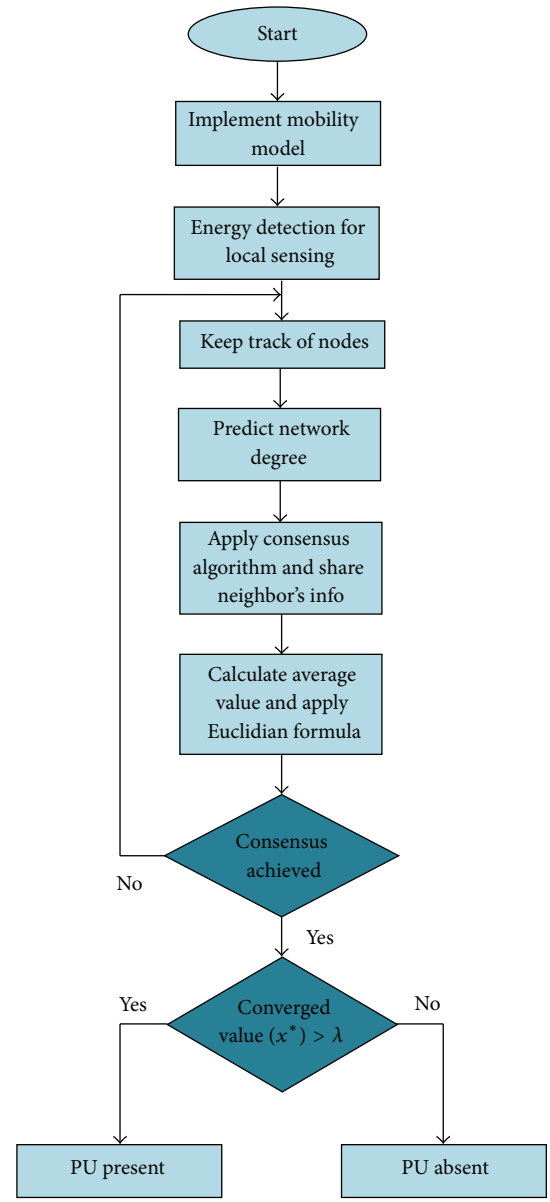

Figure 7: Flowchart of complete algorithm.

achieving consensus among MNs. The SNR here is a fixed factor having value of 10 dB.

Figure 8 shows estimated PU energy in a network with in a network of 10 nodes. From Figure 8 it is very clear that initially all MNs gave very different energy values which are their local observations. These values are then shared among neighboring MNs, and, after some iterations, consensus is achieved. This is shown in Figure 8 where, after about 13 iterations, difference between the MNs is less than 1 dB and, after about 19 iterations it is less than 0.1 dB. Here 30 iterations are shown for demonstration purpose. If we increase the number of MNs in the network, then number of iterations required to achieve consensus also increases accordingly. As a result, the algorithm also converges slowly.

4.3. Average Value Calculation. It is stated earlier that the consensus process takes place in iterations. With every time

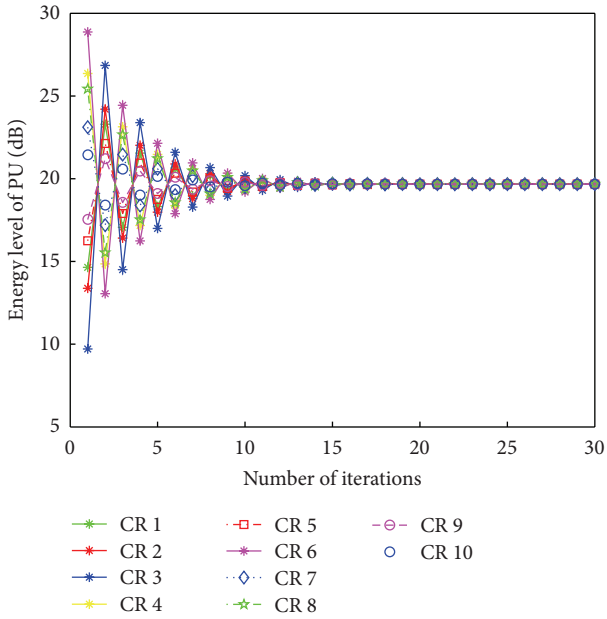

Figure 8: Consensus algorithm with prediction rule.

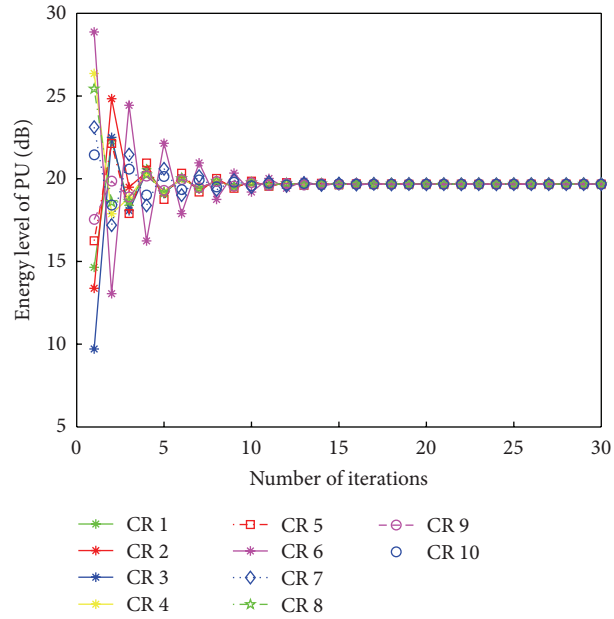

Figure 9: Consensus algorithm with distance restriction.

instant, that is, $k = 0, 1, 2, \ldots$, state of consensus variable of each MN $x_i(k)$ is updated. Along with this updating, each MN keeps track of the energy level received from the neighbor. MN calculates deviation of its neighbors from mean value. The neighbor with maximum deviation is an attacker and MN excludes this neighbor from neighbor's list. Neighbors showing maximum deviation can be an attacker which gives wrong energy values and eventually can lead to increased false alarms and reduced correct detection of PU. Due to this constraint, a safety measure was employed for network. As a result, only those energy values will be considered for state updating that are from verified neighbors.

As there was no malicious node in this network of 10 nodes, the result was the same as the result for simulation with prediction rule shown in Figure 8. The convergence value, that is, x^*, will be the same as the average of initial energy levels from MNs. In this simulation, the average value achieved is 19.6 dB, which is same as the average of initial energy levels from all MNs.

4.4. Distance Restriction. We assumed that nodes were mobile and moving considering RWMM constraints. They were moving in a cell of 20 m × 20 m area. This is also shown in Figure 6. Mobility of nodes can cause an increase in signal power and small-scale fading. Considering neighboring list, if the distance between nodes exceeds certain limit, then they can be excluded from neighbor's list. In this scenario of a 20 m × 20 m area, if the distance between nodes exceeds 15 m, then they are excluded from neighbors list. This in turn will cause variation in step size as maximum degree of node is varying. To calculate distance between nodes, Euclidian's formula was used which is given in (7). Simulation result for CDCSS, which also employed this distance restriction, is shown in Figure 9:

$$d = \sqrt{(x_2 - x_1)^2 + (y_2 - y_1)^2}. \quad (7)$$

Simulation result in Figure 9 shows that now less iterations are taken to achieve consensus compared to previous results. The difference between energy values is less than 1 dB after 10 iterations and is less than 0.1 dB after 15 iterations. Here also, the converged value is equal to the average of initial energy values of MNs, that is, 19.6 dB.

4.5. Complete Consensus Algorithm. Finally, all these constraints were simultaneously applied to achieve consensus among MN's energy values and come to a common decision about presence or absence of PU. Figure 10 shows a simulation result obtained by considering all the above rules, that is, prediction rule, average value calculation, and distance restriction.

Figure 10 revealed that convergence rate is the fastest in this case compared to all of the rest of the cases. The difference between energy values of MNs is less than 1 dB after 7 iterations and is less than 0.1 dB after 12 iterations. The final converged value is $x^* = 19.6$ dB.

5. Simulation Results

The CDCSS for distributed network does not have a central entity. Therefore, for analysis purpose, it is compared with techniques that are employed either for distributed network or centralized networks. For distributed network, CDCSS was compared with consensus algorithm given in Yu et al. [20], while, for centralized network, it was compared with EGC rule which is a soft combining rule. EGC is one of the simplest

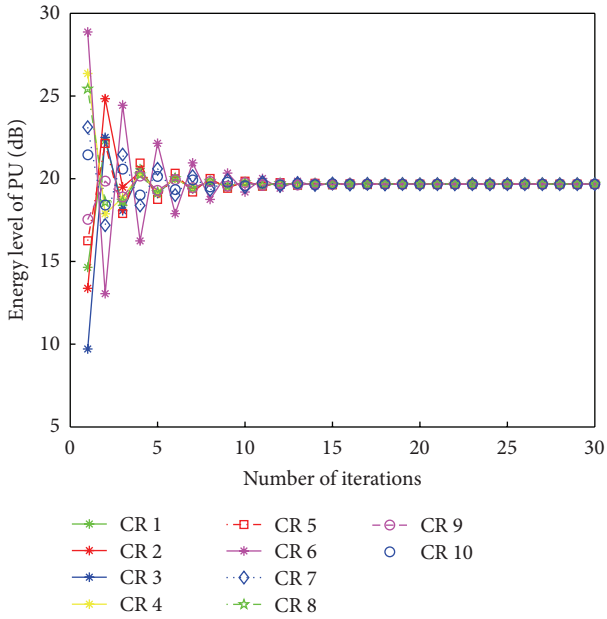

Figure 10: Complete consensus algorithm.

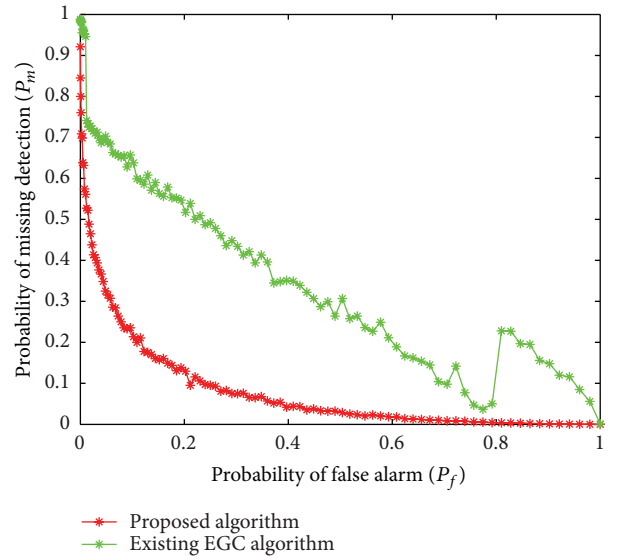

Figure 11: Comparison on the basis of P_f versus P_m with the existing EGC rule (SNR = 10 dB, $TW = 5$).

linear soft combining rules where estimated energy in each node is sent to the fusion center where they will be added together. The summation is compared with a predefined threshold, and the decision is made about presence or absence of PU accordingly. Comparisons between CDCSS and EGC rule were made on the basis of P_d and P_f and probability of missed detection (P_m).

5.1. Comparison with EGC Rule. Firstly comparison was made on the basis of P_m and P_f. If number of false alarms increases then P_f also increases which will result in low spectrum utilization. P_m is defined as

$$P_m = 1 - P_d. \tag{8}$$

As P_m increases, this will cause high missed detection of PU, which will result in disturbance to PU transmission. This means that a good scheme is the one in which both of these factors are minimized. Comparison of CDCSS with existing EGC rule is shown in Figure 11. This comparison comprises P_f and P_m.

It is clear from Figure 11 that CDCSS performs better compared to existing EGC rule. New scheme has lower P_f compared to EGC rule. This will result in less interference to PU, thus improving PU's transmission and causing more efficient and reliable spectrum sensing.

Further, in analysis, comparison is made on the basis of varying SNR and sensitivity in detection, that is, P_d. Figure 12 shows simulation result for SNR versus P_d. Here SNR varies from −20 dB to 20 dB. Time-bandwidth factor, that is, $TW = 5$ and P_f, is fixed here having a value of 0.1. From Figure 12, it is clear that, in terms of average SNR, CDCSS has considerable improvements for performing detection. For $P_d > 0.99$, CDCSS required a lesser average SNR than existing EGC-rule.

5.2. Comparison with the Existing Consensus Algorithm. CDCSS was also compared with the existing consensus algorithm which was given in Yu et al. [20]. This existing algorithm was also used for distributive network. Figure 13 shows comparison of result for CDCSS and existing consensus algorithm.

It is clear from Figure 13 that CDCSS has lower Pm than existing consensus algorithm. This means CDCSS has improved spectrum utilization and reduced PU interference. Mobility of nodes aided in better performance of CDCSS when compared to existing consensus algorithm. As in both schemes, nodes need to communicate the degree of network, so energy consumption is approximately the same in both the schemes.

Further, in the analysis, comparison is made on the basis of SNR and P_d. SNR varies from −20 dB to 20 dB. Time-bandwidth factor, that is, $TW = 5$, and decision threshold, λ, is set so as to keep P_f fixed having a value of 0.1. Simulation result in Figure 14 shows that CDCSS has a better performance than existing consensus algorithm that was given in [20]. It is also clear from Figure 14 that CDCSS has a better result for detection considering varying SNR compared to existing consensus algorithm. Even if P_d is expected to be kept above 0.99 then, the existing algorithm required a higher average SNR as compared to CDCSS.

6. Conclusion

Cooperative spectrum sensing is an efficient technique to improve spectrum exploitation. In this paper, consensus-based distributive cooperative spectrum scheme is proposed, which was applied to mobile nodes. The local sensing, in this scheme, was based on energy detection. This is the most widely used local sensing technique as it does not require

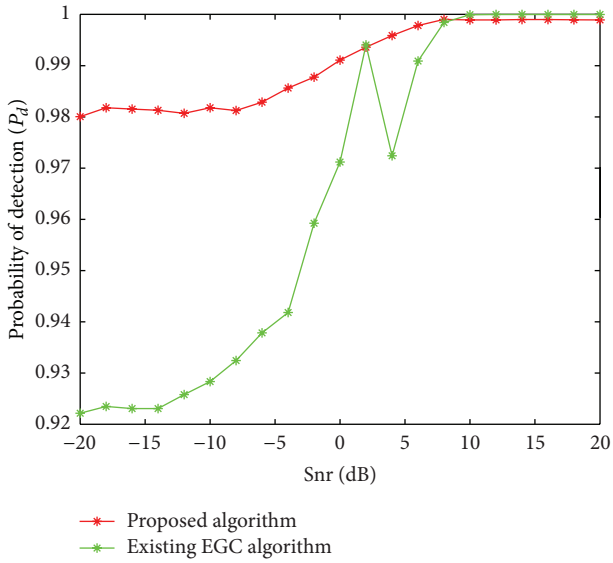

Figure 12: Comparison of the basis of SNR versus P_d with the existing EGC rule.

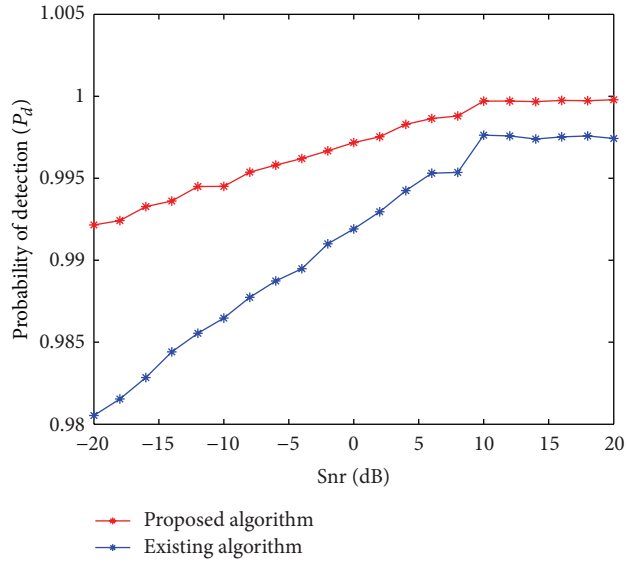

Figure 14: Comparison of the basis of SNR versus P_d with the existing consensus algorithm.

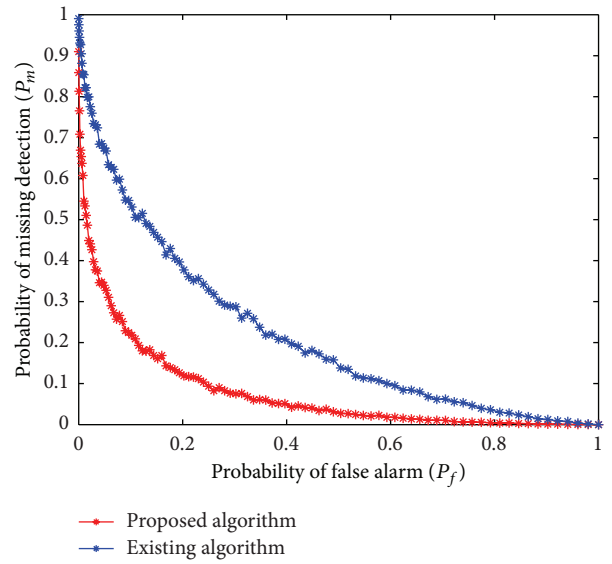

Figure 13: Comparison of the basis of P_f versus P_m with the existing consensus algorithm (SNR = 10 dB, TW = 5).

prior knowledge of network topology and is easy to implement. For cooperative sensing, the proposed algorithm was based on a set of certain rules which includes prediction rule and average value calculation for energy values of unlicensed users. Details of these rules are provided in Sections 3 and 4. This technique was applied on mobile nodes because mobility of nodes results in reducing the fading effect, thus making sensing more efficient. The goal of the proposed scheme was to provide proficient cooperative spectrum sensing technique. The results showed that our technique has the potential to contribute effectively for efficient spectrum utilization. A future direction of study is to consider sensing overheads and to provide optimal spectrum heterogeneous CR-MANET design.

Acknowledgments

This work was supported by the Ministry of Science, ICT & Future Planning (MSIP), Korea, under the Convergence Information Technology Research Center (C-ITRC) support program (NIPA-2013-H0401-13-1003) supervised by the National IT Industry Promotion Agency (NIPA). It was also supported by the Seoul R&BD Program (SS110012C0214831) and Special Disaster Emergency R&D Program from National Emergency Management Agency (2012-NEMA10-002-01010001-2012).

References

[1] I. F. Akyildiz, W. Y. Lee, M. C. Vuran, and S. Mohanty, "NeXt generation/dynamic spectrum access/cognitive radio wireless networks: a survey," *Computer Networks*, vol. 50, no. 13, pp. 2127–2159, 2006.

[2] S. Haykin, "Cognitive radio: brain-empowered wireless communications," *IEEE Journal on Selected Areas in Communications*, vol. 23, no. 2, pp. 201–220, 2005.

[3] R. W. Thomas, D. H. Friend, L. A. DaSilva, and A. B. MacKenzie, "Cognitive networks: adaptation and learning to achieve end-to-end performance objectives," *IEEE Communications Magazine*, vol. 44, no. 12, pp. 51–57, 2006.

[4] Q. Zhao and B. M. Sadler, "A survey of dynamic spectrum access," *IEEE Signal Processing Magazine*, vol. 24, no. 3, pp. 79–89, 2007.

[5] S. S. Ahmed, A. Raza, H. Asghar, and G. Ume, "Implementation of dynamic spectrum access using enhanced carrier Sense Multiple Access in Cognitive Radio Networks," in *Proceedings of the 6th International Conference on Wireless Communications,*

Networking and Mobile Computing (WiCOM '10), pp. 1–4, Chengdu, China, September 2010.

[6] D. Cabric, S. M. Mishra, and R. W. Brodersen, "Implementation issues in spectrum sensing for cognitive radios," in *Proceedings of the Conference Record of the 38th Asilomar Conference on Signals, Systems and Computers*, pp. 772–776, November 2004.

[7] A. Ghasemi and E. S. Sousa, "Spectrum sensing in cognitive radio networks: requirements, challenges and design trade-offs," *IEEE Communications Magazine*, vol. 46, no. 4, pp. 32–39, 2008.

[8] I. F. Akyildiz, W. Y. Lee, and K. R. Chowdhury, "CRAHNs: cognitive radio Ad Hoc networks," *Ad Hoc Networks*, vol. 7, no. 5, pp. 810–836, 2009.

[9] S. Basagni, M. Conti, S. Giordano, and I. Stojmenovic, *Mobile Ad Hoc Networking*, John Wiley & Sons, New York, NY, USA, 2004.

[10] I. F. Akyildiz, W. Y. Lee, M. C. Vuran, and S. Mohanty, "A survey on spectrum management in cognitive radio networks," *IEEE Communications Magazine*, vol. 46, no. 4, pp. 40–48, 2008.

[11] E. Axell, G. Leus, E. G. Larsson, and H. V. Poor, "Spectrum sensing for cognitive radio: state-of-the-art and recent advances," *IEEE Signal Processing Magazine*, vol. 29, no. 3, pp. 101–116, 2012.

[12] D. Bhargavi and C. R. Murthy, "Performance comparison of energy, matched-filter and cyclostationarity-based spectrum sensing," in *Proceedings of the IEEE 11th International Workshop on Signal Processing Advances in Wireless Communications (SPAWC '10)*, pp. 1–5, Marrakech, Morocco, June 2010.

[13] D. Cabric, A. Tkachenko, and R. W. Brodersen, "Spectrum sensing measurements of pilot, energy, and collaborative detection," in *Proceedings of the Military Communications Conference 2006 (MILCOM '06)*, pp. 1–7, Washington, DC, USA, October 2006.

[14] T. Yücek and H. Arslan, "A survey of spectrum sensing algorithms for cognitive radio applications," *IEEE Communications Surveys and Tutorials*, vol. 11, no. 1, pp. 116–130, 2009.

[15] I. F. Akyildiz, B. F. Lo, and R. Balakrishnan, "Cooperative spectrum sensing in cognitive radio networks: a survey," *Physical Communication*, vol. 4, no. 1, pp. 40–62, 2011.

[16] M. Subhedar and G. Birajdar, "Spectrum sensing techniques in cognitive radio networks: a survey," *International Journal of Next-Generation Networks*, vol. 3, pp. 37–51, 2011.

[17] W. Ejaz, N. Ul Hassan, and H. S. Kim, "Distributed cooperative spectrum sensing in cognitive radio for Ad Hoc networks," *Computer Communications*, vol. 36, no. 12, pp. 1341–1349, 2013.

[18] Q. H. Wu, G. R. Ding, J. L. Wang, X. Q. Li, and Y. Z. Huang, "Consensus-based decentralized clustering for cooperative spectrum sensing in cognitive radio networks," *Chinese Science Bulletin*, vol. 57, no. 28-29, pp. 3677–3683, 2012.

[19] F. C. Ribeiro, M. L. de Campos, and S. Werner, "Distributed cooperative spectrum sensing with adaptive combining," in *Proceedings of the IEEE International Conference on Acoustics, Speech and Signal Processing (ICASSP '12)*, pp. 3557–3560, 2012.

[20] F. R. Yu, M. Huang, and H. Tang, "Biologically inspired consensus-based spectrum sensing in mobile Ad Hoc networks with cognitive radios," *IEEE Network*, vol. 24, no. 3, pp. 26–30, 2010.

[21] F. Bai and A. Helmy, "A survey of mobility models," in *Wireless Ad Hoc Networks*, vol. 206, University of Southern California, Los Angeles, Calif, USA, 2004.

[22] H. Urkowitz, "Energy detection of unknown deterministic signals," *Proceedings of the IEEE*, vol. 55, no. 4, pp. 523–531, 1967.

[23] M. E. J. Newman, "The structure and function of complex networks," *SIAM Review*, vol. 45, no. 2, pp. 167–256, 2003.

[24] M. Tahir, H. Mohamad, N. Ramli, and Y. Lee, "Cooperative spectrum sensing using energy detection in mobile and static environment," in *Proceedings of the International Conference on Computer Networks and Communications Systems (CNCS '12)*, 2012.

[25] T. Camp, J. Boleng, and V. Davies, "A survey of mobility models for Ad Hoc network research," *Wireless Communications and Mobile Computing*, vol. 2, no. 5, pp. 483–502, 2002.

Hindawi Publishing Corporation
International Journal of Distributed Sensor Networks
Volume 2013, Article ID 724581, 8 pages
http://dx.doi.org/10.1155/2013/724581

Research Article

The User Requirement Based Competitive Price Model for Spectrum Sharing in Cognitive Radio Networks

Fang Ye,[1] Yibing Li,[1] Rui Yang,[2] and Zhiguo Sun[1]

[1] *College of Information & Communication Engineering, Harbin Engineering University, Harbin 150001, China*
[2] *China Electronics Standardization Institute, Beijing 100176, China*

Correspondence should be addressed to Yibing Li; liyibing@hrbeu.edu.cn

Received 4 September 2013; Revised 1 November 2013; Accepted 1 November 2013

Academic Editor: Al-Sakib Khan Pathan

We analyze the competitive price game model for spectrum sharing in cognitive radio networks with multiple primary users and secondary users and propose a user requirement based competitive price game model for the calculation of the shared spectrum size of cognitive user in Bertrand game. The communication requirement of the cognitive user is quantified into different requirement levels. With the application of spectrum requirement factor, cognitive user can adjust the demanded shared spectrum size according to self-requirement level and the shared spectrum price provided by licensed users. It can avoid the waste of spectrum resource caused by the overdistribution of spectrum to the cognitive user with low communication requirement. Simulation results show that the occupied spectrum of cognitive user can be adjusted with the variation of requirement levels, and the licensed users can achieve better profit performance with consideration of requirement of cognitive user by adjustment of the shared spectrum price proposed spectrum sharing model.

1. Introduction

Cognitive radio is viewed as an effective approach for improving the utilization of the radio spectrum [1]. The cognitive transceivers have flexible spectrum sensing ability and can adjust transmission parameters adaptively according to the ambient environment. The spare spectrum of licensed users (primary user) can be accessed by the cognitive users (secondary user) dynamically without causing harmful interference, and certain economic revenue can be achieved by the primary users [2, 3].

As the behaviors of the primary users and secondary users interact with each other, game theory, which is viewed as an effective tool for the analysis of interactive decision making, is applied in the spectrum sharing problem of cognitive radio networks [4]. The players in game model are primary and secondary users. The strategy space for each user consists of various actions related to spectrum sharing. Specifically, for secondary users, the strategy space includes which licensed channel they will use, what transmission parameters (e.g., transmission power or time duration) to apply, and the price they agree to pay for leasing certain channels from the primary users. For primary users, the strategy space may include which unused channel they will lease to secondary users and how much they will charge secondary users for using their spectrum resources [5, 6]. The competitive price model is applied to analyze the spectrum sharing problem in cognitive radio networks and obtain the Nash equilibrium price strategies that maximize the profits of primary users. As the price strategies of other primary users are usually not available simultaneously, the iterative equilibrium price calculation was further analyzed [7, 8]. The spectrum sharing problem with price strategies offered simultaneously and sequentially is also discussed in [9]. The selection of adjustment factor in the calculation of the equilibrium price is discussed in [10]. The auction mechanism is used to analyze the spectrum sharing of cognitive users to obtain the transmit power that satisfies the interference constraints [11], and the auction mechanism based on the signal to noise ratio and power is proposed; it can be applied to achieve the iterative calculation of the equilibrium price in distributed cognitive radio networks. The spectrum allocation algorithm based on dynamic multiband auction is discussed in [12], and the spectrum auction problem is converted to the 0/1 integer

knapsack problem. The shared spectrum price is determined according to the supply-demand relationship. The spectrum resource allocation of cognitive radio networks based on auction mechanism is also analyzed in [13]. The cognitive users bid for the spectrum resource, the licensed users as the spectrum broker determine the spectrum sharing strategies without the deterioration of its communication quality, and the iterative calculation of the spectrum bid from secondary users in distributed cognitive radio networks is discussed. With the consideration of the collaboration among cognitive users, the mechanism of monetary compensation and motivation is used to improve utility function of the cognitive uses; thus the licensed spectrum can be shared with better fairness performance [14]. The spectrum leasing problem in cognitive radio networks is discussed in [15], which is different from the spectrum leasing model mentioned above; the primary users allow the spectrum sharing with selection of the affordable interference levels. The auction mechanism based spectrum sharing between single primary user and multiple secondary users in cognitive radio networks is discussed in [16], the shared spectrum power strategies of the secondary users are determined by Vickrey auction mechanism to guarantee the interference power levels without causing harmful influence to the communication quality. The auction agent-based spectrum sharing in cognitive radio networks is analyzed in [17]. In addition to the primary users and secondary users, specialized agent is responsible for the spectrum resources allocation. It applies for the spectrum resource from the primary users and reallocates the licensed spectrum resource to the secondary users at certain price strategies. The transmit information between the primary users and secondary users can be reduced by the spectrum sharing mechanism, and effective spectrum sharing strategies can be achieved.

As the competitive price game model is applied in the cognitive radio networks with multiple primary users and single secondary user service, and the auction mechanism spectrum sharing model is applied in the cognitive radio networks with single primary user and multiple secondary users, this paper focused on the spectrum sharing problem with multiple primary users and secondary users. Moreover, on the basis of the competitive price game model, the spectrum resource demand levels of the secondary user are taken into account; the secondary service can adjust the applied spectrum resource according to the spectrum demand of secondary users and the shared spectrum price from the primary users. It is more applicable in the practical cognitive radio networks with the consideration of the spectrum requirements of secondary users, and the spectrum efficiency can be improved.

The rest of this paper is organized as follows. Section 2 describes the system model of spectrum sharing in cognitive radio networks. In Section 3, the spectrum sharing problem based on competitive price game is analyzed. Section 4 presents the simulation results, and Section 5 draws some conclusions.

2. System Model

We consider a wireless system with multiple primary users, the total number of which is denoted by N. For simplicity, assume the communication of secondary users is served by a secondary service. In this case, primary user i wants to sell portions of its spare spectrum to secondary user at price p_i. The communication requirements of secondary user should be satisfied with assurance of primary users' communication qualities, and certain economic revenue is obtained by the primary users through spectrum sharing. The demanded spectrum size of secondary user here depends on its transmission efficiency and the shared spectrum price charged by primary users. The transmission efficiency of secondary user is related to the modulation and channel qualities, which can be expressed as follows [18]:

$$k = \log_2 (1 + K\gamma), \tag{1}$$

where γ is the SNR at the secondary receiver, $K = 1.5/\ln(0.2/\mathrm{BER}^{\mathrm{tar}})$, and $\mathrm{BER}^{\mathrm{tar}}$ is the target bit error rate of the secondary user.

We apply Bertrand price model in economics to analyze the spectrum sharing problem in cognitive radio networks. The primary users provide the price strategies of shared spectrum, and the demanded spectrum size of the secondary user is determined from its utility function, which is relevant to the price strategies provided by primary users. The spectrum sharing profits of primary user depend on the economic revenue and the cost due to spectrum sharing. Here, the cost of spectrum sharing is defined as the degradation of the quality of service (QoS). The primary users constantly adjust the price strategies of shared spectrum to achieve the maxima of their own profits.

The demanded spectrum size of secondary user can be calculated through the quadratic utility function that is described as follows [5]:

$$\begin{aligned} U(\mathbf{b}) = {} & \sum_{i=1}^{N} b_i k_i^{(s)} \\ & - \frac{1}{2}\left(\sum_{i=1}^{N} b_i^2 + 2\nu \sum_{j \neq i} b_i b_j\right) - \sum_{i=1}^{N} p_i b_i, \end{aligned} \tag{2}$$

where $\mathbf{b}$ is the set of the shared spectrum size from different primary users, $\mathbf{b} = [b_1, b_2, \ldots, b_N]$; p_i is the price strategy of shared spectrum from primary user i, $\mathbf{p} = [p_1, p_2, \ldots, p_N]$; $k_i^{(s)}$ is the spectrum efficiency of secondary user that can be achieved by occupying the spectrum resource from primary user i; ν is the spectrum substitutability factor, and $\nu \in [0, 1]$. When $\nu = 0$, the spectrum resource of different primary users cannot be substituted, while when $\nu = 1$, the spectrum resource of different primary users can be substituted freely. The demanded spectrum size by secondary users can be obtained by

$$\frac{\partial U(\mathbf{b})}{\partial b_i} = 0. \tag{3}$$

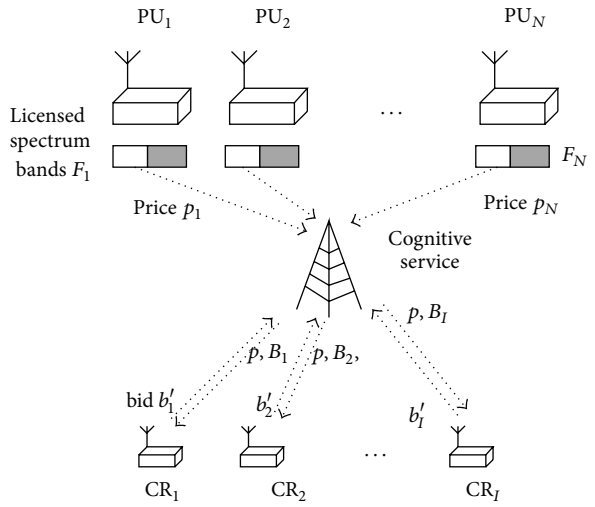

Figure 1: The improved spectrum sharing model.

The demanded spectrum resource of the secondary service from the primary users can be determined by calculating the solution of b_i. However, the spectrum resource requirement of the secondary users is not taken into account; the required spectrum resource is determined by the shared spectrum price of the primary users. It may lead to the secondary service demanding more spectrum resource than required, so that the spectrum efficiency cannot fully be improved.

3. The Competitive Price Gamed Based Spectrum Sharing with User Requirement

On the basis of the spectrum sharing model in cognitive radio networks based on the competitive price game, we take the impact of cognitive users' spectrum requirement in the spectrum sharing into account and establish an improved spectrum sharing model with the combination of competitive price game and auction mechanism as shown in Figure 1. The secondary service can collect the spectrum bids of the secondary user within the secondary user group, and the demanded spectrum resource level can be determined by the spectrum bids of the secondary users. With the acknowledgement of the shared spectrum price provided by the primary user and the spectrum demand levels of the secondary users, the secondary service determines the optimal shared spectrum size by competitive price game model. After the secondary service obtains the exclusive spectrum access right of certain spectrum resource, the secondary service reallocates the obtained spectrum resource to the secondary users by auction mechanism. Thus, the spare licensed spectrum resource can be shared between multiple primary users and secondary users.

In the spectrum sharing model based on auction mechanism, the secondary users submit the spectrum bids $\mathbf{b}' = [b_1', b_2', \ldots, b_I']$ to the secondary service according to the communication requirement, where I is the number of secondary users within the group. The secondary service collects the spectrum bids of different primary users and determines the demanded spectrum resource according to the shared spectrum price from the primary users $\mathbf{p} = \{p_1, p_2, \ldots, p_N\}$, where N is the number of primary users.

At the secondary service terminal, the demanded spectrum resource of the secondary is $\sum_{i=1}^{I} b_i'$; the quadratic utility function based on the competitive price game model can be described as follows:

$$\begin{aligned} U'(\mathbf{b}) &= \sum_{i=1}^{N} b_i k_i^{(s)} - \frac{1}{2}\left(\sum_{i=1}^{N} b_i^2 + 2v\sum_{j\neq i} b_i b_j\right) \\ &\quad - \sum_{i=1}^{N} p_i b_i - \sigma\left(\sum_{i=1}^{N} b_i - \sum_{k=1}^{I} b_k'\right)^2, \end{aligned} \tag{4}$$

where σ is constant factor. In order to achieve the shared spectrum size that maximizes the utility function of the secondary service, the demanded spectrum size by secondary users can be obtained by

$$\frac{\partial U'(\mathbf{b})}{\partial b_i} = 0. \tag{5}$$

From (5), we can get

$$\begin{aligned} &(1+2\sigma)\, b_i + (v+2\sigma)\sum_{j\neq i} b_j \\ &\quad = k_i^{(s)} - p_i + 2\sigma\sum_{k=1}^{I} b_k'. \end{aligned} \tag{6}$$

The size of shared spectrum can be rewritten as the linear equations according to (6):

$$\begin{aligned} &(1+2\sigma)\, b_1 \\ &\quad + (v+2\sigma)\, b_2 + (v+2\sigma)\, b_3 + \cdots + (v+2\sigma)\, b_N \\ &\qquad = k_1^{(s)} - p_1 + 2\sigma\sum_{k=1}^{I} b_k', \\ &(v+2\sigma)\, b_1 + (1+2\sigma)\, b_2 \\ &\quad + (v+2\sigma)\, b_3 + \cdots + (v+2\sigma)\, b_N \\ &\qquad = k_2^{(s)} - p_2 + 2\sigma\sum_{k=1}^{I} b_k', \\ &\quad \vdots \\ &(v+2\sigma)\, b_1 + (v+2\sigma)\, b_2 \\ &\quad + (v+2\sigma)\, b_3 + \cdots + (1+2\sigma)\, b_N \\ &\qquad = k_N^{(s)} - p_N + 2\sigma\sum_{k=1}^{I} b_k'. \end{aligned} \tag{7}$$

The size of demanded spectrum can be obtained by

$$\mathbf{D} = \mathbf{A}^{-1}\mathbf{F}, \tag{8}$$

where

$$\mathbf{A} = \begin{bmatrix} 1+2\sigma & \nu+2\sigma & \cdots & \nu+2\sigma \\ \nu+2\sigma & 1+2\sigma & \cdots & \nu+2\sigma \\ \vdots & \vdots & \ddots & \vdots \\ \nu+2\sigma & \nu+2\sigma & \cdots & 1+2\sigma \end{bmatrix}, \tag{9}$$

$$\mathbf{D} = \begin{bmatrix} b_1 \\ b_2 \\ \vdots \\ b_N \end{bmatrix}, \tag{10}$$

$$\mathbf{F} = \begin{bmatrix} k_1^{(s)} - p_1 + 2\sigma \sum_{k=1}^{I} b_k' \\ k_2^{(s)} - p_2 + 2\sigma \sum_{k=1}^{I} b_k' \\ \vdots \\ k_N^{(s)} - p_N + 2\sigma \sum_{k=1}^{I} b_k' \end{bmatrix}. \tag{11}$$

The elements in the inverse of $\mathbf{A}$ matrix can be achieved by elementary transform:

$$a_{ij}' = \begin{cases} \dfrac{1+2\sigma+(N-2)(\nu+2\sigma)}{(1-\nu)(1+2\sigma+(N-1)(\nu+2\sigma))} & i = j \\ -\dfrac{\nu+2\sigma}{(1-\nu)(1+2\sigma+(N-1)(\nu+2\sigma))} & i \neq j. \end{cases} \tag{12}$$

With the acknowledgement of shared spectrum price strategies $\mathbf{p}$, the size of demanded spectrum can be expressed as follows:

$$\begin{aligned} b_i &= \left(\left(k_i^{(s)} - p_i + 2\sigma \sum_{k=1}^{I} b_k' \right) \right. \\ &\quad \times (1+2\sigma+(N-2)(\nu+2\sigma)) - (\nu+2\sigma) \\ &\quad \left. \times \sum_{j \neq i} \left(k_j^{(s)} - p_j + 2\sigma \sum_{k=1}^{I} b_k' \right) \right) \\ &\quad \times ((1-\nu)(1+2\sigma+(N-1)(\nu+2\sigma)))^{-1}. \end{aligned} \tag{13}$$

3.1. Adaption of the Shared Spectrum Price. The cost of spectrum sharing in this paper is defined by the QoS degradation of primary users. The revenue function R_i and cost function C_i for the primary user i that provides certain size of shared spectrum are defined as follows, respectively [7, 8]:

$$R_i = c_1 M_i, \tag{14}$$

$$C_i(b_i) = c_2 M_i \left(B_i^{\text{req}} - k_i^{(p)} \frac{W_i - b_i}{M_i} \right), \tag{15}$$

where c_1, c_2 are constants that denote the weights between revenue function and cost function, B_i^{req} is the bandwidth requirement of primary user, W_i is the total size of available spectrum, M_i is the number of primary connections, and $k_i^{(p)}$ is the transmission efficiency of primary users.

In Bertrand price model, the players of the game are the primary users, the strategies of the players are prices of shared spectrum, that is, $\{p_i\}$, and the utility function is the achieved profit, that is, $\{P_i\}$. If the spectrum demand of cognitive user can be satisfied by the primary users, that is, the available spectrum resource of the primary users is larger than the spectrum demand $D_i(\mathbf{p})$ of the secondary user, the profit function of primary users i is given by

$$\begin{aligned} P_i(\mathbf{p}) &= p_i D_i(\mathbf{p}) \\ &\quad + c_1 M_i - c_2 M_i \left(B_i^{\text{req}} - k_i^{(p)} \frac{W_i - D_i(\mathbf{p})}{M_i} \right)^2. \end{aligned} \tag{16}$$

However, in practical spectrum sharing model for cognitive radio networks, the spectrum resources of the primary users are usually restricted. The spectrum demand of the secondary users will not be definitely satisfied by the primary users. Thus, it needs to consider the constraints of the shared spectrum size. $B_i^{\max}$ is the maximum shared spectrum size of primary user i, and the competitive price game based spectrum sharing model with constraints of shared spectrum for cognitive radio networks can be formulated as (17), that is, determining the price strategy $\mathbf{p}^*$ satisfies

$$\begin{aligned} \mathbf{p}^* &= \arg\max_{\mathbf{p}} \left(\sum_{i=1}^{N} P_i(\mathbf{p}) \right), \\ \text{s.t.} \quad & D_i(\mathbf{p}) > 0, \quad i = 1, 2, \ldots, N, \\ & D_i(\mathbf{p}) < B_i^{\max}, \quad i = 1, 2, \ldots, N, \end{aligned} \tag{17}$$

where $\mathbf{p}^*$ is also defined as the Nash equilibrium price of the competitive price game. In order to achieve the $\mathbf{p}^*$ that satisfies (17):

$$\frac{\partial P_i(\mathbf{p})}{\partial p_i} = 0. \tag{18}$$

It can be achieved from (16)–(18) that

$$\begin{aligned} & D_i(\mathbf{p}) + p_i \frac{\partial D_i(\mathbf{p})}{\partial p_i} \\ & \quad - 2c_2 k_i^{(p)} \left(B_i^{\text{req}} - k_i^{(p)} \frac{W_i - D_i(\mathbf{p})}{M_i} \right) \frac{\partial D_i(\mathbf{p})}{\partial p_i} = 0, \end{aligned} \tag{19}$$

where

$$\begin{aligned} & \frac{\partial D_i(\mathbf{p})}{\partial p_i} \\ & \quad = -\frac{1+2\sigma_1+(N-2)(\nu+2\sigma_1)}{(1-\nu)(1+2\sigma_1+(N-1)(\nu+2\sigma_1))}. \end{aligned} \tag{20}$$

In practical cognitive radio networks, the price strategies of other primary users cannot be achieved simultaneously; the Nash equilibrium price strategy of the competitive price model cannot be achieved through the linear equations formed by (19). Thus, it is needed to further discuss the iterative method without acknowledgment of price strategies from other primary users.

Assume the price strategies of other primary users cannot be achieved simultaneously, but the price strategies of primary users during last cycle are available. The Nash equilibrium price that maximizes the system profits of the primary users can be achieved iteratively.

The linear gradient descent algorithm is one of the effective tools to calculate the maximum and minimum value of continuous target function during the optimization problems. For the primary users, the profit function is convex with the variation of shared spectrum price. At the kth iteration, p_i^k is the shared spectrum price of primary user i and $P_i^k(\mathbf{p})$ is the profit of primary user i. We can establish the improved system profit function $\varphi^k(\mathbf{p})$ using the Lagrange function in the condition of limited spectrum resource [3]. If the available spectrum resource of the primary users is larger than the spectrum demand of the secondary user, the value of the improved system profit function of primary users increases with p_i^k until the maximum of the improved system profit function is obtained, at which $\partial\varphi(\mathbf{p})/\partial p_i^k$ is positive, and p_i will increase iteratively until the equilibrium price is achieved or the spectrum constraints of the primary users cannot be satisfied. The value of the improved system profit function will decrease with the decrease in the demanded spectrum size of the cognitive users when the price of the shared spectrum is too high for the cognitive user. At this time, $\partial\varphi(\mathbf{p})/\partial p_i^k$ is negative, and the shared spectrum price p_i decreases until the equilibrium price is achieved. Otherwise, with the increase of p_i^k, the spectrum demand of the secondary user decreases and the profit of the primary user also decreases accordingly, $\partial\varphi(\mathbf{p})/\partial p_i^k$ is negative, and p_i^k tends to decrease by (21) until the Nash equilibrium price strategy is achieved. When the spectrum demand of the secondary user cannot be satisfied by the available spectrum resource of primary users, that is, the cognitive user tends to apply for more spectrum resource than spectrum constraints, the value of the improved profit function decreases. Thus the equilibrium price of the shared spectrum that maximizes the improved system profit function and satisfies the constraints of spectrum resource can be achieved iteratively:

$$p_i^{k+1} = p_i^k + a\frac{\partial\phi(\mathbf{p})}{\partial p_i^k}, \tag{21}$$

where a is a nonnegative adjustment factor. With appropriate adjustment factor, the shared spectrum price that maximizes the improved system profit function can be achieved iteratively.

3.2. Reallocation of Achieved Spectrum Resource. The secondary users submit the spectrum bids $\mathbf{b}'$ to the secondary service. Here, we use the demanded spectrum size as spectrum bids of the secondary users, where $0 \le b_i' \le B^{\text{tot}}$ and $B^{\text{tot}} = \sum_{i=1}^{N} b_i$ is the total achieved spectrum resource of the secondary service from the primary users. The secondary service, as the spectrum resource broker, collects the spectrum bids from the secondary users and determines the shared spectrum size to the secondary users $\mathbf{B} = [B_1, B_2, \ldots, B_I]$:

$$B_k = \frac{b_k'}{\sum_{k=1}^{I} b_k' + \beta} B^{\text{tot}}, \tag{22}$$

where β is a positive reserve bid used by the PU to control the remaining portion of the spectrum for its own usage [13], which is set by PU to satisfy

$$B^{\text{tot}} - \sum_{k=1}^{I} B_k > \sum_{i=1}^{N} B_i^{\text{req}}. \tag{23}$$

With the shared spectrum resource B_i, the revenue R_i of the secondary user i can be shown as

$$R_i = r_i k_i B_i, \tag{24}$$

where r_i is the revenue of secondary user i per unit of achievable transmission rate, which relates to the QoS in a real network; that is, the higher the QoS required by the secondary user i is, the greater the revenue r_i will be. k_i is spectral efficiency of transmission, which can be obtained from (1).

The economical cost C_i of secondary user i with shared spectrum size B_i can be shown as

$$C_i = p\theta_i b_i, \tag{25}$$

where θ_i is the priority factor of secondary user. The profit function of secondary user i that can be achieved through spectrum sharing is defined as follows:

$$\begin{aligned} U_i\left(b_i', \mathbf{b}_{-i}', p\right) &= R_i\left(B_i\left(b_i', \mathbf{b}_{-i}'\right)\right) - C_i\left(b_i', p\right) \\ &= r_i k_i \frac{b_i'}{\sum_{i=1}^{I} b_i' + \beta} B^{\text{tot}} - p\theta_i b_i', \end{aligned} \tag{26}$$

where $\mathbf{b}_{-i}' = [b_1', b_2', \ldots, b_{i-1}', b_{i+1}', \ldots, b_I']$ is the spectrum bids of secondary users except secondary user i. The secondary user i adjusts its spectrum bid to achieve the maximal profit function according to the communication parameters. Thus the equilibrium price strategies can be obtained, and the secondary users cannot get higher profit with price strategy variation; the equilibrium price strategy $(b_i')^*$ must satisfy

$$\left(b_i'\right)^* = \underset{0 \le b_i' \le B^{\text{tot}}}{\operatorname{argmax}} U_i\left(b_i', \mathbf{b}_{-i}', p\right), \tag{27}$$

where $(\mathbf{b}')^* = [(b')_i^*, (\mathbf{b}_{-i}')^*]$. In order to obtain the price strategies that maximize its spectrum sharing profits, we can get

$$\frac{\partial U_i\left(b_i', \mathbf{b}_{-i}', p\right)}{\partial b_i'} = 0. \tag{28}$$

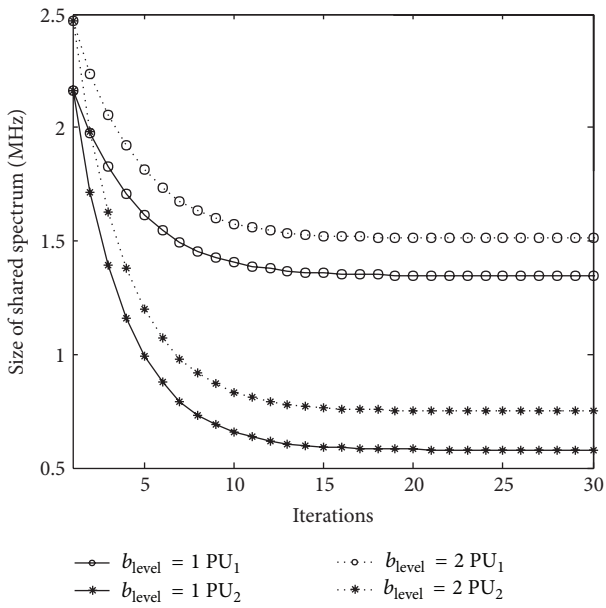

Figure 2: The shared spectrum size under different requirement levels of cognitive users.

Thus

$$r_i k_i B^{\text{tot}} \frac{\sum_{j=1, j\neq i}^{I} b_i' + \beta}{\left(\sum_{j=1}^{I} b_i' + \beta\right)^2} - p\theta_i = 0. \tag{29}$$

When the cognitive user cannot get acknowledgment of the spectrum bids from other cognitive user, which is similar with the calculation of the shared spectrum price in competitive price game model discussed in Section 3.1, the spectrum bids of the secondary user can be achieved by

$$\left(b_i'\right)^{t+1} = \left(b_i'\right)^{t} + \alpha_i \left(b_i'\right)^{t} \frac{\partial U_i\left(b_i', \mathbf{b}_{-i}', p\right)}{\partial b_i'}, \tag{30}$$

where $(b_i')^t$ is the spectrum bid of secondary user i at time slot t and α_i is the speed adjustment parameter (i.e., learning speed) of secondary user i, which makes the spectrum sharing stable and Nash equilibrium reached.

4. Simulation Results

We consider a cognitive radio network with two primary users and two secondary users sharing a frequency spectrum of size 20 MHz. The target BER for each secondary user is $\text{BER}_i^{\text{tar}} = 10^{-4}$. Each secondary user knows its revenue per unit transmission rate $r_i = 10$, and it also knows its spectral efficiency of transmission through channel estimation. The primary user sets the price $p = 10$ per unit bandwidth and reserves bid $\beta_1 = \beta_2 = 0.2$. The speed adjustment parameter is set as $\alpha_1 = \alpha_2 = 0.1$.

Figure 2 shows simulation results of the shared spectrum size of the secondary service under different spectrum requirements from the secondary users, where spectrum requirement $b_{\text{level}} = \sum_{i=1}^{I} b_i'$. It can be concluded from Figure 2 that, with the increasing spectrum requirement of secondary users, the secondary service can demand more spectrum resource from the primary users.

Figure 3 shows the simulation results of the system profit of the primary users by providing spectrum sharing to the secondary users. It can be concluded from Figure 3 that, with the increasing spectrum requirement of the secondary users, more shared spectrum size can be obtained by the secondary users, and the primary users can also achieve more spectrum sharing profits.

Then, we compare the proposed approach with the conventional approach which combines the competitive price game and auction mechanism directly without considering different spectrum requirement levels from the secondary users. Figure 4 shows the simulation results of spectrum bids with different spectrum requirement levels from the secondary users, when applying the proposed spectrum leasing model and the conventional competitive price game model for cognitive radio networks. The factor θ is reduced to control the cost function in the improved spectrum leasing model. On the contrary, with the increase of factor θ, the spectrum requirements of the secondary users are increased. Where the signal to noise ratio of the secondary receiver 1 is 18 dB and the signal to noise ratio of the secondary receiver 1 is 22 dB. In the conventional spectrum leasing model with the combination of the competitive price game and auction mechanism, $\theta_1 = 1$, and in the improved spectrum leasing model $\theta_2 = 0.8$ to improve the spectrum requirement of the secondary users. It can be concluded from Figure 4 that, with the increase of the spectrum requirement levels from the secondary user, the improved spectrum leasing model can achieve more spectrum resource with higher shared spectrum price.

Figure 5 shows the simulation results of the shared spectrum resource size of the secondary service by the improved spectrum leasing model and the conventional spectrum leasing model with direct combination of the competitive price game and auction mechanism. It can be concluded from Figure 5 that, in the improved spectrum leasing model, the secondary user can increase the spectrum bids to apply for more licensed spectrum resource. It is more suitable for the spectrum leasing problem in cognitive radio networks.

5. Conclusion

In this paper, we analyze the spectrum leasing problem of the cognitive radio networks with multiple primary users and multiple secondary users, and propose an improved spectrum sharing model considering the spectrum requirement of the secondary users. This approach introduces the demanded spectrum resource of the secondary users into the utility function base on the competitive price game model and uses a spectrum requirement level to quantify the communication requirements of the secondary users. Then the secondary service can determine the size of shared spectrum according to the spectrum requirement of the secondary users and the provided spectrum sharing price,

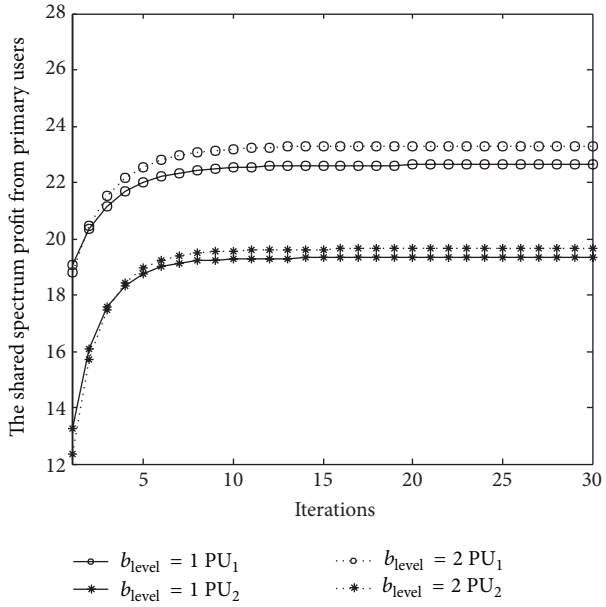

Figure 3: The profit of primary users by providing spectrum resource under different requirement levels of cognitive users.

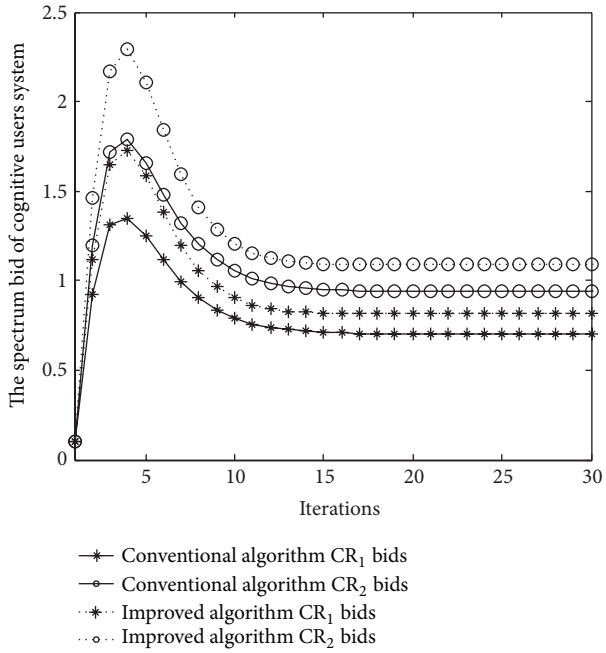

Figure 4: The spectrum bid of cognitive users system revenue performance of primary users in the improved spectrum trading model.

and the primary users adjust the price of shared spectrum to maximize their spectrum sharing profits. The simulation results show that the achieved spectrum resource of the secondary user can be adjusted flexibly according to its spectrum requirements and the shared spectrum price of the primary user, especially when the demand spectrum size of the secondary users cannot be satisfied by the primary users.

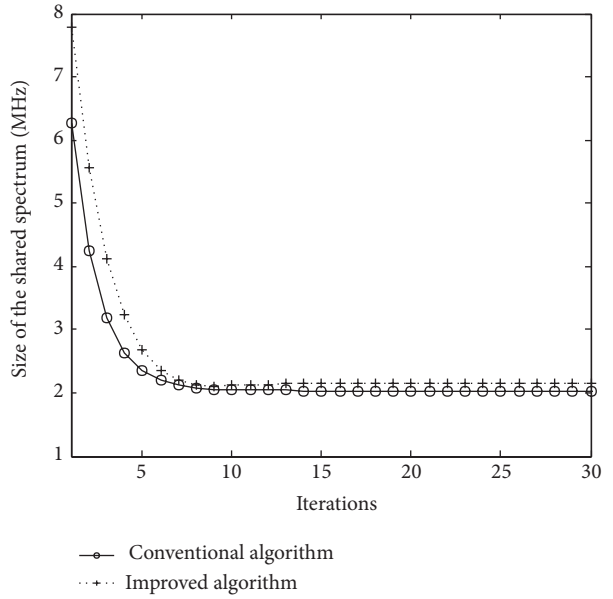

Figure 5: The achieved shared spectrum resource of the cognitive service management by the improved spectrum trading model.

It can also avoid the waste of spectrum resource when the spectrum requirement of the secondary user is low.

Conflict of Interests

The authors declare that there is no conflict of interests regarding the publication of this paper.

Acknowledgments

This paper is supported by the Young Scientists Fund of the National Natural Science Foundation of China (Grant no. 61101141), the Natural Science Foundation of Heilongjiang Province, China (Grant no. QC2012C070), and the Fundamental Research Funds for the Central Universities of Ministry of Education of China (Grant no. HEUCF1308).

References

[1] S. Haykin, "Cognitive radio: brain-empowered wireless communications," *IEEE Journal on Selected Areas in Communications*, vol. 23, no. 2, pp. 201–220, 2005.

[2] I. F. Akyildiz, W.-Y. Lee, M. C. Vuran, and S. Mohanty, "Next generation/dynamic spectrum access/cognitive radio wireless networks: a survey," *Computer Networks*, vol. 50, no. 13, pp. 2127–2159, 2006.

[3] Y. Li, R. Yang, Y. Lin, and F. Ye, "The spectrum sharing in cognitive radio networks based on competitive price game," *Radio Engineering*, vol. 21, no. 3, pp. 802–808, 2012.

[4] Z. Ji and K. J. R. Liu, "Dynamic spectrum sharing: a game theoretical overview," *IEEE Communications Magazine*, vol. 45, no. 5, pp. 88–94, 2007.

[5] O. Raoof and H. S. Al-Raweshidy, "Spectrum sharing in cognitive radio networks: an adaptive game approach," *IET Communications*, vol. 6, no. 11, pp. 1495–1501, 2012.

[6] T. Zhang and X. Yu, "Spectrum sharing in cognitive radio using game theory—a survey," in *Proceedings of the 6th International Conference on Wireless Communications, Networking and Mobile Computing (WiCOM '10)*, pp. 1–5, Chengdu, China, September 2010.

[7] D. Niyato and E. Hossain, "Competitive pricing for spectrum sharing in cognitive radio networks: dynamic game, inefficiency of nash equilibrium, and collusion," *IEEE Journal on Selected Areas in Communications*, vol. 26, no. 1, pp. 192–202, 2008.

[8] D. Niyato and E. Hossain, "Optimal price competition for spectrum sharing in cognitive radio: a dynamic game-theoretic approach," in *Proceedings of the 50th Annual IEEE Global Telecommunications Conference*, pp. 4625–4629, Washington, DC, USA, November 2007.

[9] H. Hong, K. Niu, and Z. He, "A game thezoretic analysis of pricing for spectrum sharing in cognitive radio networks," in *Proceedings of the 1st IEEE International Conference on Communications Technology and Applications*, pp. 467–471, Beijing, China, October 2009.

[10] A. J. Goldsmith, "Variable-rate variable-power MQAM for fading channels," *IEEE Transactions on Communications*, vol. 45, no. 10, pp. 1218–1230, 1997.

[11] J. Huang, R. A. Berry, and M. L. Honig, "Auction-based spectrum sharing," *Mobile Networks and Applications*, vol. 11, no. 3, pp. 405–418, 2006.

[12] G. Wu, P. Ren, and M. Zhan, "Dynamic spectrum assignment based on FADM algorithm in cognitive networks," *Journal of University of Science and Technology of China*, vol. 39, no. 10, pp. 1070–1075, 2009.

[13] X. Wang, Z. Li, P. Xu, Y. Xu, X. Gao, and H.-H. Chen, "Spectrum Sharing in cognitive radio networks: an auction-based approach," *IEEE Transactions on Systems, Man, and Cybernetics B*, vol. 40, no. 3, pp. 587–596, 2010.

[14] W.-F. Zhou and Q. Zhu, "Novel auction-based spectrum sharing scheme with the compensation and motivation mechanism," *Journal on Communications*, vol. 32, no. 10, pp. 86–91, 2011.

[15] S. K. Jayaweera, G. Vazquez-Vilar, and C. Mosquera, "Dynamic spectrum leasing: a new paradigm for spectrum sharing in cognitive radio networks," *IEEE Transactions on Vehicular Technology*, vol. 59, no. 5, pp. 2328–2339, 2010.

[16] H.-B. Chang and K.-C. Chen, "Auction-based spectrum management of cognitive radio networks," *IEEE Transactions on Vehicular Technology*, vol. 59, no. 4, pp. 1923–1935, 2010.

[17] L. Qian, F. Ye, L. Gao et al., "Spectrum trading in cognitive radio networks: an agent-based model under demand uncertainty," *IEEE Transactions on Communications*, vol. 59, no. 11, pp. 3192–3203, 2011.

[18] S.-G. Chua and A. Goldsmith, "Variable-rate variable-power MQAM for fading channels," in *Proceedings of the 46th IEEE Vehicular Technology Conference*, pp. 815–819, Atlanta, Ga, USA, May 1996.